

COMPUTATION OF THE MOTION AND
DRIFT FORCE FOR A FLOATING BODY

CENTRE FOR NEWFOUNDLAND STUDIES

**TOTAL OF 10 PAGES ONLY
MAY BE XEROXED**

(Without Author's Permission)

CHUAN-CHEUNG TSE



**COMPUTATION OF THE MOTION AND DRIFT FORCE
FOR A FLOATING BODY**

C

BY

CHUAN-CHEUNG TSE, M. SC. (ENG.)

**A Thesis submitted to the School of Graduate
Studies in partial fulfillment of the
requirements for the degree of
Master of Engineering**

Faculty of Engineering and Applied Science

Memorial University of Newfoundland

April 1984

*** St. John's**

Newfoundland

ABSTRACT

A computer program based on the linear wave diffraction theory, using 3-D source distribution method, is set up. This program calculates the first-order wave forces, response motions, steady (mean) horizontal drift forces and vertical drift moment for a floating body in a regular wave system. The steady drift forces (moment) are evaluated by the far field approach.

Some modified numerical schemes are proposed, in this work that save a certain amount of the computer cpu time.

Computations were carried out for two typical floating bodies (hemisphere and rectangular box). The computed results are in good agreement with the published data.

ACKNOWLEDGEMENT

The author wishes to express his sincere gratitude to Professor C. C. Hslung and Professor Don Bass for their valuable suggestions and comments. Sincere thanks are also due to Dr. G. R. Peters, Dean of Engineering and Applied Science, and Dr. T. R. Charl, Associate Dean of Engineering and Applied Science, for their encouragement. The author is also grateful to Mr. J. M. Chuang and Mr. D. Sen for devoting much of their time in discussions. Acknowledgement is also given for the University Fellowship provided by Memorial University of Newfoundland.

Table of Contents

	Page
ABSTRACT	II
ACKNOWLEDGEMENT	III
LIST OF TABLES AND FIGURES	vi
NOMENCLATURE	viii
CHAPTER 1: INTRODUCTION	1
CHAPTER 2: MATHEMATICAL MODEL	3
CHAPTER 3: STEADY HARMONIC POTENTIAL	6
CHAPTER 4: SOLUTION OF $\phi(\vec{x})$ BY USING GREEN'S FUNCTION METHOD AND STEADY MOTION $\eta_j(t)$	12
4.1 Integral-equation formulation	13
4.2 Numerical solution	15
CHAPTER 5: STEADY DRIFT FORCES AND MOMENTS	18
5.1 General description	18
5.2 Formulation of steady horizontal drift forces and vertical drift moment	19
CHAPTER 6: NUMERICAL PROGRAMMING SCHEMES	28
6.1 Body surface panel	28
6.2 Evaluation of the Green's function and its derivative	29
6.3 Evaluation of α_{pq} and β_{pq}	33
6.4 Properties of α_{pq} due to the symmetry of the body geometry	35
6.5 Properties elements of α_{pq} and β_{pq}	37
6.6 Complex matrix Inversion	38
6.7 Miscellaneous	39
CHAPTER 7: RESULTS OF COMPUTED EXAMPLES	41
7.1 General description	41
7.2 Comparison with published data	42
7.3 Discussion of computed results	45
7.4 Irregular frequency	46
CHAPTER 8: CONCLUSION	49

REFERENCES	51
TABLES AND FIGURES	54
APPENDIX A	84
APPENDIX B	91

LIST OF TABLES AND FIGURES

	Page
Table (1) Data for hemisphere	54
Table (2) Data for rectangular box	55
Figure (1) Coordinate system and sign convention for translatory and angular displacements	56
Figure (2) Typical partitioning of x-z plane symmetric body	56
Figure (3) Added mass and damping in surge for a hemisphere	57
Figure (4) Added mass and damping in heave for a hemisphere	58
Figure (5) Surge exciting force and phase for a hemisphere	59
Figure (6) Heave exciting force and phase for a hemisphere	60
Figure (7) Surge motion and phase for a hemisphere	61
Figure (8) Heave motion and phase for a hemisphere	62
Figure (9) Drift force for a hemisphere	63
Figure (10) Added mass and damping in surge for rectangular box	64
Figure (11) Added mass and damping in heave for rectangular box	65
Figure (12) Added mass and damping in pitch for rectangular box	66
Figure (13) Added mass and damping in yaw for rectangular box	67
Figure (14.a) Surge motion and phase for rectangular box (heading = 0 Deg.)	68
Figure (14.b) Surge motion and phase for rectangular box (heading = 45 Deg.)	69
Figure (15.a) Heave motion and phase for rectangular box (heading = 0 Deg.)	70
Figure (15.b) Heave motion and phase for rectangular box (heading = 45 Deg.)	71

Figure (16.a) Pitch motion and phase for rectangular box (heading = 0 Deg.)	72
Figure (16.b) Pitch motion and phase for rectangular box (heading = 45 Deg.)	73
Figure (17.a) Surge exciting force and phase for rectangular box (heading = 0 Deg.)	74
Figure (17.b) Surge exciting force and phase for rectangular box (heading = 45 Deg.)	75
Figure (18.a) Heave exciting force and phase for rectangular box (heading = 0 Deg.)	76
Figure (18.b) Heave exciting force and phase for rectangular box (heading = 45 Deg.)	77
Figure (19.a) Pitch exciting force and phase for rectangular box (heading = 0 Deg.)	78
Figure (19.b) Pitch exciting force and phase for rectangular box (heading = 45 Deg.)	79
Figure (20.a) Drift force in x-component for rectangular box (heading = 0 Deg.)	80
Figure (20.b) Drift force in x-component for rectangular box (heading = 45 Deg.)	81
Figure (21) Drift force in x-component for rectangular box at various heading angles	82
Figure (22) Vertical Drift moment for rectangular box at various heading angles	83

NOMENCLATURE

A_j	Angular momentum
A_{jk}	Added-mass coefficients
A_{wp}	Area of water plane
B_{jk}	Damping coefficients
C_{jk}	Restoring coefficients
G	Green's function
F_j	Complex amplitude of wave exciting force
F_d	Steady drift force
$(F_j)_{ex}$	External force
g	Gravitational acceleration
I_{jk}	Moment of inertia
Im	Imaginary part of a complex function
$\sqrt{-1}$	
J_0	Bessel function of first kind of zero order
K_0	Modified Bessel function of second kind of zero order
k	Wave number
L_j	Linear momentum
M	Mass of the body
M_d	Steady drift moment
\vec{n}	Unit normal vector (into the fluid)
n_i	See equation (2.8); $i=1 \dots 6$
P	Fluid pressure
Q_j	Source densities; $j=1 \dots 7$
R	$= [(x-\xi)^2 + (y-\eta)^2 + (z-\zeta)^2]^{1/2}$
R'	$= [(x-\xi)^2 + (y-\eta)^2 + (z+2h+\zeta)^2]^{1/2}$
Re	Real part of a complex function
r	$= [(x-\xi)^2 + (y-\eta)^2]^{1/2}$

- ix -

\vec{r} Position vector of the body/surface

S_b Mean wetted body surface

$S_{b(t)}$ Instantaneous wetted body surface

S_∞ Vertical cylindrical surface of large radius

$T(\theta)$ See equation (5.20)

t Time variable

U_j Generalized rigid body velocity, ($j=1, \dots, 6$), see equation (2.2)

V Displaced volume of water

V_j Fluid velocity

V_r, V_θ, V_z Fluid velocity components in cylindrical co-ordinate system

$x, y, z = (x_1, x_2, x_3)$ Co-ordinate system as defined in figure (1).

Y_0 Bessel function of second kind of zero order

z_b z co-ordinate of center of buoyancy

z_c z co-ordinate of center of gravity

β Incident angle of waves system (measured from the positive x -axis to the direction of wave propagation).

ϕ Velocity potential

ϕ_j Complex velocity potential, $j = 1, \dots, 7$.

η_j Complex rigid body displacement (see figure 1)

η_j Rigid body displacement

λ Wave length

ν $(\omega^2/g) = k \tanh kh$

ξ $= (\xi, \eta, \zeta)$, position vector of a point

ρ Mass density of water

ρ_b Mass density of the floating body

$\tau(\theta)$ See equation (5.20)

ω Circular frequency of incident wave

c_s Wave amplitude of incident wave

Chapter 1

INTRODUCTION

When a floating body is exposed to an incident wave system, in addition to apparent oscillatory motions, the body has a tendency to drift away in the direction of the wave propagation and to change its orientation in the horizontal plane. This phenomenon is due to the reflection of the wave and the phase lag of the oscillatory motion with respect to the incident wave system.

The forces and moments exerted on the floating body by the surrounding fluid will include not only the conventional unsteady exciting components which give rise to the oscillatory motion in waves, but also higher order steady and unsteady forces due to various nonlinear effects. These higher order forces are generally too small to influence the first order oscillatory motions of the floating body, but nevertheless can be important in certain circumstances, particularly in considering the drifting force and drifting moment of the body in the horizontal plane. For example, the drifting velocity of the body will be governed by the drifting force while the stable heading angle of the floating body will be governed by the corresponding drifting moment. These forces and moments are therefore of importance in the design of mooring systems and bow thrusters.

Although the theory of motion was well established [15], [16], the

complete analysis of the drifting force acting on a ship with zero mean forward speed was not obtained until Maruo [21](1980), who clarified the relationship between drifting force and all aspects of wave interaction. Newman [23](1967), generalized the theory such that the vertical drifting moment was included.

In the past decade, due to the demands of larger floating offshore structures, e.g., floating drill platforms and storage tankers, the conventional methods in the motion calculation based on the strip theory [27], or the slender body approximation [22] are sometimes inadequate; therefore many computations turn to the three dimensional source distribution method. The basic contributions to the application of this technique are the papers of Lebreton and Cormault [19](1969) and Garrison and Seetharama Rao [7](1971).

Faltinsen and Michelsen [4](1974) used the same technique to calculate the motions of a rectangular box, and also the drifting force and moment based on Newman's "far field" approach.

The main purpose of the present work is to develop a computer program to calculate the oscillatory motion, drift force and moment. Special attention has been given in the design of the program to simplicity of input data for generating of required body shapes, and also some modified numerical schemes were incorporated, so that a certain amount of the computer cpu time could be saved. Although the theory and the method of calculation used are not new it is believed that the experience gained from this computation is helpful for future advanced studies.

Chapter 2

MATHEMATICAL MODEL

The mathematical model of the problem is derived from the dynamic equilibrium between forces and moments. A right hand cartesian coordinate system $(x, y, z) = (x_1, x_2, x_3)$, see figure (1), fixed with respect to the mean position of the body, is used with positive z vertically upwards through the center of gravity of the body and the origin in the plane of the undisturbed free surface.

We assume the flow field is in an ideal fluid and irrotational, so there exists a velocity potential Φ , which satisfies Laplace's equation in the whole domain of the fluid

$$\nabla^2 \Phi = 0 \quad (2.1)$$

Let U_i be the component of the generalized body velocity vector of the floating body. (U_1 = surge, U_2 = sway, U_3 = heave, U_4 = roll, U_5 = pitch, U_6 = yaw), and n_i be the generalized "unit" outward normal vector of the body surface, i.e.

$$U_i = \begin{cases} \vec{u}, & i=1,2,3 \\ \vec{\omega}, & i=4,5,6 \end{cases} \quad (2.2)$$

$$n_i = \begin{cases} \vec{n}, & i=1,2,3 \\ (\vec{r} \times \vec{n}), & i=4,5,6 \end{cases} \quad (2.3)$$

where \vec{u} is the linear velocity of the body, $\vec{\omega}$ is the angular velocity of the body, \vec{n} is the unit outward normal vector of the body surface, and \vec{r} is the position vector of the body surface.

Assuming that the motion of the body is small so that coupled higher order terms of the linear velocity and angular velocity can be neglected, then the linearized kinematic boundary condition on the body surface S_b can be obtained

$$\begin{aligned}\frac{\partial \phi}{\partial n} &= (\vec{U} + \vec{\Omega} \times \vec{r}) \cdot \vec{n} = \vec{U} \cdot \vec{n} + \vec{\Omega} \cdot (\vec{r} \times \vec{n}) \\ &= U_j n_j, \quad j=1\dots 6 \quad \text{on } S_b\end{aligned}\quad (2.4)$$

The kinematic boundary condition on the sea bed which is assumed to be flat reads

$$\frac{\partial \phi}{\partial n} = 0, \quad \text{on } z=-h \quad (2.5)$$

where h is the water depth.

If the atmospheric pressure is assumed to be constant above the free surface and the incident wave amplitude is small, then the combined linearized kinematic and dynamic boundary condition on the free surface is

$$\frac{\partial^2 \phi}{\partial z^2} + g \frac{\partial \phi}{\partial z} = 0, \quad \text{on } z=0 \quad (2.6)$$

From equations (2.1), (2.4), (2.5) and (2.6), it is noticed that ϕ can not be completely solved since U_j , in equation (2.4) is still not known. The relationship between ϕ and U_j can be found from the dynamic boundary condition of ϕ on the body surface. This condition is obtained by using Bernoulli's equation and Newton's law of motion.

$$\begin{aligned}\int_{S_b(t)} \left(\rho \frac{\partial \phi}{\partial t} + \frac{\rho}{2} \frac{\partial \phi}{\partial x_k} \frac{\partial \phi}{\partial x_k} + \rho g z \right) n_j ds + (F_{ex})_j \\ = M_{jk} \dot{U}_k, \quad j, k=1\dots 6\end{aligned}\quad (2.7)$$

Equation (2.7) is known as the equation of motion of the body. The first

term on the left-hand side of equation (2.7) represents the generalized forces due to the integration of pressure distribution over the instantaneous wetted surface $S_b(t)$ of the body. $(F_{ex})_j$ are the external generalized forces, which are assumed to be known, due to other sources. (for example, mooring cables or bow thrusters) the right hand side of (2.7), are the generalized inertia forces, where U_k is the acceleration of the body (the dot sign stands for the total time derivative), and M_{jk} is the generalized mass tensor of the body; If the body geometry is symmetric with respect to x-z plane, (i.e. x_1-x_3 plane), M_{jk} can be written in the matrix form:

$$M_{jk} = \begin{bmatrix} M & 0 & 0 & 0 & Mz_c & 0 \\ 0 & M & 0 & -Mz_c & 0 & 0 \\ 0 & 0 & M & 0 & 0 & 0 \\ 0 & -Mz_c & 0 & I_{44} & 0 & -I_{46} \\ Mz_c & 0 & 0 & 0 & I_{55} & 0 \\ 0 & 0 & 0 & -I_{64} & 0 & I_{66} \end{bmatrix} \quad (2.8)$$

where M is the mass of the body, z_c is the z-coordinate of the center of gravity. I_{jk} is the moment of inertia with respect to the coordinate system and is defined as:

$$I_{j+3,k+3} = \int_{V_b} \rho_b [x_i x_j \delta_{jk} - x_j x_k] dv \quad j, k, l = 1, 2, 3$$

where ρ_b is the density of the body. V_b is the volume of the body. δ_{ij} is the Kronecker delta.

At this stage, the formulation of the problem in equations (2.1)(2.4)(2.5)(2.6)(2.7), for the motion of a floating body is completed, and from these equations \dot{x}_i and U_i are to be solved.

Chapter 8

STEADY HARMONIC POTENTIAL

Since the general solution of the problem is rather complicated, only the steady harmonic solution and steady drift forces due to the harmonic incident waves are considered in the present work.

From equation (2.1), (2.7), (2.4), (2.5), (2.6), we notice that in equation (2.1) and equation (2.7), ϕ and U_j are related only through the kinematic body boundary condition equation (2.4), therefore, ϕ "might" firstly be solved, in terms of U_j , then substitute this ϕ into equation (2.7) and solve for U_j . This is the basic idea of the mathematical scheme.

Firstly it is assumed that the external force (F_{ex}) in equation (2.7) is such that it is just equal to the summation of all the second or higher order fluid forces acting on the body. Here the "higher order forces" means the forces due to the product terms of first order ϕ and/or its derivative. In this situation, the motion of the body would become purely harmonic with the same frequency as that of the incident wave, then equation (2.7) can be rewritten as (see [24]),

$$\int_{S_b} \rho \frac{\partial \phi}{\partial t} n_j ds - C_{jk} \eta_k^*(t) = M_{jk} \dot{U}_k = M_{jk} \frac{\partial^2}{\partial t^2} [\eta_k^*(t)] \quad j, k=1, \dots, 6 \quad (3.1)$$

where S_b is the time-independent mean wetted body surface, $\eta_k^*(t)$ are the time-dependent first order linear ($k=1, 2, 3$) and angular ($k=4, 5, 6$) rigid

body displacements of the floating body. C_{jk} are the restoring coefficients of the body. If the body is symmetric with respect to x-z plane, then C_{jk} can be written as

$$\begin{aligned} C_{33} &= \rho g A_{wp} & C_{35} = C_{53} = -\rho g \int \frac{x ds}{A_{wp}} \\ C_{44} &= \rho g V (z_b - z_c) + \rho g \int \frac{y^2 ds}{A_{wp}} \end{aligned} \quad (3.2)$$

$$C_{55} = \rho g V (z_b - z_c) + \rho g \int \frac{x^2 ds}{A_{wp}}$$

where A_{wp} is the water plane area, V is the displaced volume of fluid, z_b , z_c are the z-coordinates of the center of buoyancy and center of gravity of the body.

For equations (2.1), (3.1), (2.4), (2.5), (2.6), since we are looking for the harmonic solution only, it is more convenient to represent Φ , and η_j by the real part of a complex function. Let

$$\begin{aligned} \Phi(\vec{x}, t) &= \text{Re}[\phi(\vec{x})] e^{-i\omega t} \\ \eta_j(t) &= \text{Re}[\eta_j(t)] = \text{Re}[\bar{\eta}_j e^{-i\omega t}] \end{aligned} \quad (3.3)$$

where ω is the frequency of the incident wave. $\phi(\vec{x})$ and $\bar{\eta}_j$ are the corresponding time independent complex amplitudes of $\Phi(\vec{x}, t)$ and $\eta_j(t)$, and $i = \sqrt{-1}$.

Substituting these expressions into equation (2.1), (3.1), (2.4), (2.5), (2.6), it can be shown that it is sufficient to take $\phi(\vec{x})$ and $\eta_j(t)$ to be the solutions of the following problem in complex space:

$$\nabla^2 \phi = 0 \quad (3.4)$$

$$\frac{\partial \phi}{\partial n} = -i\omega \bar{\eta}_j n_j, \quad j=1, \dots, 6 \quad \text{on } S_b \quad (3.5)$$

$$-\omega^2 \phi + g \frac{\partial \phi}{\partial z} = 0, \quad \text{on } z=0 \quad (3.6)$$

$$\frac{\partial \phi}{\partial n} = 0, \quad \text{on } z=-h \quad (3.7)$$

$$\int_{S_b} \rho(-i\omega) \phi e^{-i\omega t} n_j ds = C_{jk} \eta_k(t) = M_{jk} \ddot{\eta}_k(t), \quad j, k=1, \dots, 6 \quad (3.8)$$

Using the principle of superposition for linear problems, $\phi(\vec{x})$ can be broken down into three parts, i.e. let

$$\phi = \phi_0 + \phi_7 + (-i\omega \bar{\eta}_j) \phi_j, \quad j=1, \dots, 6 \quad (3.9)$$

where ϕ_0 is chosen to be the incident wave potential, ϕ_7 is known as the scattering potential due to the restrained body, ϕ_j ($j=1, \dots, 6$) is known as the radiation potential due to the corresponding modes of body motions.

The incident wave potential can be obtained from small amplitude wave theory, namely

$$\phi_0 = \frac{g c_a}{\omega} \frac{\cosh kh}{\cosh kh} e^{i(kx \cos \beta + ky \sin \beta)} \quad (3.10)$$

where c_a is the incident wave amplitude, β is the incident angle of the incident wave, which is measured as the angle between the direction of the wave propagation and positive x -axis, k is the wave number which is related to the wave frequency by the dispersion relationship

$$\frac{\omega^2}{g} = k \tanh kh \quad (3.11)$$

Since ϕ_0 satisfies equation (3.4), (3.6), (3.7), one may take ϕ_j ($j=1, \dots, 7$), to be the solution of the following problem

$$\nabla^2 \phi_j = 0, \quad j=1 \dots 7 \quad (3.12)$$

$$\frac{\partial \phi_7}{\partial n} = -\frac{\partial \phi_0}{\partial n}, \quad \text{on } S_b \quad (3.13)$$

$$\frac{\partial \phi_j}{\partial n} = n_j, \quad j=1 \dots 6, \quad \text{on } S_b$$

$$-\omega^2 \phi_j + g \frac{\partial \phi_j}{\partial z} = 0, \quad j=1 \dots 7 \quad \text{on } z=0 \quad (3.14)$$

$$\frac{\partial \phi_j}{\partial n} = 0, \quad j=1 \dots 7 \quad \text{on } z=-h \quad (3.15)$$

and equation (3.8) becomes

$$\int_{S_b} \rho(-i\omega) \cdot (\phi_0 + \phi_7) e^{-kz} n_j ds + \int_{S_b} \rho(-i\omega) \cdot (-i\omega \bar{n}_k \phi_k) e^{-kz} n_j ds = C_{jk} \eta_k(t) \\ - M_{jk} \ddot{\eta}_k(t), \quad j, k=1 \dots 6 \quad (3.16)$$

If one defines

$$F_j = (-i\omega) \cdot \rho \int_{S_b} (\phi_0 + \phi_7) n_j ds \quad (3.17)$$

$$A_{jk} = -\rho \operatorname{Re} \left[\int_{S_b} \phi_j n_k ds \right] \quad (3.18)$$

$$B_{jk} = -\rho \omega \operatorname{Im} \left[\int_{S_b} \phi_j n_k ds \right] \quad (3.19)$$

where Im denotes the imaginary part, then equation (3.16), after some rearrangements, can be written in a more standard form as a 2nd order ordinary differential equation:

$$(M_{jk} + A_{jk}) \ddot{\eta}_k(t) + B_{jk} \dot{\eta}_k(t) + C_{jk} \eta_k(t) = F_j \cdot e^{-kz} \quad j, k=1 \dots 6 \quad (3.20)$$

From the boundary condition of equation (3.13), the physical meaning of ϕ_j ($j=1 \dots 7$) is obvious. Generally, $(\phi_0 + \phi_7)$ is known as the solution of the wave diffraction problem. It is the potential due to the

incident wave and the interaction with the restrained body. On the other hand, ϕ_j ($j=1 \dots 6$), are known as the solutions of the radiation problem. They are the potentials due to the forced body motions of the corresponding modes in still water.

In equation (3.20), A_{jk} and B_{jk} are tensor quantities, called the Added Mass and the Damping coefficients of the body. It can be shown that they are symmetric in j, k . Also since equation (3.14) is frequency dependent, hence the values of A_{jk} and B_{jk} are also dependent on the frequency. F_j is the complex amplitude of what is generally known as the wave exciting force. By using Haskind's relation [24], it can be shown that the wave exciting force, F_j , can be expressed in term of ϕ_0 and ϕ_j ($j=1 \dots 6$), so that the solution of ϕ_7 is not necessary. However this relationship is of little help in the present computation work, since the labor of calculating ϕ_7 is minor. On the other hand, it is troublesome to use the Haskind's relations when one wishes to calculate the wave exciting force acting on a fixed body. Therefore this relationship is not made use of in this computation.

At this stage, the original problem of solving $\Phi(\vec{x}, t)$, and $U_j(t)$ in chapter 1 is now transformed, by equation (3.3), (3.9) to a problem of finding the solution of the boundary-value problem for $\phi_j(\vec{x})$ ($j=1 \dots 7$), and the steady solution of the initial-value problem for $n_j(t)$ ($j=1 \dots 6$).

Nevertheless, the solution of the boundary-value problem is not unique. It can be seen that since any arbitrary constant times the diffraction potential $(\phi_0 + \phi_7)$ can be added to any one of the potentials ϕ_j ($j=1 \dots 7$), without violating the boundary conditions equation (3.13), a

so called radiation condition at infinity is added to ensure uniqueness. the general form of this condition is :

$$\phi_j = \frac{\cosh k(z+h)}{\cosh kh} r^{-1/2} e^{ikr} \text{ as } r \rightarrow \infty \quad (3.21)$$

where $r = \sqrt{x^2 + y^2}$

and the constant of proportionality in equation (3.21) may depend on θ , where $\theta = \tan^{-1}(y/x)$, but not on r and z . The choice of equation (3.21) is more or less based on "intuition". It restricted the class of ϕ_j ($j=1\dots 7$) to those having the property that the waves associated with them are always propagating outward (i.e. in the direction of increasing r) at infinity.

In the next chapter, the method of solving ϕ_j ($j=1\dots 7$) subject to equations (3.12)-(3.15), and (3.21), by using the integral-equation technique is discussed. after that, the calculation of the steady solution of $\eta_j(t)$ governed by equation (3.20) is straightforward. The calculation of the steady drifting force and moment will be discussed later on.

Chapter 4

SOLUTION OF $\phi_i(\vec{x})$ BY USING GREEN'S FUNCTION METHOD AND STEADY MOTION $\eta_j(t)$

The treatment of the boundary-value problem stated in the previous chapter by the integral-equation method is classical. The use of singularity distributions to solve problems of Neumann and Dirichlet type are well known from texts such as Kellogg [17](1929). These formulations lead to Fredholm integral-equations of the second type, for which a rather complete mathematical theory of existence and uniqueness has been developed.

Lamb [18] has shown through the application of Green's theorem that, for the infinite fluid case, the velocity potential associated with the flow about a body can be described by either a simple source or doublet distribution over the body surface. Very little progress was made towards solving them, except for those few cases of special geometry. With the advent of the hight speed computer and the discretization techniques developed by Hess & Smith [11](1964), calculation of flow about arbitrary shaped bodies in an infinite fluid became possible. These techniques have been extended to the case of fluid of finite depth with free surface by many authors, such as Lebreton & Margnac [19](1968), Garrison & Rao [7](1971), Faltinsen & Michelsen [4](1976).

4.1 Integral-Equation Formulation

Let us consider a function of \vec{x} , $G(\vec{x}, \vec{z})$, that satisfies the following conditions

$$\nabla^2 G(\vec{x}, \vec{z}) = \delta(\vec{x} - \vec{z}), \quad -h < z < 0 \text{ and } -h < \zeta < 0 \quad (4.1)$$

$$-\omega^2 G + g \frac{\partial G}{\partial z} = 0, \quad \text{on } z=0 \quad (4.2)$$

$$\frac{\partial G}{\partial n} = 0, \quad \text{on } z=-h \quad (4.3)$$

$$G \sim \frac{\cosh k(z+h)}{\cosh kh} r^{-1/2} e^{ikr}, \quad \text{as } r \rightarrow \infty \quad (4.4)$$

where the right hand side of equation (4.1) is the Dirac delta function which can be defined (in a generalized sense) by the functional

$$\int_D h(\vec{x}) \cdot \delta(\vec{x} - \vec{z}) dV(\vec{x}) = h(\vec{z}), \quad \text{for } \vec{z} \text{ in } D \quad (4.5)$$

where $h(\vec{x})$ is any testing function within some prescribed class.

Applying Green's theorem to $G(\vec{x}, \vec{z})$, and ϕ_j in the region bounded by S_b , $z=0$, and $z=-h$. It can be shown that ϕ_j may be represented as

$$\phi_j(\vec{x}) = \int_{S_b} Q_j(\vec{z}) \cdot G(\vec{x}, \vec{z}) ds \quad (4.6)$$

where Q_j is known as the source density function which is to be determined, the kernel function $G(\vec{x}, \vec{z})$ is known as the Green's function of the problem for ϕ_j . Such a function can be written in two general forms, according to Wehausen & Laitone [28], they are the "integral form":

$$\begin{aligned}
 G(\vec{x}, \vec{z}) = & \frac{1}{R} + \frac{1}{R'} \\
 & + 2PV \int_0^\infty (\mu + \nu) e^{-\mu h} \frac{\cosh[\mu(z+h)] \cdot \cosh[\mu(z+h)]}{\mu \sinh(\mu h) - \nu \cosh(\mu h)} \cdot J_0(\mu r') d\mu \\
 & + i \frac{2\pi(k^2 - \nu^2)}{k^2 h - \nu^2 h + \nu} \cdot \cosh[k(z+h)] \cdot \cosh[k(z+h)] - J_0(\mu r') \quad (4.7)
 \end{aligned}$$

and the "series form":

$$\begin{aligned}
 G(\vec{x}, \vec{z}) = & \frac{2\pi(\nu^2 - k^2)}{k^2 h - \nu^2 h + \nu} \cdot \cosh[k(z+h)] \cdot \cosh[k(z+h)] - [Y_0(kr') - iJ_0(kr')] \\
 & + 4 \sum_{j=1}^{\infty} \frac{(\mu_j^2 + \nu^2)}{\mu_j^2 h - \nu^2 h + \nu} \cdot \cos[\mu_j(z+h)] \cdot \cos[\mu_j(z+h)] \cdot K_0(\mu_j r') \quad (4.8)
 \end{aligned}$$

where

$$\nu = \frac{\omega^2}{g} = k \tanh kh \quad (4.9)$$

$$R = [(x-\xi)^2 + (y-\eta)^2 + (z-\zeta)^2]^{1/2} \quad (4.10)$$

$$R' = [(x-\xi)^2 + (y-\eta)^2 + (z+2h+\zeta)^2]^{1/2} \quad (4.11)$$

$$r' = [(x-\xi)^2 + (y-\eta)^2]^{1/2} \quad (4.12)$$

J_0 and Y_0 denote, respectively, the Bessel function of the first kind and the second kind of order zero, and K_0 denotes the modified Bessel function of the second kind of order zero. PV in equation (4.7) indicates the principal value of the integral: μ_j in equation (4.8) are the real positive roots of the equation:

$$\mu_j \tan(\mu_j h) + \nu = 0 \quad (4.13)$$

Since equation (4.6) is also valid for \vec{x} as a point on the body boundary, taking the normal directional derivative of ϕ in equation (4.6) and applying the boundary condition equation (3.13) yields the following integral equation for Q_j :

$$\int_{S_b} Q_j(\xi) \frac{\partial G}{\partial n}(\vec{x}, \xi) d\xi = -\frac{\partial \phi_0}{\partial n} \quad j=1 \dots 6. \quad (4.14)$$

The solution to the boundary value problem stated in chapter 3 now rests on the determination of the source density function Q_j , which is governed by equation (4.14). If this Q_j can be obtained, then the potential ϕ_j can be calculated directly from equation (4.6).

From equation (4.14) it can be seen that a distinct advantage of the integral equation formulation over the space-discretization formulation, such as the finite-difference or finite element method, is that the space dimension of the problem is reduced by one. In the present work, the integral-equation treatment seems particularly suitable since physical quantities of primary interest, such as wave height and fluid pressure, are required only on the body boundary. Space-discretization techniques would appear inefficient and wasteful since they yield massive amounts of interior data that are normally of minor use [29].

4.2 Numerical Solution

The integral-equation (4.14) may be solved numerically beginning with the partitioning of the body surface into N panels of area ΔS_k ($k=1 \dots N$). Since the source density function Q_j ($j=1 \dots 7$) in equations (4.6) and (4.14) is a continuous, well-behaved function, then if the source density is assumed to be uniformly distributed on each panel, these integrals may be approximated by summations, therefore, equation (4.14) becomes

$$a_{pq}(Q_j)_q = \left\{ \frac{\partial \phi_0}{\partial n} \right\}_p \quad p=1 \dots 6 \quad p,q=1 \dots N \quad (4.15)$$

where

$$\alpha_{pq} = \int_{\Delta S_q} \frac{\partial G}{\partial n} (\vec{x}_p, \vec{z}) ds, \quad p, q = 1-N \quad (4.16)$$

here α_{pq} has the physical meaning that it is the influence at the p^{th} control point (within the p^{th} panel) due to the unit density source distribution on the q^{th} panel. $(Q_j)_q$ is the source density of the j^{th} ($j=1\dots 7$) "mode" potential on the q^{th} panel.

Similarly, equation (4.6) can be approximated as:

$$(\phi_j)_p = \beta_{pq} \cdot (Q_j)_q, \quad j = 1\dots 7, \quad p, q = 1, N \quad (4.17)$$

where

$$\beta_{pq} = \int_{\Delta S_q} G(\vec{x}_p, \vec{z}) ds \quad (4.18)$$

From equations (4.15)–(4.18), it is noticed that once α_{pq} and β_{pq} are calculated from equations (4.16)–(4.18), then finding $(Q_j)_q$ is reduced to a problem of solving sets of N simultaneous linear algebraic equations of equation (4.15); after that $(\phi_j)_p$ can be calculated straightforwardly from equation (4.17).

There are certain difficulties in the actual computation of α_{pq} and β_{pq} . The numerical schemes will be discussed in chapter 6.

4.3 Solution of The Steady State Body Motion $\eta_j(t)$

Once $(Q_j)_p$ ($j=1\dots 7$) has been calculated by the surface discretization technique mentioned earlier, the coefficients A_{jk} , B_{jk} , F_j , defined by equations (3.17)–(3.19) can be computed in the same way

$$F_j = (-i\omega) \cdot p \sum_{q=1}^N (\phi_0 + \phi_7)_q (n_j)_q \Delta S_q, \quad j = 1\dots 6 \quad (4.19)$$

$$A_k = -\rho \operatorname{Re} \left[\sum_{q=1}^N (\Phi)_q (n_k)_q \Delta S_q \right], \quad 1, k = 1, \dots, 6 \quad (4.20)$$

$$B_k = -\rho \omega \operatorname{Im} \left[\sum_{q=1}^N (\Phi)_q (n_k)_q \Delta S_q \right], \quad 1, k = 1, \dots, 6 \quad (4.21)$$

Substituting the $n_j(t) = \bar{n}_j e^{-kot}$ into equation (3.20), it becomes

$$([-\omega^2(A_k + M_k) + C_k] + i[-\omega B_k]) \bar{n}_k = F_j, \quad 1, k = 1, \dots, 6 \quad (4.22)$$

the complex amplitude of the body motion \bar{n}_k can be obtained by solving this set of equations.

The solution of Φ_j and $n_j(t)$ by using the integral-equation formulation and surface discretization technique is now completed.

Chapter 5

STEADY DRIFT FORCES AND MOMENTS

5.1 General description

In the first paragraph of chapter 1, it has been mentioned that when a floating body is exposed to an incident wave system, it has a tendency to drift away in the direction of wave propagation and to change its orientation in the horizontal plane, and yet in chapter 3, the steady state body motion, which is obviously without drift phenomenon was computed. An explanation of this apparent inconsistency is necessary.

In equation (2.7), the exact equation of motion (which may be regarded as the dynamic body surface boundary condition of Φ). It has been assumed that the "external" force (F_{ex})₁ is just equal to the summation of all second or higher order fluid forces acting on the body, so that equation (3.1) was obtained. Therefore, the steady component of (F_{ex})₁ is the force required to maintain the body's mean position unchanged while the body undergoes an oscillatory motion. Here, therefore, the steady drift forces (and moments) mean the forces equal to the steady components of (F_{ex})₁, but with opposite sign. In other words, it is the constant part of all higher order fluid forces acting on the body while it undergoes an oscillatory motion without drifting.

When a freely floating body or fixed object is exposed to regular

Incident waves, the second order force contains a constant part and a part which oscillates with twice the frequency of the incident wave. In the present work, only the constant part i.e., the steady component is considered. Gerritsma [8] (1971) has shown experimentally that this constant force is proportional to the square of the wave height as the theory predicted. However according to the tests done by Clauss, Sukan, and Schellin [3] (1982), these drift forces are not proportional to the wave amplitude squared but they are proportional to some power greater than two particularly for waves with periods in the vicinity of the natural pitch period.

Another interesting question is, how large is the difference between this wave drift force (without drifting motion) compared to that while the floating body undergoes drifting motion? Since these higher order forces are generally too small to influence the first order motion, one might expect that the difference is usually small provided that the drifting velocity, which also depends on the viscous drag force, is small. Also it is worth mentioning here that in head seas the "small" higher order forces are not the sum of small contributions with the same sign but rather the difference between large contributions from the fore and aft body each of which may be considerably larger than the total [28].

5.2 Formulation of steady horizontal drift forces and vertical drift moment

The steady horizontal drift forces and vertical moment can be expressed as

$$(F_d)_j = \left\langle \int_{S_b(l)} P n_j ds \right\rangle \quad j=1,2 \quad (5.1)$$

$$(M_d)_z = \langle \int_{S_b(t)} P (\vec{r} \times \vec{n})_z ds \rangle \quad (5.2)$$

where the $\langle \rangle$ sign denotes the time average over one period. $(F_d)_i$ ($i = 1, 2$) denotes the drift force in x and y directions. $(M_d)_z$ is the drift moment about the z -axis. P is the hydrodynamic pressure. \vec{r} is the position vector of the time-dependent wetted surface. $\vec{n} = (n_1, n_2, n_3)$ denotes the unit normal vector of $S_b(t)$. For the sake of convenience, here, we take \vec{n} to be positive when it points into the body, i.e. outward from the fluid domain.

When equations (5.1) (5.2) are used to calculate the drift forces and moment (this is generally known as the "near field" approach), the second order effect due to the instantaneous wetted surface $S_b(t)$ must be taken into account. That makes this approach more complicated [3][26]. Newman related these expressions, by using the principle of conservation of momentum, to the so called "far field" expression, from which these forces and moments can be evaluated on some cylindrical control surface, thus avoiding the necessity to determine some second-order disturbances in the near field.

Let us consider the control volume, D , of the fluid domain, which is bounded by the body surface $S_b(t)$, the free surface S_f , the sea bed S_h and a chosen fixed control surface at infinity S_∞ . The time rate of change of linear momentum of fluid in D is

$$\begin{aligned} \frac{dL}{dt} &= \frac{d}{dt} \int_D \rho V_i dv \\ &= \rho \int_D \frac{\partial V_i}{\partial t} dv + \rho \int_S V_i U_k n_k ds \quad i, k = 1, 2, 3 \end{aligned} \quad (5.3)$$

where $S = S_b(1) + S_\infty + S_f + S_h$. L_j ($j=1,2,3$) is the linear momentum in x,y,z directions. V_j is the fluid velocity vector. U_k is the velocity vector of the corresponding surface. n_k is the "outward" (from D) unit normal vector of S.

By using Eulers's equation of motion for fluid particles, i.e.

$$\frac{\partial V_j}{\partial t} + V_k \frac{\partial V_j}{\partial x_k} = - \frac{\partial}{\partial x_j} [P/\rho + g x_3] \quad j,k=1,2,3 \quad (5.4)$$

substitute equation (5.4) into (5.3) to eliminate $\frac{\partial V_j}{\partial t}$ and notice that $\frac{\partial V_k}{\partial x_k} = 0$, $k=1,2,3$, one obtains

$$\begin{aligned} \frac{dL_j}{dt} &= -\rho \int_D \left(\frac{\partial}{\partial x_j} (P/\rho + g x_3) + \frac{\partial}{\partial x_k} (V_j V_k) \right) dv + \rho \int_S V_j U_k n_k ds \\ &= - \int_S (P/\rho + g x_3) n_j ds - \rho \int_S V_j (V_k n_k - U_k n_k) ds \\ &= -\rho \int_S ((P/\rho + g x_3) n_j + V_j (V_n - U_n)) ds \quad j,k=1,2,3 \end{aligned} \quad (5.5)$$

where V_n is the normal velocity component of fluid particles on S, U_n is the normal velocity component of the surface S.

Since the hydrostatic term $\int_S g x_3 n_j ds = \int_D \delta_{jj} dv$, (δ_{ij} is the Kroenecker delta), has no contribution in x and y directions, then, if only drift forces in the horizontal plane are considered, equation (5.5) can be rewritten as:

$$\frac{dL_1}{dt} = - \int_S (P n_1 + \rho V_1 (V_n - U_n)) ds \quad j=1,2 \quad (5.6)$$

Applying the corresponding boundary condition on S, i.e.

$$P = 0, \quad V_n = U_n, \quad \text{on } S_f$$

$$\vec{n} = (0, 0, n_3), \quad V_n = U_n = 0, \quad \text{on } S_h$$

$$V_n = U_n, \quad \text{on } S_b(t)$$

$$U_n = 0, \quad \text{on } S_\infty$$

to equation (5.6), it becomes:

$$\int_{S_b(t)} P n_j ds = - \int_{S_\infty} (P n_j + \rho V_j V_n) ds - \frac{dL}{dt} \quad /=1.2 \quad (5.8)$$

Since there should be no net increase of linear momentum in D over one period of harmonic motion, taking the time average of equation (5.8) over one period, one then obtains the far field expression for drift forces in the horizontal plane:

$$\langle \int_{S_b(t)} P n_j ds \rangle = - \langle \int_{S_\infty} (P n_j + \rho V_j V_n) ds \rangle \quad /=1.2 \quad (5.9)$$

The merit of the far field expression is evident, since the shape of the fixed control surface S_∞ can be chosen as desired. When this surface is chosen to be a vertical cylindrical surface of large radius r extending from the free surface down to $z = -h$, cylindrical polar coordinate (r, θ, z) are used with $x = r \cos \theta$, $y = r \sin \theta$; V_r and V_θ are the radial and tangential velocity components; the drift forces can then be expressed as:

$$(F_d)_x = - \langle \int_{S_\infty} [P \cos \theta + \rho V_r (V_r \cos \theta - V_\theta \sin \theta)] r d\theta dz \rangle \quad (5.10)$$

$$(F_d)_y = - \langle \int_{S_\infty} [P \sin \theta + \rho V_r (V_r \sin \theta + V_\theta \cos \theta)] r d\theta dz \rangle$$

The far-field expression for the vertical drift moment can be obtained in a similar way. Let A_i ($i=1, 2, 3$) be the angular momentum of fluid

particles in D, then the time rate of change of this angular momentum in D is:

$$\begin{aligned}\frac{dA_i}{dt} &= \rho \frac{d}{dt} \int_D (\vec{r} \times \vec{v}) dv \\ &= \rho \int_D \epsilon_{ijk} x_j \frac{\partial v_k}{\partial t} dv + \rho \int_S \epsilon_{ijk} x_j v_k U_n ds \quad i, j, k = 1, \dots, 3 \quad (5.11)\end{aligned}$$

where ϵ_{ijk} is the permutation symbol. Again using Euler's equation of motion and continuity equation in equation (5.11), it becomes:

$$\begin{aligned}\frac{dA_i}{dt} &= -\rho \int_D \epsilon_{ijk} x_j \left[\frac{\partial}{\partial x_k} (P/\rho + g x_3) + \frac{\partial}{\partial x_p} (V_p V_k) \right] dv + \rho \int_S \epsilon_{ijk} x_j V_k U_p n_p ds \\ &= -\rho \int_D \frac{\partial}{\partial x_k} [\epsilon_{ijk} x_j (P/\rho + g x_3)] dv \\ &\quad - \rho \int_D \frac{\partial}{\partial x_p} [\epsilon_{ijk} x_j V_k V_p] dv \\ &\quad + \rho \int_D \epsilon_{ijk} V_k V_p \frac{\partial x_j}{\partial x_p} dv \\ &\quad + \int_S \epsilon_{ijk} x_j V_k U_n ds \quad i, j, k, p = 1, 2, 3 \quad (5.12)\end{aligned}$$

for the first term on the right hand side of equation (5.12), we have used the fact that $\frac{\partial}{\partial x_k} [\epsilon_{ijk} x_j] = \epsilon_{ijk} \frac{\partial x_j}{\partial x_k} = \epsilon_{ijk} \delta_{jk} = 0$.

By using the divergence theorem, equation (5.12) can be written as:

$$\begin{aligned}
 \frac{dA_i}{dt} = & -\rho \int_S \epsilon_{ijk} x_j [P/\rho + g x_3] n_k ds \\
 & - \rho \int_S \epsilon_{ijk} x_j V_k V_r n_r ds \\
 & + \rho \int_D \epsilon_{ijk} V_j V_k dv \\
 & + \rho \int_S \epsilon_{ijk} x_j V_k U_n ds \quad i, j, k, r = 1, 2, 3
 \end{aligned} \tag{5.13}$$

Since $\epsilon_{ijk} V_j V_k = 0$, the third term on the right hand side of equation (5.13) vanishes, then equation (5.13) becomes:

$$\begin{aligned}
 \frac{dA_i}{dt} = & -\rho \int_S \epsilon_{ijk} x_j [P/\rho + g x_3] n_k ds \\
 & - \rho \int_S \epsilon_{ijk} x_j V_k (V_n - U_n) ds \quad i, j, k = 1, 2, 3
 \end{aligned} \tag{5.14}$$

If only the vertical angular momentum, i.e. A_3 , is considered in equation (5.14), since the integral $\int_S \epsilon_{ijk} x_j x_3 n_k ds = \int_D \epsilon_{ijk} (x_3 \delta_{jk} + x_j \delta_{ik}) dv$
 $= \int_D \epsilon_{ijk} x_j dv$ has no contribution for $i=3$, one obtains:

$$\begin{aligned}
 \frac{dA_i}{dt} = & - \int_S P \epsilon_{ijk} x_j n_k ds \\
 & - \rho \int_S \epsilon_{ijk} x_j V_k (V_n - U_n) ds, \quad i=3; \quad i, k = 1, 2, 3
 \end{aligned} \tag{5.15}$$

Employing the relationship $\epsilon_{3jk} x_j n_k = 0$ on the cylindrical surface S_∞ and substituting the boundary conditions of equation (5.7) for S , one has:

$$\int_{S_b(t)} P \epsilon_{ijk} x_j n_k ds = - \rho \int_{S_\infty} \epsilon_{ijk} x_j V_k V_n ds - \frac{dA_i}{dt} \quad i=3; \quad i, k = 1, 2, 3 \tag{5.16}$$

Again taking time averages in equation (5.16) over one period of time, the last term vanishes, then one obtains the following vector form:

$$\left\langle \int_{S_b(t)} P(\vec{r} \times \vec{n})_z ds \right\rangle = -\rho \left\langle \int_{S_\infty} V_n(\vec{x} \times \vec{v})_z ds \right\rangle \quad (5.17)$$

Using cylindrical coordinates on the right hand side of equation (5.17), one has the far-field expression for steady vertical moment:

$$(M_d)_z = -\rho \left\langle \int_{S_\infty} V_r V_\theta r^2 d\theta dz \right\rangle \quad (5.18)$$

Using the expressions of equation (3.9) (3.10) (4.6) and the asymptotic expansion of the Green's function (4.7), the far field expression for the first order potential is:

$$\begin{aligned} \phi \sim & \frac{\alpha c_s}{\omega} \frac{\cosh k(z+h)}{\cosh kh} \cdot e^{i(kx \cos \beta + ky \sin \beta - \omega t)} \\ & + T(\theta) e^{iT(\theta)} \cosh [k(z+h)] \cdot \sqrt{1/r} \cdot e^{i(kr - \omega t)} \end{aligned} \quad (5.19)$$

where $T(\theta)$ and $\tau(\theta)$ are real functions of θ , and $T(\theta) \cdot e^{iT(\theta)}$ is given by:

$$\begin{aligned} T(\theta) \cdot e^{iT(\theta)} = & \frac{2\pi(v^2 - k^2)}{k^2 h - v^2 h + v} \sqrt{27(\pi k)} \cdot e^{-i3\pi/4} \\ & \cdot \int_{S_b} (Q(\xi) \cosh [k(\xi + h)]) \cdot e^{-i(k\xi \cos \theta + k\eta \sin \theta)} ds \end{aligned} \quad (5.20)$$

where $Q(\xi)$ is the "total source" density:

$$Q(\xi) = Q_7 + (-i\omega \bar{\eta}_j) Q_j \quad j=1 \dots 6 \quad (5.21)$$

It can be shown [20] that the error associated with the approximate far field potential in equation (5.19) is small when r is large. It is of order $r^{-1.5}$.

Substitute relations:

$$V_r = \operatorname{Re} \left[\frac{\partial \phi}{\partial r} e^{-i\omega t} \right] \quad (5.22)$$

$$V_\theta = \operatorname{Re} \left[\frac{1}{r} \frac{\partial \phi}{\partial \theta} e^{-i\omega t} \right]$$

and equation (5.19) into equations (5.10) and (5.18). If only contributions up to second order terms of ϕ are retained, then equations (5.10), (5.18) can be written in terms of the first order far field potential:

$$(F_d)_x = -\frac{\rho}{2} \frac{\omega C_a}{\sinh kh} \sqrt{2\pi/k} \left(\frac{1}{4} \sinh 2kh + \frac{kh}{2} \right) \cdot 2T(\beta) \cdot \cos[\tau(\beta) + \pi/4] \cdot \cos \beta - \frac{\rho k}{2} \left(\frac{1}{4} \sinh 2kh + \frac{kh}{2} \right) \cdot \int_0^{2\pi} T^2(\theta) \cdot \cos \theta d\theta \quad (5.23)$$

$$(F_d)_y = -\frac{\rho}{2} \frac{\omega C_a}{\sinh kh} \sqrt{2\pi/k} \left(\frac{1}{4} \sinh 2kh + \frac{kh}{2} \right) \cdot 2T(\beta) \cdot \cos[\tau(\beta) + \pi/4] \cdot \sin \beta - \frac{\rho k}{2} \left(\frac{1}{4} \sinh 2kh + \frac{kh}{2} \right) \cdot \int_0^{2\pi} T^2(\theta) \cdot \sin \theta d\theta \quad (5.24)$$

$$(M_d)_z = \left(\frac{\sinh 2kh}{4k} + \frac{h}{2} \right) \cdot \left(-\frac{\rho \omega C_a}{\sinh kh} \cdot \sqrt{2\pi/k} \cdot T'(\beta) \cdot \sin [\tau(\beta) + \pi/4] - \frac{\rho \omega C_a}{\sinh kh} \cdot \sqrt{2\pi/k} \cdot T'(\beta) \cdot T(\beta) \cdot \cos [\tau(\beta) + \pi/4] \right) - \frac{\rho k}{2} \cdot \int_0^{2\pi} T^2(\theta) \cdot T'(\theta) d\theta \quad (5.25)$$

where $T'(\beta)$, ($T'(\beta)$) is interpreted as $\frac{dT}{d\theta}$ ($\frac{dT}{d\theta}$) evaluated at $\theta=\beta$.

The working formulas (5.23)-(5.25) enable us to evaluate the horizontal drift forces and vertical moment. The detail of the derivation is rather complicated and lengthy. It can be found in [4], and hence is omitted here. Only a brief outline is given as below:

1. In equation (5.19), the first term on the right hand side is the potential due to the incident wave system (i.e. ϕ_0), the second term is

the potential due to the presence of the body (i.e. $\phi_j + \phi_b$, $j=1\dots 6$). This equation can be written as $\phi \sim \phi_0 + \phi_b$. Substitute this representation, by using the relationship of equation (5.22), into equation (5.10) and equation (5.18). The result will involve terms which are quadratic in ϕ_0 and ϕ_b separately, plus terms involving products of ϕ_0 and ϕ_b . The contribution from ϕ_0 alone must vanish since there can be no force or moment associated with the undisturbed incident wave system. Thus only the cross product terms and terms which are quadratic in ϕ_b need to be considered.

2. The integrals in equation (5.10) and (5.18) involving r can be evaluated by the method of stationary phase, after taking the limit $r \rightarrow \infty$, one arrives at the expression in which no r is involved.

3. If one set all $\bar{\eta}_j$, $j=1\dots 6$ to be zero, i.e. taking $Q(\vec{z}) = Q_7$, in equation (5.21), then equations (5.23)-(5.25) give the drift forces and moments of a fixed object.

4. The "Kochlin's function" $T(\theta) e^{i\tau(\theta)}$, defined by equation (5.20) can be calculated numerically by the same surface discretization technique without difficulty, since $Q(\vec{z})$ is well behaved over S_b .

Chapter 6

NUMERICAL PROGRAMMING SCHEMES

A computer program has been set up to calculate the motions, horizontal drift forces and vertical moment. In order to reduce computer cpu time, this program is especially designed for ocean structures with at least one plane (say x-z plane) of symmetry. Generally, this restriction is satisfied in most ocean engineering applications. Numerical schemes used in this program are discussed in the following section:

6.1 Body surface panel

It has been mentioned in section 4.2 that the integral-equation (4.14) may be solved numerically beginning with the partitioning of the body surface into N panels. As far as the surface panel is concerned, it should be emphasized that the shape of the panel is not important. The important thing is that the panel should have the area ΔS_k , the control point, and the normal vector of each panel as close to the real body surface as possible. It is worth quoting Hess and Smith[1] "It should be kept in mind that the elements are simply devices for obtaining the surface source distribution and that the polyhedral-type body has no direct physical significance, in the sense that the flow eventually calculated is not the flow about the polyhedral-type body. Even if the edges of adjacent elements are coincident, the normal velocity is zero at only one point (the control point) of each element, over the remainder of the element

there is flow through it". Further more, Garrison [5] has shown that when a curved surface is approximated by plane elements, an error of the order of the surface curvature may be expected to result. These concepts are important when one uses the surface discretization technique; It indicates that the body boundary conditions are guaranteed to be satisfied only at a certain control point in each panel. Also since there is "initial error" due to the curvature of the surface, certain "more accurate" computations used by most authors are theoretically and practically not necessary (see section 6.3).

In this program, the triangular panel, is used for a simply connected smooth body surface. (for example a ship). These triangular shaped panels are generated systematically from the given "ship-offsets", and the centroid of each panel is taken as the control point. The reason for using the triangular shaped panel is that its normal vector, centroid and area can be determined uniquely by three adjacent offset points.

6.2 Evaluation of the Green's function and its derivative

1. Comparing the Integral and Series form for the Green's function: equations (4.7) and (4.8), generally speaking, the series form has better convergence properties than that of the integral form, since the modified Bessel's function K_0 decays much faster than J_0 , except when r' is small, where K_0 and also Y_0 are not well-behaved numerically.

The number of terms needed in equation (4.8) depends on the rate of decay of $K_0(\mu_j r')$. When $\mu_j r'$ is large

$$K_0(\mu_j r') \sim \frac{1}{\sqrt{\pi/(2\mu_j r')}} e^{-\mu_j r'}$$

and the j^{th} positive root of equation (4.19), μ_j , lies in the range

$$(1 - 1/2) \pi < \mu_1 h < 1/\pi$$

or

$$(1 - 1/2) \pi r'/h < \mu_1 r' < 1/\pi r'/h$$

Usually, one may terminate the series around $\mu_1 r' = 5$. In the present work, we terminate the series at $\mu_1 r' = 10$, since the derivative of G has the form of $K_1(\mu_1 r')$, which converges slower than $K_0(\mu_1 r')$, hence the number of terms needed in equation (4.8) is determined by:

$$J_{\max} = 2 + 10 \cdot h / (\pi r') \quad (6.1)$$

In the program a maximum of $J_{\max} = 1000$ is allowed. The integral form is used whenever $J_{\max} > 1000$. The positive roots of equation (4.13) are calculated by using the Half-Range method.

2 Whenever the integral form of G is used, notice that the integral in equation (4.7) decays as $e^{\mu(z+\zeta)}$ when μ is large, hence, in the program, this integration is terminated at

$$\mu_{\max} = -10 / (z + \zeta) \quad (6.2)$$

The most troublesome thing in the integral form is the evaluation of the principal value of the integral, since the integrand becomes singular at $\mu = k$. This principal value can be evaluated by the following scheme. Let

$$F(\mu) = 2(\mu + v) e^{-\mu h} \frac{\cosh[\mu(z+h)] \cdot \cosh[\mu(z+h)]}{\mu \sinh(\mu h) - v \cosh(\mu h)} \cdot J_0(\mu r') \quad (6.3)$$

then the third term on the right-hand side of equation (4.7) can be written as:

$$\begin{aligned}
 PV \int_0^\infty F(\mu) d\mu &= PV \int_0^{2k} F(\mu) d\mu + PV \int_{2k}^\infty F(\mu) d\mu \\
 &= PV \int_{-k}^{+k} F(\mu+k) d\mu + \int_{2k}^\infty F(\mu) d\mu
 \end{aligned} \tag{6.4}$$

In equation (6.4), the singularity has been shifted to the point $\mu = 0$. If the integrand of the first integral on the right-hand side of equation (6.4) is decomposed into an even function and an odd function of μ , i.e.

let

$$F(\mu+k) = F_e(\mu) + F_o(\mu) \tag{6.5}$$

where

$$\begin{aligned}
 F_e(\mu) &= 1/2 [F(\mu+k) + F(-\mu+k)] \\
 F_o(\mu) &= 1/2 [F(\mu+k) - F(-\mu+k)]
 \end{aligned} \tag{6.6}$$

then equation (6.4) becomes

$$\begin{aligned}
 PV \int_0^\infty F(\mu) d\mu &= PV \int_{-k}^{+k} F_e(\mu) d\mu + PV \int_{-k}^{+k} F_o(\mu) d\mu + PV \int_{2k}^\infty F(\mu) d\mu \\
 &= PV \int_0^{+k} 2F_e(\mu) d\mu + \int_{2k}^\infty F(\mu) d\mu \\
 &= \int_0^{+k} [F(\mu+k) + F(-\mu+k)] d\mu + \int_{2k}^\infty F(\mu) d\mu
 \end{aligned} \tag{6.7}$$

In arriving at equation (6.7), the fact that $PV \int_{-k}^{+k} F_o(\mu) d\mu = 0$, and that the integrand $[F(\mu+k) + F(-\mu+k)]$ should be finite at $\mu = 0$ have been used. Since the well-behaved analytical form of $[F(\mu+k) + F(-\mu+k)]$ is rather complicated, in the program, equation (6.7) is approximated as:

$$PV \int_0^{\infty} F(\mu) d\mu = 0.01k \cdot [F(\mu+k) + F(-\mu+k)]_{\mu=0.01k} + \int_{0.01k}^k [F(\mu+k) + F(-\mu+k)] d\mu + \int_{2k}^{\mu_{max}} F(\mu) d\mu \quad (6.8)$$

The numerical integration in equation (6.8) is carried out in a way similar to that of the Simpson's Integration method, but the Gaussian's 16-point formula was used in each subinterval. Numerical experiment shows that this technique converges much faster than Simpson's method.

The summation in the series form of Green's function is carried out in reverse order, so that possible truncation error can be minimized. Some values of the Green's function were checked by the series form and the integral form simultaneously. They agree up to at least three digits.

As was mentioned above the series form of Green's function is used when $J_{max} < 1000$, otherwise the integral form is used. This "two-path" criterion for choosing the Green's function does not work well in the following cases:

A When $J_{max} < 1000$, but $k=0$. $Y_0(kr')$ in equation (4.8) might numerically overflow, hence, in the program, the integral form of Green's function is again used when $kr' < 0.01$. This path is actually not necessary in general practical applications since the motion and drift forces for extreme long waves are trivial.

B Since the Green's function expression for the infinite water depth case has not been incorporated in the program. In deep water case (i.e., $h \rightarrow \infty$), it might happen that $J_{max} > 1000$ always. In this case, a suitable

choice of h , to approximate the infinite water depth case, is necessary. In order to make the program work more efficiently.

6.3 Evaluation of α_{pq} and β_{pq}

Most cpu time is taken up in the evaluation of the matrices α_{pq} and β_{pq} defined in equation (4.16) and (4.18). For $p \neq q$, α_{pq} and β_{pq} represent the influence at the p^{th} control point (centroid of the P^{th} panel) by the source distribution on the q^{th} panel. We assume the distributed source on the q^{th} panel is concentrated at the q^{th} control point (centroid of the q^{th} panel). In this case α_{pq} and β_{pq} can be approximated as:

$$\alpha_{pq} = \nabla G(\vec{x}_p, \vec{z}_q) \cdot \vec{n}(\vec{x}_p) \Delta S_q, \quad \text{when } p \neq q \quad (6.9)$$

$$\beta_{pq} = G(\vec{x}_p, \vec{z}_q) \Delta S_q, \quad \text{when } p \neq q \quad (6.10)$$

For $p = q$, i.e. the influence at the p^{th} control point by the source distribution on its own panel, the approximate method mentioned above can not be used. Therefore, the analytical expression for α_{pq} and β_{pq} according to equation (4.16) and (4.18) is needed. If the panel size is small, the predominant contribution to α_{pq} and β_{pq} when $p = q$, comes from the "source part", $1/R$, of the Green's function, hence equations (4.16) and (4.18) can be approximated as

$$\alpha_{pq} = \int_{\Delta S_q} \frac{\partial}{\partial n} \frac{1}{R} (\vec{x}_p, \vec{z}) ds, \quad p=q \quad (6.11)$$

$$\beta_{pq} = \int_{\Delta S_q} \frac{1}{R} (\vec{x}_p, \vec{z}) ds, \quad p=q \quad (6.12)$$

The analytical expression for equation (6.11) can be obtained as the limiting case when the field point, \vec{z} , approaches \vec{x}_p along the normal direction of the panel at \vec{x}_p , then equation (6.11) becomes

$$\alpha_{pq} = -2\pi \text{ when } p = q \quad (6.13)$$

It is worth noticing that the expression for α_{pq} in equation (6.13) is independent of the shape of the panel. On the other hand, the analytical form for β_{pq} ($p = q$) is more lengthy, since it depends on the panel shape. Nevertheless, if one replaces the panel by a circular disk, (we call it the "equivalent disk") with the same area, then one has:

$$\beta_{pq} = 2\sqrt{\pi \Delta S_q} \text{ when } p = q \quad (6.14)$$

Summarizing, in the program, α_{pq} and β_{pq} are evaluated by:

$$\alpha_{pq} = -2\pi s_{pq} + (1 - s_{pq}) \nabla G(\bar{x}_p, \bar{z}_q) \cdot \vec{n}(\bar{x}_p) \cdot \Delta S_q, \text{ no sum } q \quad (6.15)$$

$$\beta_{pq} = 2\sqrt{\pi \cdot \Delta S_q} s_{pq} + (1 - s_{pq}) G(\bar{x}_p, \bar{z}_q) \cdot \Delta S_q, \text{ no sum } q \quad (6.16)$$

It should be emphasized that most authors, e.g. [4] [5] [12], have used some other "more accurate" formula to evaluate β_{pq} when $p = q$, rather than using equation (6.14). It does not appear to be necessary. Using these "more accurate" formulas does not necessarily lead to a more precise result since theoretically, one may use panels of arbitrary shape as long as the distance from the boundary of the panel to its control point is small. One thing for sure is that using those shape dependent formulas takes more computing time.

This "equivalent disk" technique is not new and we actually have used it unconsciously. Since when computing α_{pq} and β_{pq} for $p \neq q$, one assumes that the source distribution in the q^{th} panel is concentrated at the q^{th} control point, this is equivalent to saying that one shrank the q^{th} panel into a "very small disk" while keeping the total source strength ($Q_q \Delta S_q$) unchanged.

Garrison [30] has pointed out that the value of β_{pq} when ($p = q$) changed significantly with the change of aspect ratio of a rectangular panel. It is therefore expected that the values of β_{pq} for a triangular panel and an "equivalent disk" might have a "large difference", but this "large difference" does not mean that it will induce a "large error" in the whole computation, since it doesn't make sense to compare two approximation schemes "locally" while not knowing the "exact value". Computed examples as will be seen in chapter 7, indicate that this technique works quite well.

6.4 Properties of α_{pq} due to the symmetry of the body geometry

As was mentioned earlier, this program requires the body geometry to be symmetric with respect to the x-z plane. If the total number of the panels of the body is N, equation (4.15) indicates that one has to compute a $N \times N$ complex matrix inversion. Taking advantage of the symmetric body geometry one only needs to invert two ($N/2 \times N/2$) complex matrices. The scheme used in the program is illustrated in the following example.

Let Q_j denote any Q_j ($j=1-7$), b denote the corresponding boundary value of the right-hand side of equation (4.15), then equation (4.15) can be rewritten as

$$\alpha_{pq} \cdot Q_q = b_p \quad (6.17)$$

For the sake of convenience, let us take the total panel number $N=4$, and let the panel indices 1 and 2 be on one side, the indices 3 and 4 on the opposite symmetric side, as shown in figure (2), then equation (6.17) becomes

$$\begin{bmatrix} \alpha_{11} & \alpha_{12} & \alpha_{13} & \alpha_{14} \\ \alpha_{21} & \alpha_{22} & \alpha_{23} & \alpha_{24} \\ \alpha_{31} & \alpha_{32} & \alpha_{33} & \alpha_{34} \\ \alpha_{41} & \alpha_{42} & \alpha_{43} & \alpha_{44} \end{bmatrix} \begin{bmatrix} Q_1 \\ Q_2 \\ Q_3 \\ Q_4 \end{bmatrix} = \begin{bmatrix} b_1 \\ b_2 \\ b_3 \\ b_4 \end{bmatrix} \quad (6.18)$$

after partitioning, equation (6.18) can be written as:

$$\begin{bmatrix} \bar{\alpha}_{11} & \bar{\alpha}_{12} \\ \bar{\alpha}_{21} & \bar{\alpha}_{22} \end{bmatrix} \begin{bmatrix} \bar{Q}_1 \\ \bar{Q}_2 \end{bmatrix} = \begin{bmatrix} \bar{b}_1 \\ \bar{b}_2 \end{bmatrix} \quad (6.19)$$

where

$$\bar{\alpha}_{11} = \begin{bmatrix} \alpha_{11} & \alpha_{12} \\ \alpha_{21} & \alpha_{22} \end{bmatrix}, \quad \bar{\alpha}_{12} = \begin{bmatrix} \alpha_{13} & \alpha_{14} \\ \alpha_{23} & \alpha_{24} \end{bmatrix} \text{ etc...}$$

$$Q_1 = \begin{bmatrix} Q_1 \\ Q_2 \end{bmatrix}, \quad Q_2 = \begin{bmatrix} Q_3 \\ Q_4 \end{bmatrix} \quad (6.20)$$

$$\bar{b}_1 = \begin{bmatrix} b_1 \\ b_2 \end{bmatrix}, \quad \bar{b}_2 = \begin{bmatrix} b_3 \\ b_4 \end{bmatrix}$$

Due to the symmetry of the body, it can be shown that

$$\bar{\alpha}_{11} = \bar{\alpha}_{22}; \quad \bar{\alpha}_{12} = \bar{\alpha}_{21} \quad (6.21)$$

Furthermore, if the boundary values are also symmetric with respect to x-z plane, i.e. $\bar{b}_1 = \bar{b}_2$, then it can be shown that $Q_1 = Q_2$. Similarly, if the boundary values are antisymmetric with respect to x-z plane, i.e. $\bar{b}_1 = -\bar{b}_2$, one will have $Q_1 = -Q_2$. Therefore, summarizing, equation (6.19) can be rewritten in two special cases:

IF $\bar{b}_1 = \bar{b}_2$ then $Q_1 = Q_2$

$$\text{and } (\bar{\alpha}_{11} + \bar{\alpha}_{12}) (Q_1) = (\bar{b}_1) \quad (6.22)$$

IF $\bar{b}_1 = -\bar{b}_2$ then $Q_1 = -Q_2$

$$\text{and } (\bar{\alpha}_{11} - \bar{\alpha}_{12}) (Q_1) = (\bar{b}_1) \quad (6.23)$$

In equation (4.15), since the boundary values n_j are symmetric when $j=1, 3, 5$ and are antisymmetric when $j=2, 4, 6$. If one splits the boundary value of $j=7$, i.e., $-\frac{\partial \Phi_0}{\partial n}$, into symmetric and antisymmetric parts, then, using the scheme illustrated above, Q_j ($j=1, \dots, 7$) can be obtained by solving two $N/2 \times N/2$ complex matrix inversions and eight matrix product operations.

Using a similar scheme, the amount of computation can be further reduced if the body geometry has two planes of symmetry, say $x-z$ plane and $y-z$ plane. But advantage has not been taken of this in the present work.

6.5 Properties of elements of α_{pq} and β_{pq}

Generally speaking, elements in α_{pq} and β_{pq} have neither symmetric nor antisymmetric properties, yet some properties of the Green's function are rather well-behaved, by which the computation time of α_{pq} and β_{pq} can be reduced by almost one half. Using the typical four-panel partitioning as an example, figure (2), these properties are outlined in the following:

$$1 \quad G(p, q) = G(q, p) \quad p, q = 1-4$$

$$2 \quad \frac{\partial G}{\partial x}(p, q) = -\frac{\partial G}{\partial x}(q, p) \quad p, q = 1-4$$

$$\frac{\partial G}{\partial y}(p, q) = -\frac{\partial G}{\partial y}(q, p) \quad p, q = 1-4$$

$$3 \quad \frac{\partial G}{\partial n}(1:4) = \frac{\partial G}{\partial n}(3, 2) \quad \frac{\partial G}{\partial n}(1, 3) = \frac{\partial G}{\partial n}(3, 1)$$

$$\frac{\partial G}{\partial n}(2, 3) = \frac{\partial G}{\partial n}(4, 1) \quad \frac{\partial G}{\partial n}(2, 4) = \frac{\partial G}{\partial n}(4, 2)$$

$$\text{where } G(p, q) = G(\vec{x}_p, \vec{z}_q), \quad \frac{\partial G}{\partial x}(p, q) = \frac{\partial G}{\partial x}(\vec{x}_p, \vec{z}_q).$$

The property 3 can be written as

$$\frac{\partial G}{\partial n}(p, q') = \frac{\partial G}{\partial n}(p')$$

where p and p' (also q and q') denote two corresponding symmetric panel indices on either side of the x - z plane, e.g. If $p = 1$ then $p' = 3$, if $q = 2$ then $q' = 4$.

Properties 1 and 2 are due to the Green's function itself. Property 3 is due to the symmetry of the body. This property has been used in obtaining equations (6.22) and (6.23).

6.6 Complex matrix inversion

The complex equation (4.15) can be written in the form

$$\alpha_{pq} Q_q = b_p$$

Splitting the complex variables into real and imaginary parts, one has:

$$(\kappa_{pq} + i\gamma_{pq})(R_q + iS_q) = (c_p + i d_p) \quad (6.24)$$

where

$$\alpha_{pq} = (\kappa_{pq} + i\gamma_{pq})$$

$$Q_q = (R_q + iS_q) \quad (6.25)$$

$$b_p = (c_p + i d_p)$$

From equation (6.24), one has:

$$\kappa_{pq} R_q - \gamma_{pq} S_q = c_p \quad (6.26)$$

$$\gamma_{pq} R_q + \kappa_{pq} S_q = d_p$$

In the program, the solutions for R_q and S_q of equation (6.26) are obtained by the method of Gaussian elimination.

6.7 Miscellaneous

1 In the program, the restoring coefficients C_{jk} , defined in equation (3.2), are calculated by the following relationships:

$$\begin{aligned} A_{wp} &= \int_{S_b} n_z ds \\ A_{wp} &= \int_{S_b} x ds = - \int_{S_b} x n_z ds \\ A_{wp} &= \int_{S_b} x^2 ds = - \int_{S_b} x^2 n_z ds \quad (6.27) \\ A_{wp} &= \int_{S_b} y^2 ds = - \int_{S_b} y^2 n_z ds \\ V &= \frac{1}{3} \int_{S_b} x_i n_i ds \quad i=1-3 \\ z_b &= \frac{1}{2V} \int_{S_b} z^2 n_z ds \end{aligned}$$

the surface integrals in equation (6.27) are approximated by the same panel summation scheme as is used in evaluating A_{pq} .

2 Consider the Green's function in equation (4.7), when the water depth h is large, the integrand

$$e^{-\mu h} \frac{\cosh(\mu(z+h)) \cdot \cosh(\mu(z+h))}{\mu \sinh(\mu h) - \nu \cosh(\mu h)} \quad (6.28)$$

might numerically overflow due to the value of the hyperbolic function, this term can be replaced by

$$\frac{0.5 e^{\mu(z+\zeta)} (1 + e^{-2\mu(z+h)}) (1 + e^{-2\mu(z+h)})}{(\mu + \nu) - (\mu + \nu) \cdot \exp(-2\mu h)} \quad (6.29)$$

The expression (6.29) is well-behaved in water of any depth. In the program, all expressions with similar properties to (6.28) are treated in a similar way, in order to minimize possible truncation errors.

Chapter 7

RESULTS OF COMPUTED EXAMPLES

The motions and drift forces of two typical floating bodies, a hemisphere and a rectangular box, were computed to check the validity and accuracy of the numerical process. Comparisons with published data are made.

7.1 General description

1. The particulars of the hemisphere are given in Table (1), the computed results are given in figures (3)-(9). 128 triangular panels were used in this computation.

2. The particulars of the rectangular box are given in Table (2). The computed results are given in figures (10)-(22). In this case, since it is rather clumsy to use triangular shape panels, rectangular shaped panels were used. 72 panels were used in this computation, except when calculating the drift force and moment at various heading angles, where 84 panels were used, since the previous panel configuration (72 panels) gives non-zero (though small) vertical drift moment at 45 degrees heading. This made the drift moment curve look awkward.

3. All the computed values are indicated by small triangles in figures (3)-(22). The solid line is the spline curve fitting results.

4. According to convention, the phase angle of the body motions and wave exciting forces presented here, are with respect to the free surface elevation, due to the incident wave, at the origin of the coordinate system. For example, the linearized free surface elevation at the origin, (denoted by ζ_0), due to the incident wave is:

$$\zeta_0(t) = -\frac{1}{g} \frac{\partial}{\partial t} [\Phi_0 e^{-kx}]_{x,y,z=0} \quad (7.1)$$

using the expression of equation (3.10) in equation (7.1) we have

$$\zeta_0(t) = \zeta_a / e^{-i\omega t} \quad (7.2)$$

If $F e^{-i\omega t}$ is the complex wave exciting force, then the phase angle, δ_F , of this exciting force with respect to $\zeta_0(t)$ is calculated by

$$\delta_F = \pi/2 - \text{Arg}(F) \quad (-\pi/2 < \text{Arg}(F) < 3/2\pi) \quad (7.3)$$

where $\text{Arg}(F)$ is the principal argument of F . $\delta_F > 0$ means the exciting force "leads" $\zeta_0(t)$.

7.2 Comparison with published data

Figures (3)-(22) show the computed results. Published data taken from Garrison's paper [5] [6], and Faltinsen's paper [4] are reproduced in Appendix A, they are taken as a comparison base. For the sake of simplicity, we use the same non-dimensional units as those used in the respective papers; and the results of comparison are put in the following tabular form:

1. Floating Hemisphere

Present work	Contents of Figure	Garrison's Data [5][6]	Result of comparison
Fig.(3)	Surge Added mass and Damping Coeff.	Fig.(A-1)	Good
Fig.(4)	Heave Added mass and Damping Coeff.	Fig.(A-2)	Good
Fig.(5)	Surge exciting force and Phase	Fig.(A-3)	Good
Fig.(6)	Heave exciting force and Phase	Fig.(A-3)	Good
Fig.(7)	Surge Motion and Phase	Fig.(A-4) Fig.(A-5)	Good
Fig.(8)	Heave Motion and Phase	Fig.(A-4) Fig.(A-5)	Good
Fig.(9)	Drift Force	Fig.(A-6)	See discussion (1)

2. Floating Rectangular Box

Present work	Contents of Figure	Faltinsen's Data [4]	Result of comparison
Fig.(10)	Surge Added mass and Damping Coeff.	Fig.(A-7.a) Fig.(A-7.b)	Good
Fig.(11)	Heave Added mass and Damping Coeff.	Fig.(A-8.a) Fig.(A-8.b)	Good
Fig.(12)	Pitch Added mass and Damping Coeff.	Fig.(A-9.a) Fig.(A-9.b)	Good
Fig.(13)	Yaw Added mass and Damping Coeff.	Fig.(A-10.a) (No Damping Coef. data)	Good
Fig.(14-a)	Surge motion and phase (0 Deg.)	Fig.(A-11.a)	Good
Fig.(14-b)	Surge motion and phase (45 Deg.)	Fig.(A-11.b)	Good
Fig.(15-a)	Heave motion and phase (0 Deg.)	Fig.(A-12.a)	Good
Fig.(15-b)	Heave motion and phase (45 Deg.)	Not Available	see Discussion(2)
Fig.(16-a)	Pitch motion and phase (0 Deg.)	Fig.(A-13.a)	see Discussion (3)
Fig.(16-b)	Pitch motion and phase (45 Deg.)	Fig.(A-13.a)	see Discussion (3)
Fig.(17-a)	Surge Exciting force and Phase (0 Deg.)	Fig.(A-14.a)	Good
Fig.(17-b)	Surge Exciting force and Phase (45 Deg.)	Fig.(A-14.b)	Good
Fig.(18-a)	Heave Exciting force and Phase (0 Deg.)	Fig.(A-15.a)	Good
Fig.(18-b)	Heave Exciting force and Phase (45 Deg.)	Not Available	see Discussion (2)
Fig.(19-a)	Pitch Exciting force and Phase (0 Deg.)	Fig.(A-16.a)	Good
Fig.(19-b)	Pitch Exciting force and Phase (45 Deg.)	Fig.(A-16.b)	Good

Fig.(20-a)	Drift force in x-component (0 Deg.)	Fig.(A-17.a)	Good
Fig.(20-b)	Drift force in x-component (45 Deg.)	Fig.(A-17.b)	Good
Fig.(21)	Drift force in x-com. at various Heading	Not Available	
Fig.(22)	Vertical Drift Moment	Not Available	

7.3 Discussion of computed results

Generally speaking, the computed results are in good agreement with the published data.

1. For the drift force on the hemisphere, comparing figure (9) and figure (A-6) which is reproduced from Maruo's paper [21], it can be seen that the trends and the locations of the peak value are in agreement (notice that Maruo used $a/\lambda = a k/(2\pi)$ unit in the abscissa), but the magnitudes are quite different. This result is not surprising since Maruo has neglected the effect of the surge motion, and only the heave motion of the hemisphere was taken into account when computing the drift force.

2. The heave exciting force (and heave motion) are exactly the same for 0 and 45 degrees heading.

3. For the rectangular box, the pitch motion at 0 and 45 degrees heading angles are shown in figures (16-a) and (16-b). When compared with the corresponding Faltinsen's results which are given in figures (A-18.a) and (A-18.b), it can be seen that the results of the present work are about twice as large as Faltinsen's. Also the trends of the phase angle are completely different. It is rather difficult to give any

confident explanation about this discrepancy. It is conceivable that there might be some misplotting in Faltinsen's curve, since in the interval of wave period from 10 to 14 seconds, the nondimensional pitch motion amplitude varies rather "monotonically", the change of phase angle in the same interval is unlikely to be that large, which is about 180 degrees. In Faltinsen result.

4. Figure (21) shows that the steady drift force (x-component) on the rectangular box decreases monotonically as the heading angle increases.

5. Figure (22) shows the steady vertical drift moment of the rectangular box at various heading angles. It can be seen that this drift moment attains its extreme values at 22.5 and 67.5 degrees heading, and vanishes at 0, 45 and 90 degrees. It is interesting to notice that the 0 and 90 degrees are stable heading angles, while 45 degrees is an unstable one. This means that the floating rectangular box has the tendency to orientate its side to face the direction of the wave propagation.

7.4 Irregular frequency

There is a discrete set of frequencies, called irregular frequencies, at which the matrix α_{pq} becomes singular or numerically ill conditioned. This fact, as was first pointed out by John [15] [16], is due to the nontrivial or unbounded solution of the interior Dirichlet problem. The source distribution method therefore breaks down when the frequencies of the incident wave coincide with these irregular frequencies (i.e. the eigen values of the interior problem). Since these irregular frequencies depend

on the body shape. It is difficult to locate them precisely. Fortunately, there is always a non-zero lower bound of the set though it is unknown generally.

In the present work, we avoided this problem by calculating in the frequency range for which no (or seemingly no) irregular frequency exists.

For a floating rectangular box (length=L, beam=B, draught=D) in infinite water depth, the irregular frequency (ω_i) can be determined analytically [14] as

$$\omega_i = [g \gamma \coth(\gamma D)]^{1/2} \quad (7.4)$$

where

$$\gamma^2 = \left(\frac{m\pi}{L}\right)^2 + \left(\frac{n\pi}{B}\right)^2 \quad m, n = 1, 2, 3, \dots \quad (7.5)$$

In the present computed example (L=90m, B=90m, D=40m) the lowest irregular frequencies predicted by equation (7.4) are:

m\n	1	2	3
1	0.7091	0.8766	1.0403
2	0.8766	0.9840	1.1107
3	1.0403	1.1107	1.2048

The lower bound for ω_i is seen to be 0.7091 rad/sec, equivalent to the period T=8.86 sec., therefore, the irregular frequency problem can be circumvented if one chooses the lowest period in computation to be larger than 8.86 second. It is worth noting that around T=9 sec., the computed results (not presented here) indeed gave some peculiar behavior. Whether

the peculiar behavior was due to the influence of this lowest irregular frequency or, on the other hand, due to the effect of an insufficient number of panels (since the higher the frequency, the more the panels should be used in order to keep a consistent numerical error). Before a detailed numerical experiment is done, no definite conclusion can be made at present.

For the hemisphere case, no analytical formula such as equation (7.4) was found. Since the heave added mass and damping coefficient, Figure (4), appears to suddenly change at $k \cdot a = 2.5$, it seems better to stop the computation there.

Although equation (7.4) was derived for the rectangular box in the infinite water depth case, it is useful to take it as a general rough guide for non-rectangular bodies. A brief outline is given below:

1. For $L/B = 1.0$, $B/D = 5.0$, the lowest irregular frequency occurs around $\lambda/L = 1.0$, where λ is the wave length.
2. Increasing the value of length to beam ratio (i.e., L/B) significantly increases the value of the lowest irregular frequency.
3. Decreasing the draught (D) of the body for a fixed beam (B) also increases the value of the lowest irregular frequency.

In our example $L/B = 1.0$, $B/D = 2.25$, the lowest irregular frequency occurs at $\lambda/L = 1.361$.

Chapter 8

CONCLUSION

A brief summary of the present work is given below:

1. A brief outline of the mathematical technique for calculating the Harmonic motion, and the steady drift forces on a floating body were reviewed.
2. A computer program has been set up, to calculate these motions, horizontal drift forces and vertical drift moment. The results of the computation are quite good when comparing with published data. For the rectangular box (72 panels) case, the average cpu time for one frequency and one heading angle is about one minute in VAX 11/780 system.
3. The "equivalent disk" concept suggested in the numerical scheme proved to work well. This scheme saves a certain amount of computation and simplifies the input data.
4. A numerical scheme is proposed in this work for evaluating the principal value in the integral of the Green's function. Using this scheme along with the Gaussian integration formula (16-point formula was employed in the present computation) makes the calculation converge much faster.

5. The computed results show that the shape of the panel is not important. Generally speaking a triangular panel is preferable, since it can be uniquely determined by three adjacent body offsets.

6. The vertical drift moment calculation is useful in the determination of the stable heading angle. It enables one to choose a "better" orientation of the floating body with respect to the incident wave direction.

7. This computer program can be used as a "basic building block" to other advanced motion calculations; for example

A. Employing the iterative process suggested by Arai [1], by slightly modifying the present program one can calculate the motions of a moored floating body.

B. Employing the assumption suggested by Hsu [13], the steady drift force computed in this program can be used to evaluate the slow oscillating drift force in a random sea.

REFERENCES

- [1] Arai, S. I. & Nekado, Y. & Takagi, M. (1976). "Study on the motion of a moored vessel among irregular waves". J.S.N.A. Vol. 140
- [2] Chang, M. S. (1977). "Computations of three-dimensional ship motions with forward speed". Proc. Int. Conf. Numer. Ship Hydrodyn., 2nd, pp. 124-135. Univ. California, Berkeley.
- [3] Clauss, G. & Sukan, M. & Schellin, T. E. (1982). "Drift forces on compact offshore structures in regular and irregular waves". App. Ocean Res. 4: 1982
- [4] Faltinsen, O. M. / Michelsen, F. C. (1974). "Motions of large structures in waves at zero Froude number". Int. Symp. on the Dynamics of Marine Vehicles and Structures in Waves. Univ. College, London, pp. 99-114
- [5] Garrison, C. J. (1974). "Hydrodynamics of large objects in the sea . Part I- Hydrodynamic analysis". Journal of Hydraulics. 8: 5-12
- [6] Garrison, C. J. (1975). "Hydrodynamics of large objects in the sea. Part II- Motion of free-floating bodies". Journal of Hydraulics. 9: 58-83
- [7] Garrison, C. J., Seetharama Rao, V. (1971). "Interaction of waves with submerged objects". Proc. ASCE. J. Waterways, Harbors, Coastal Eng. Div. 97: 257-77
- [8] Gerritsma, J. and Beukelman, W. (1971). "Analysis of the resistance in waves of a fast cargo ship". Report No. 334. Laboratorium voor Scheepsbouwkunde. Tech., Univ., Delft.
- [9] Greenberg, M. D. (1971). "Application of Green's function in science and engineering". Prentice-Hall. Inc. 141 pages.
- [10] Havelock, T. H. (1963). "Collected Works." ACR-103. Off. Nav. Res., Washington, D. C.
- [11] Hess, J. L., Smith A. M. O. (1964). "Calculation of non-lifting potential flow about arbitrary three-dimensional bodies". J. Ship Res. 8: 22-44
- [12] Hogben, N. and Standing, R. G. (1974). "Wave loads on large body". Int. Sym. on the dynamics of marine vehicles and structures in waves. London, England. pp. 258-277
- [13] Hsu, F. A. and Blendarn, K. A. (1970). "Analysis of peak mooring forces by slow vessel drift oscillation in random sea". O.T.C. paper No. 1159.

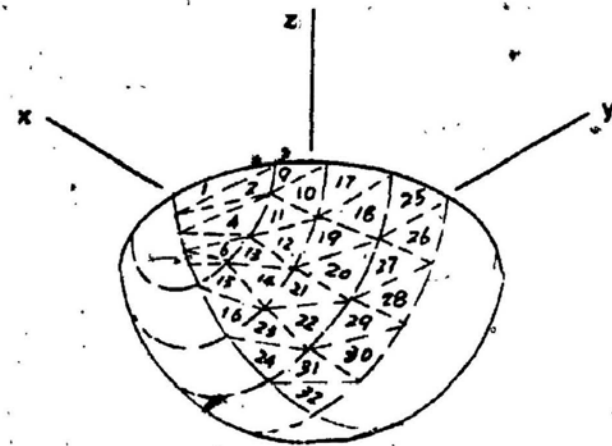
- [14] Inglis, R. B. and Price, W. G. (1981). "Irregular frequencies in three dimensional source distribution techniques". I.S.P.
- [15] John, F. (1949). "On the motion of floating bodies -I". Comm. Pure Appl. Math. 2: 13-57
- [16] John, F. (1950). "On the motion of floating bodies -II". Comm. Pure Appl. Math. 3: 45-101
- [17] Kellogg, O. D. (1929). "Foundations of Potential Theory". Berlin: Springer
- [18] Lamb, H. (1932). "Hydrodynamics". 6th ed. Cambridge University Press.
- [19] Lebreton J. C. Margnac, A. (1968). "Calcul des mouvements d'un navire ou d'une plateforme amarrés dans la houle". La Houille Blanche, 23: 379-89
- [20] Loken, A. E. and Olsen, O. A. (1976). "Diffraction theory and statistical methods to predict wave induced motions and loads for large structures". O.T.C. 2502
- [21] Maruo, H. (1960). "The drift of a body floating on waves". J.S.R. 4: 1-10
- [22] Newman, J. N. (1978). "The theory of ship motions". Adv. Appl. Mech. 18: 221-83
- [23] Newman, J. N. (1967). "The drift force and moment on ships in waves". J.S.R.
- [24] Newman, J. N. (1977). "Marine Hydrodynamics". M.I.T. press.
- [25] Newman, J. N. & Tuck, E.O. (1964). "Current Progress in the Slender body theory for ship motion". Fifth Sym. on naval hydrodynamics, Norway.
- [26] Pinkster, J. A. (1977). "Low frequency second order wave forces over vessels moored at sea". I.Mech.E. 1977
- [27] Salvassen, N. & Tuck, E. O. & Faltinsen, O. M. (1970). "Ship motions and sea loads". Tran. of SNAME 78: 1-30
- [28] Wehausen, J. V., Laitone, E. V. (1960). "Surface waves. Handbuch der Physik". 9: 446-778 Berlin: Springer.

[29] Young, R. W. (1982). "Numerical method in free-surface flows".
Ann. Rev. Fluid Mech. 14: 395-442

[30] Zienkiewicz, O. C. & Lewis R. W. & Stagg K. G. (1978).
"Numerical method in offshore engineering".

Table (1) Data for Hemisphere

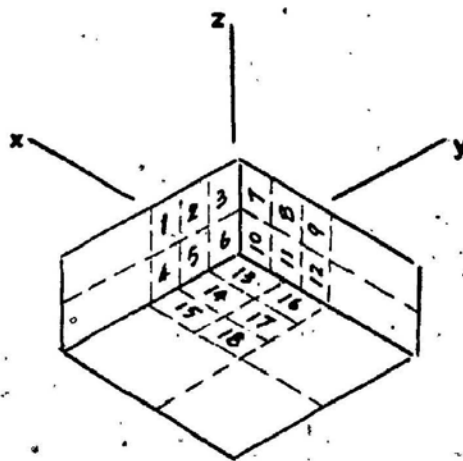
Radius (a)	1.0
Center of gravity (x_c, y_c, z_c)	(0, 0, 0)
Volume	$2/3 \pi a^3$
$I_{44} = I_{55} = I_{66}$	$2/5 \pi a^2 \rho V$
Water depth	10.0
Number of panels	128
Shape of panels	Triangular



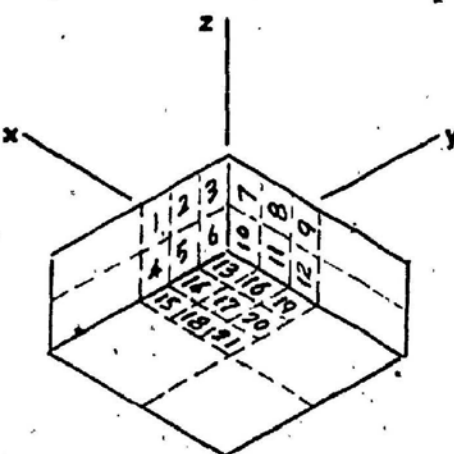
128 panels configuration

Table (2) Data of Rectangular Box

Length-Beam-Draught (m)	90-90-40
Center of gravity (x_c, y_c, z_c) (m)	(0.0, 0.0, 10.62)
Volume, V (m^3)	$3.24 \cdot 10^5$
I_{44} ($m^2 \cdot \text{mass}$)	$33.04^2 \cdot \rho V$
I_{55} ($m^2 \cdot \text{mass}$)	$32.09^2 \cdot \rho V$
I_{66} ($m^2 \cdot \text{mass}$)	$32.92^2 \cdot \rho V$
Water depth, h (m)	500
Number of panels	72 : 84
Shape of panels	Rectangular



72 panels configuration



84 panels configuration

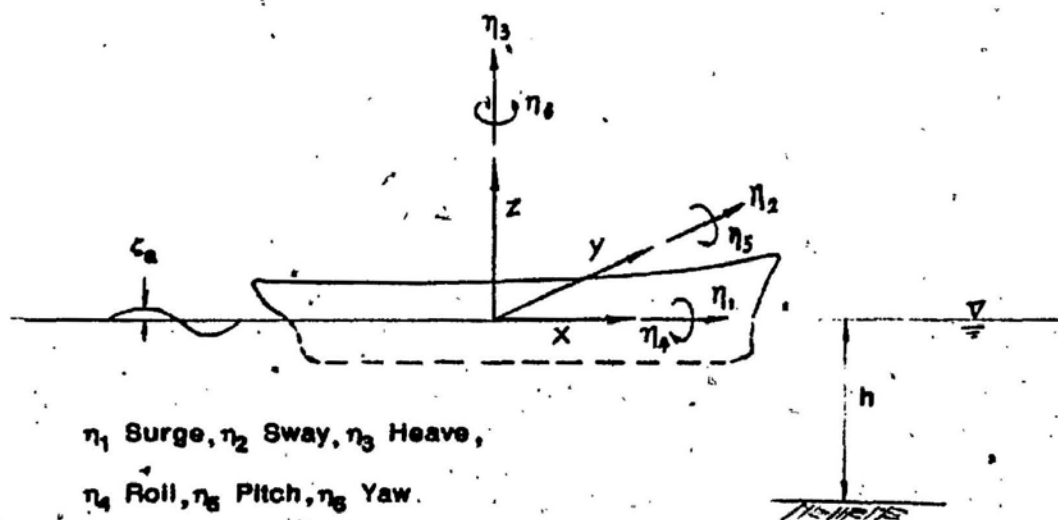


Figure (1) Coordinate system and sign convention for translatory and angular displacements

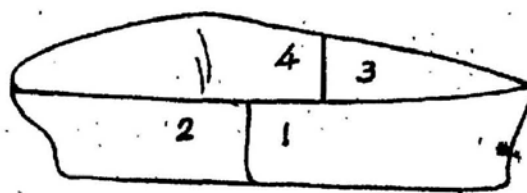


Figure (2) typical partitioning of x - z plane symmetric body

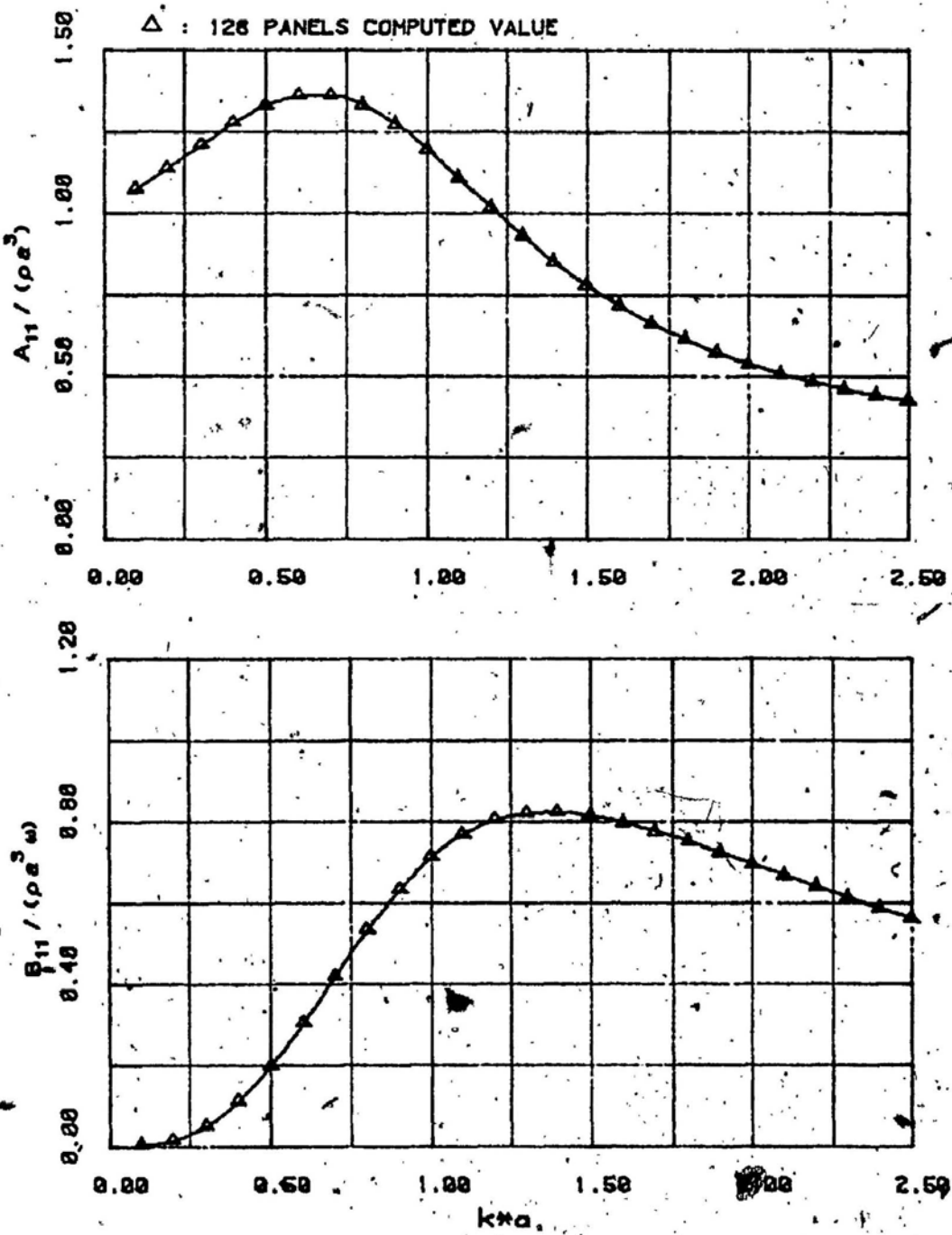


Figure (8) Added mass and damping in surge for a hemisphere ($h/a = 10$)

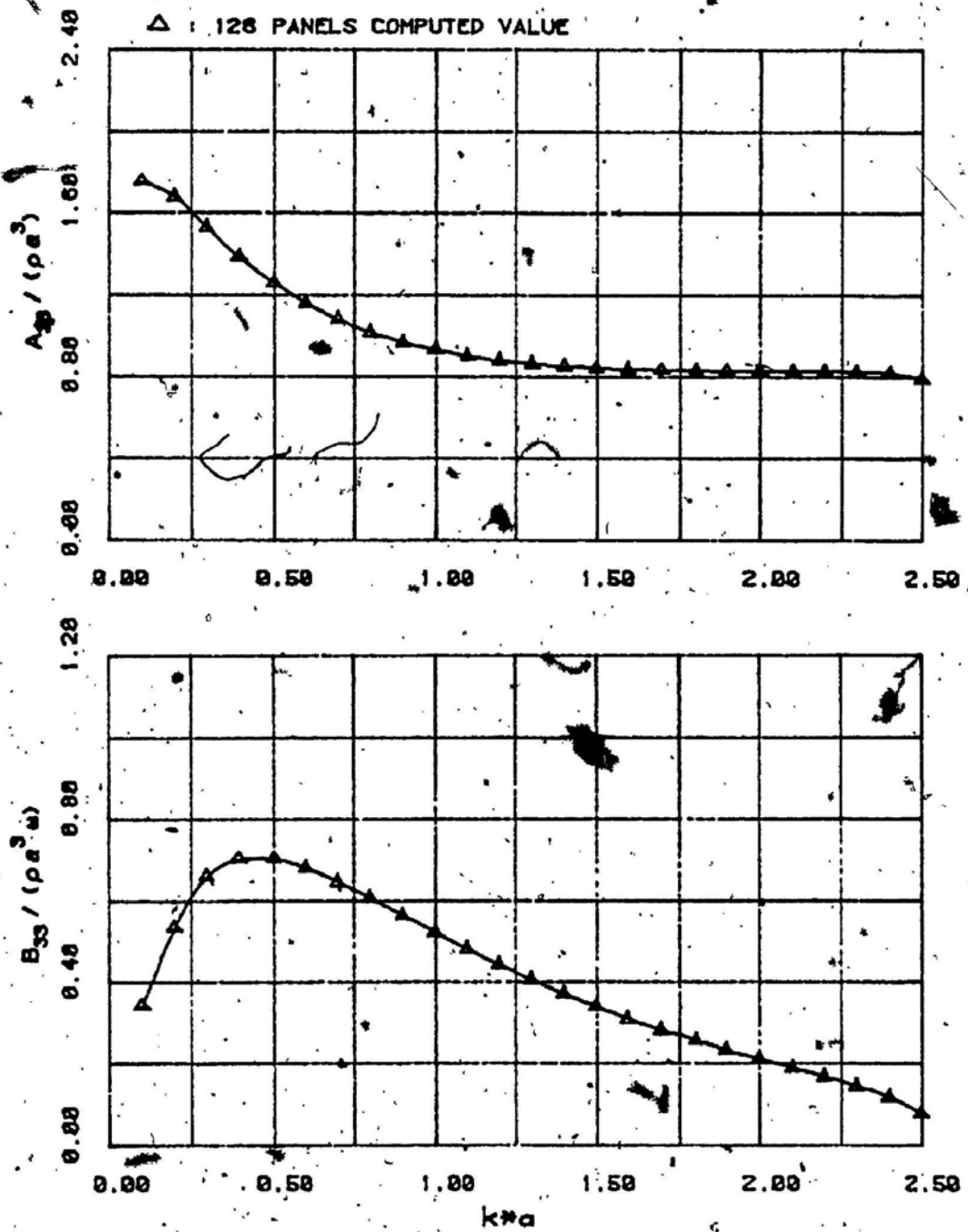


Figure (4) Added mass and damping in heave for a hemisphere (h/a = 10)

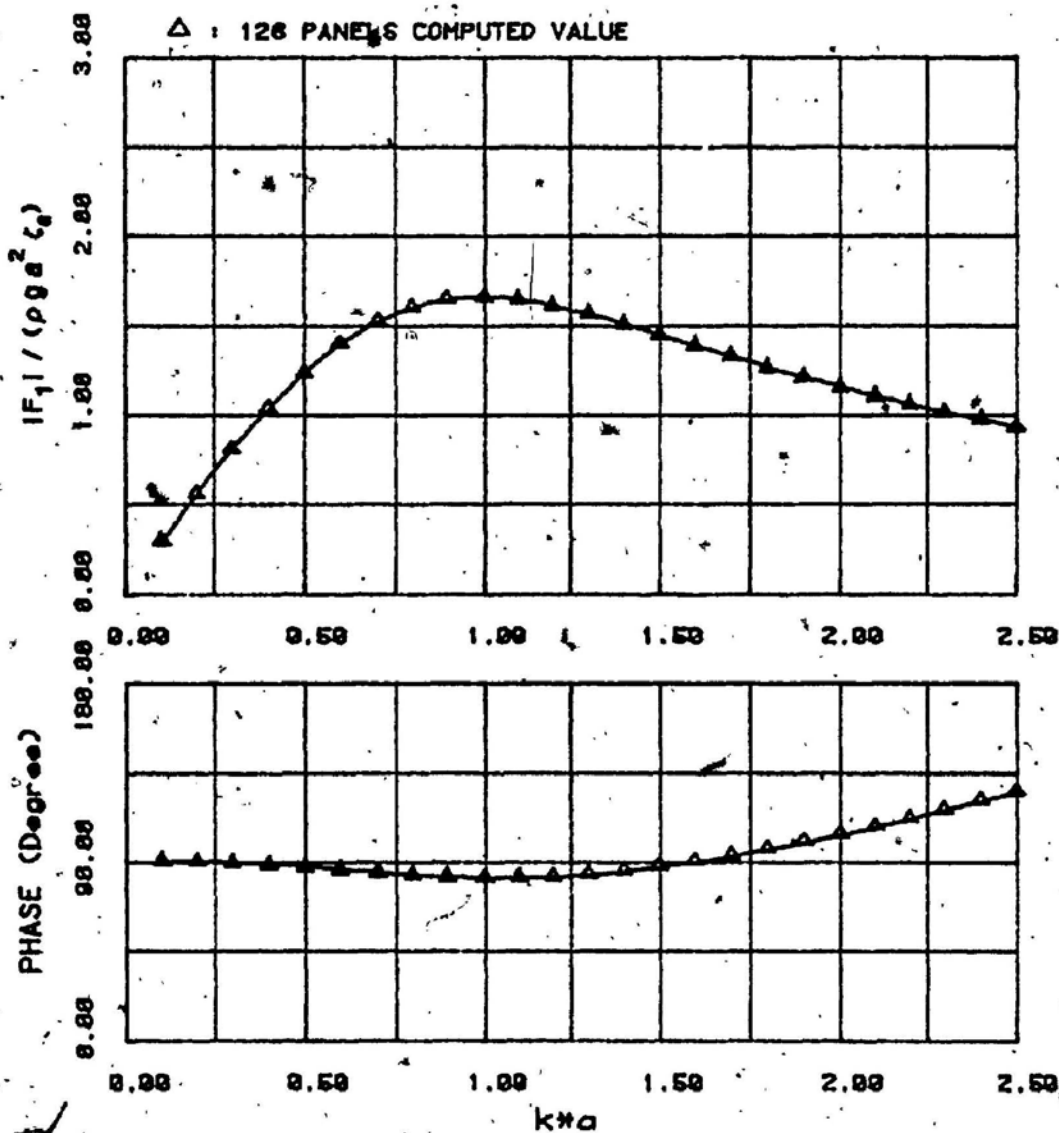


Figure (5) Surge exciting force and phase for a hemisphere ($h/a = 10$)

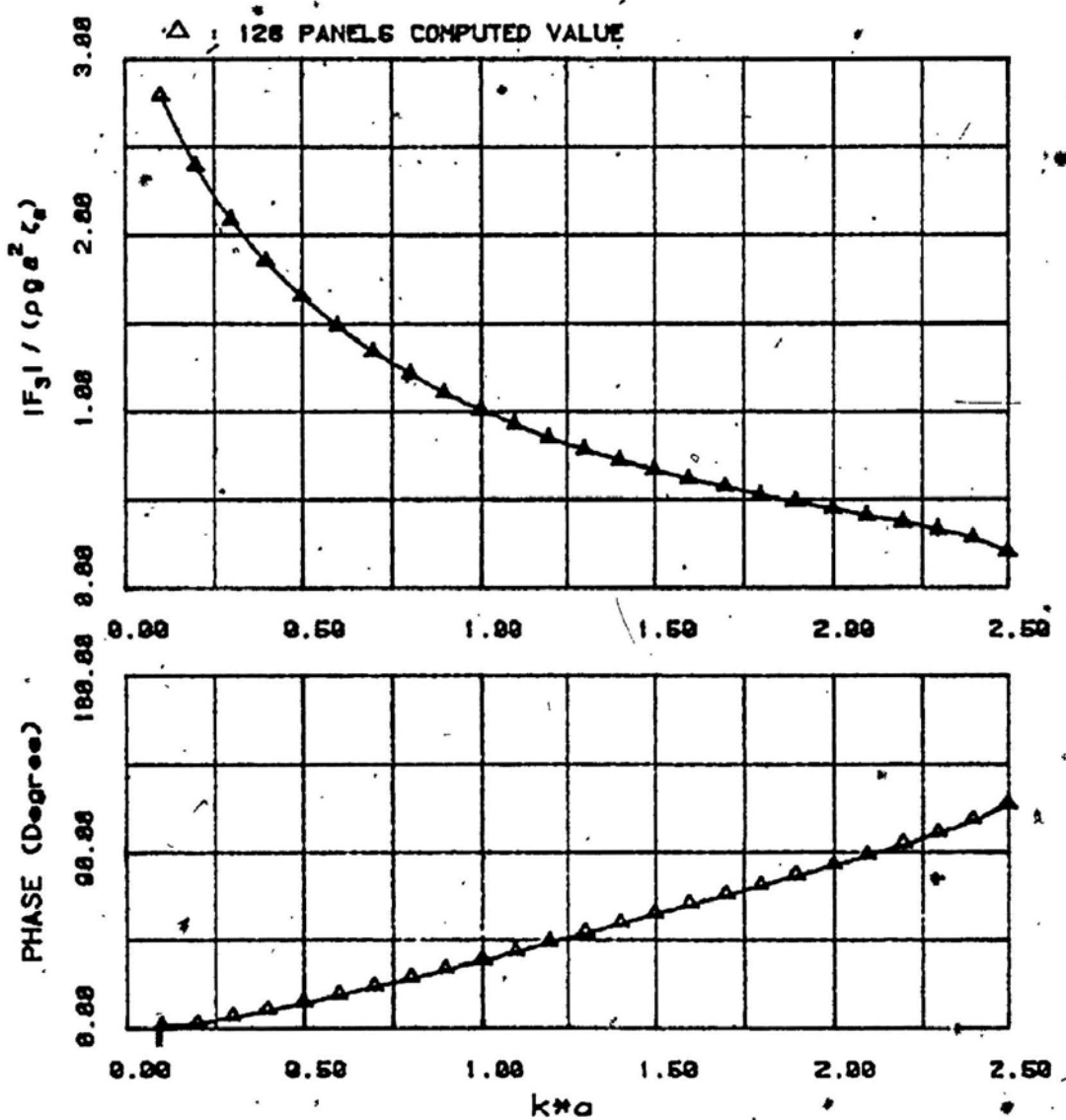


Figure (6) Heave exciting force and phase for a hemisphere ($h/a = 10$)

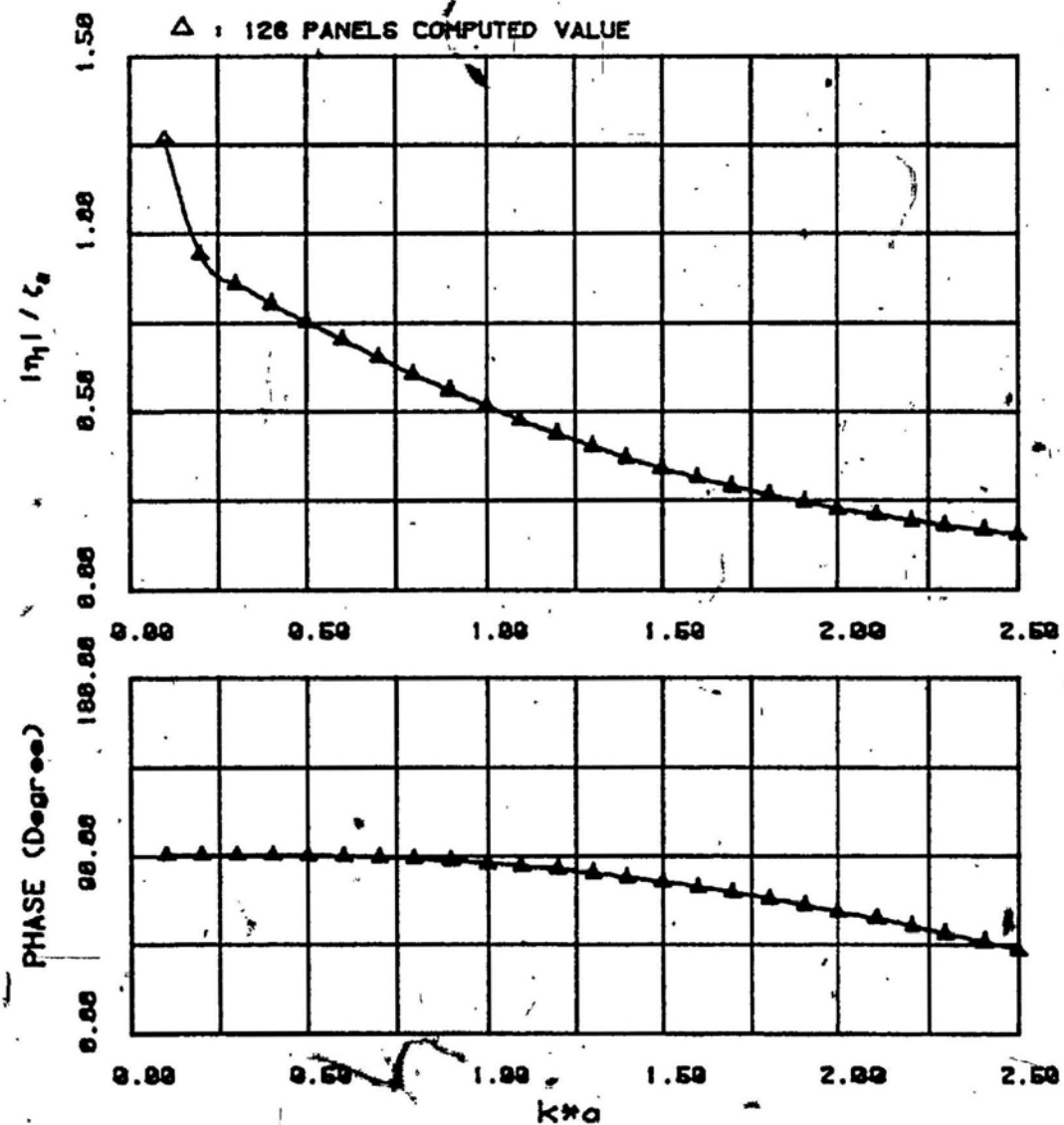


Figure (7) Surge motion and phase for a hemisphere ($h/a = 10$)

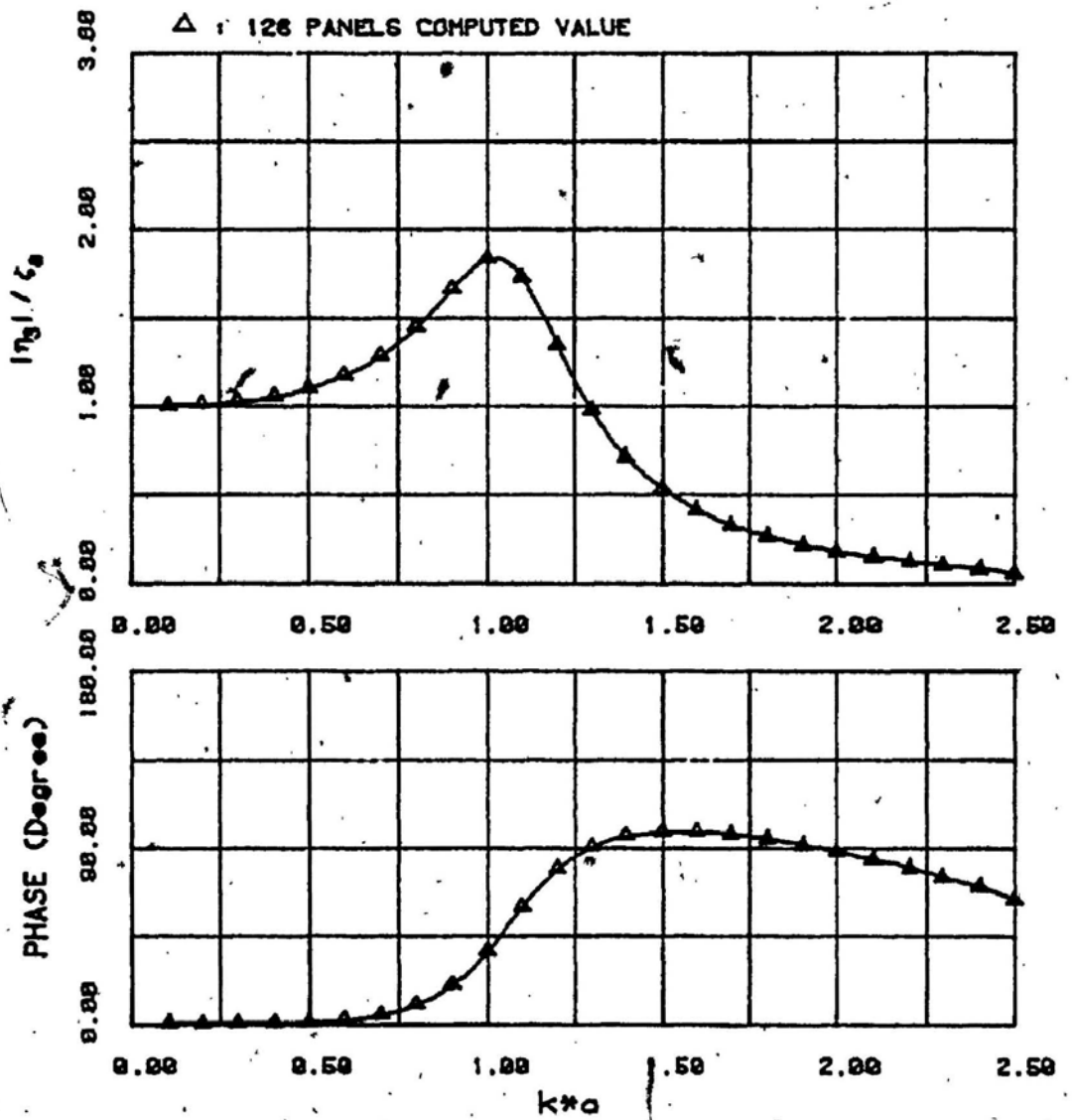


Figure (8) Heave motion and phase for a hemisphere ($h/a = 10$).

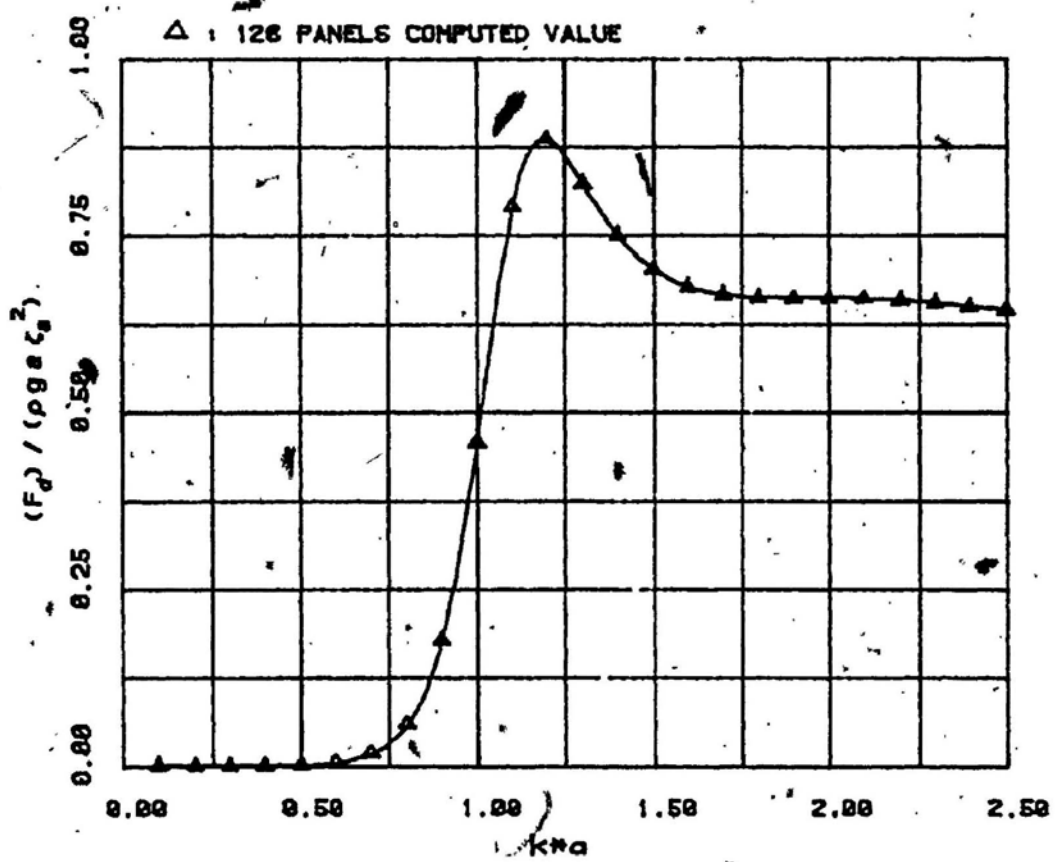


Figure (8) Drift force for a hemisphere ($h/a = 10$)

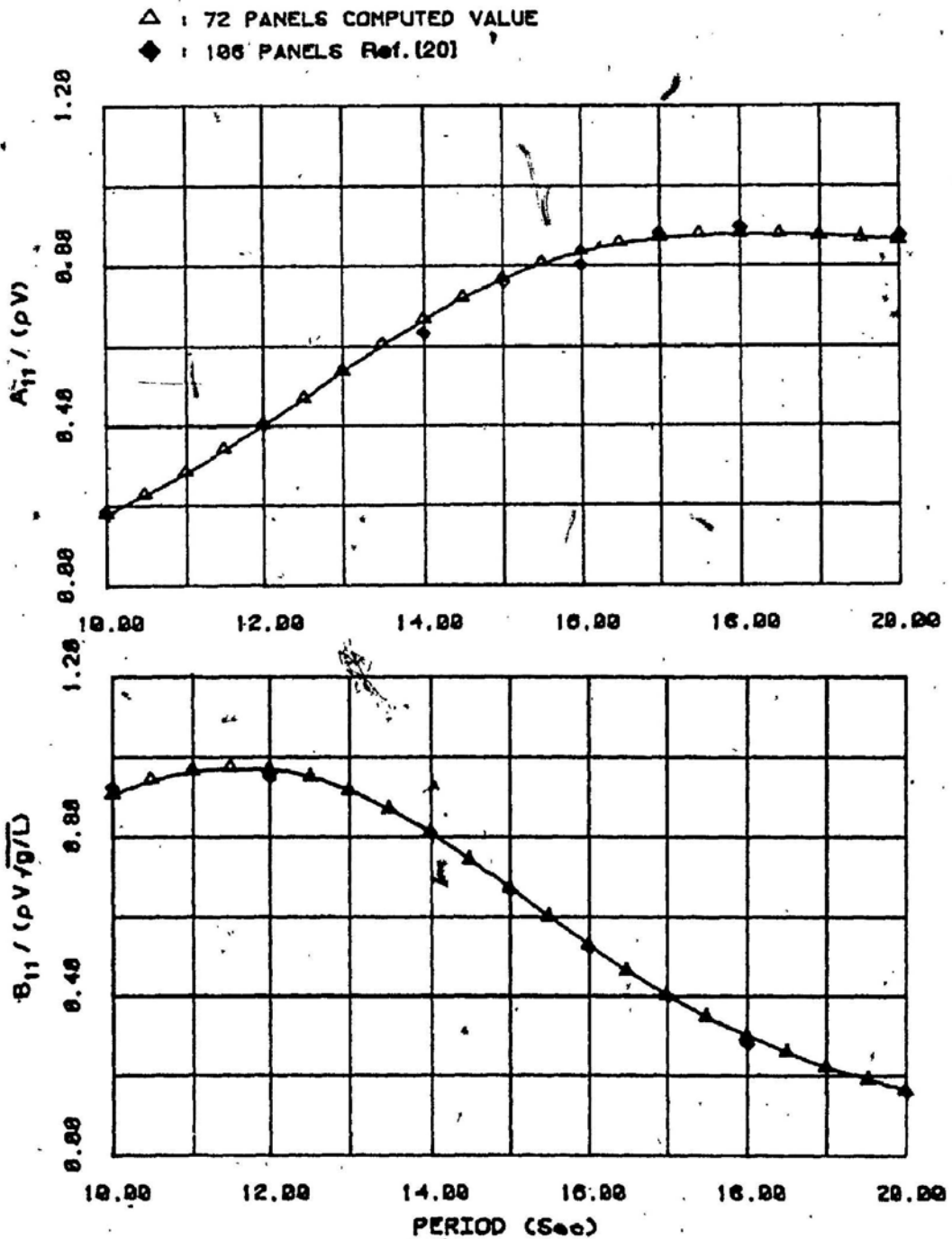


Figure (10) Added mass and damping in surge for rectangular box
($L \times B \times D = 90 \times 90 \times 40$ m, water depth = 500m)

△ : 72 PANELS COMPUTED VALUE
◆ : 186 PANELS Ref. [20]

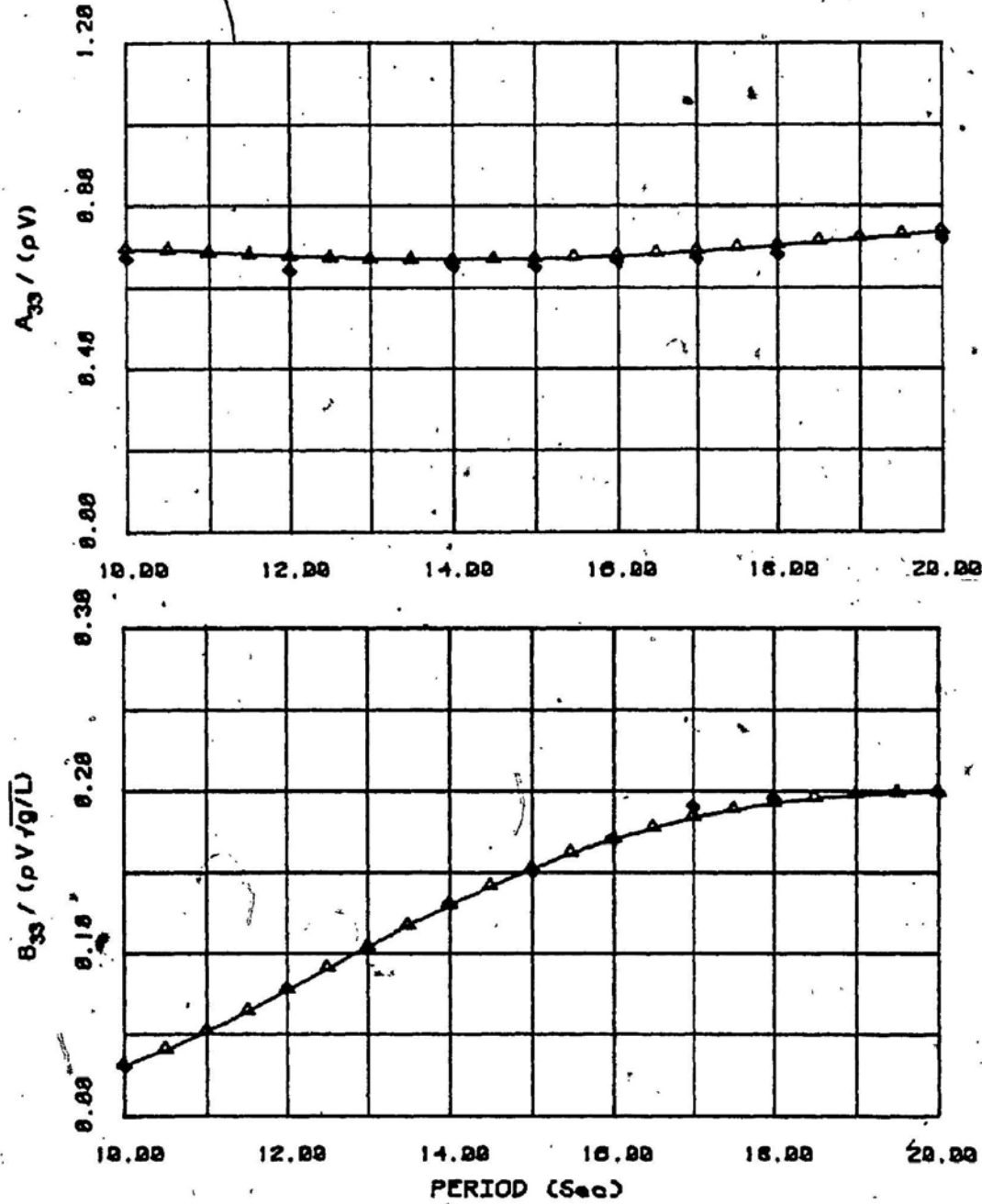


Figure (11) Added mass and damping in heave for rectangular box
($L=B=D = 90 \times 90 \times 40$ m, water depth = 500m)

- 66 -

△ : 72 PANELS COMPUTED VALUE
◆ : 186 PANELS Ref. [20]

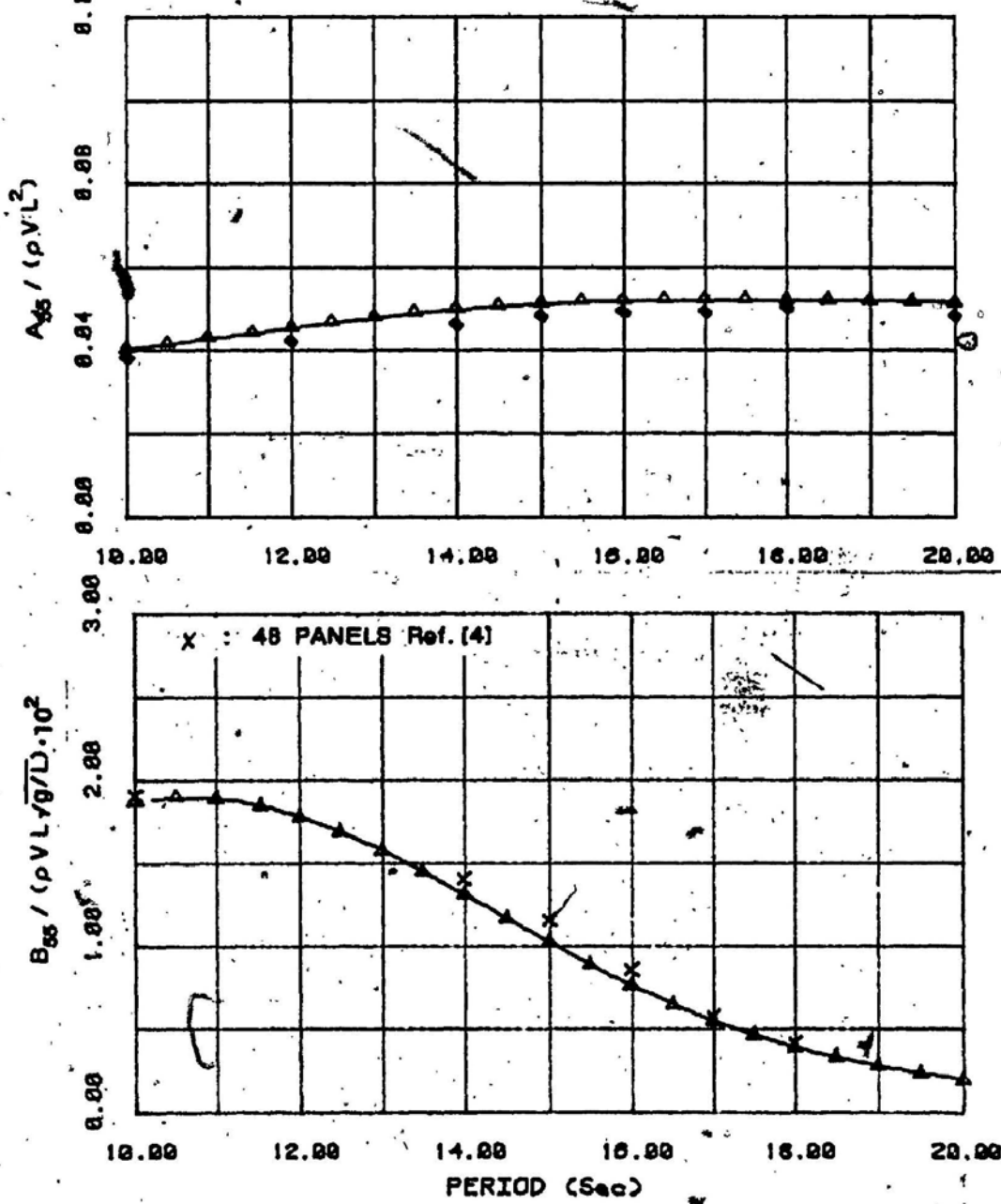


Figure (12) Added mass and damping in pitch for rectangular box
($L \times B \times D = 90 \times 90 \times 40$ m, water depth = 500m)

- 67 -

△ : 72 PANELS COMPUTED VALUE
◆ : 106 PANELS Ref. [20]

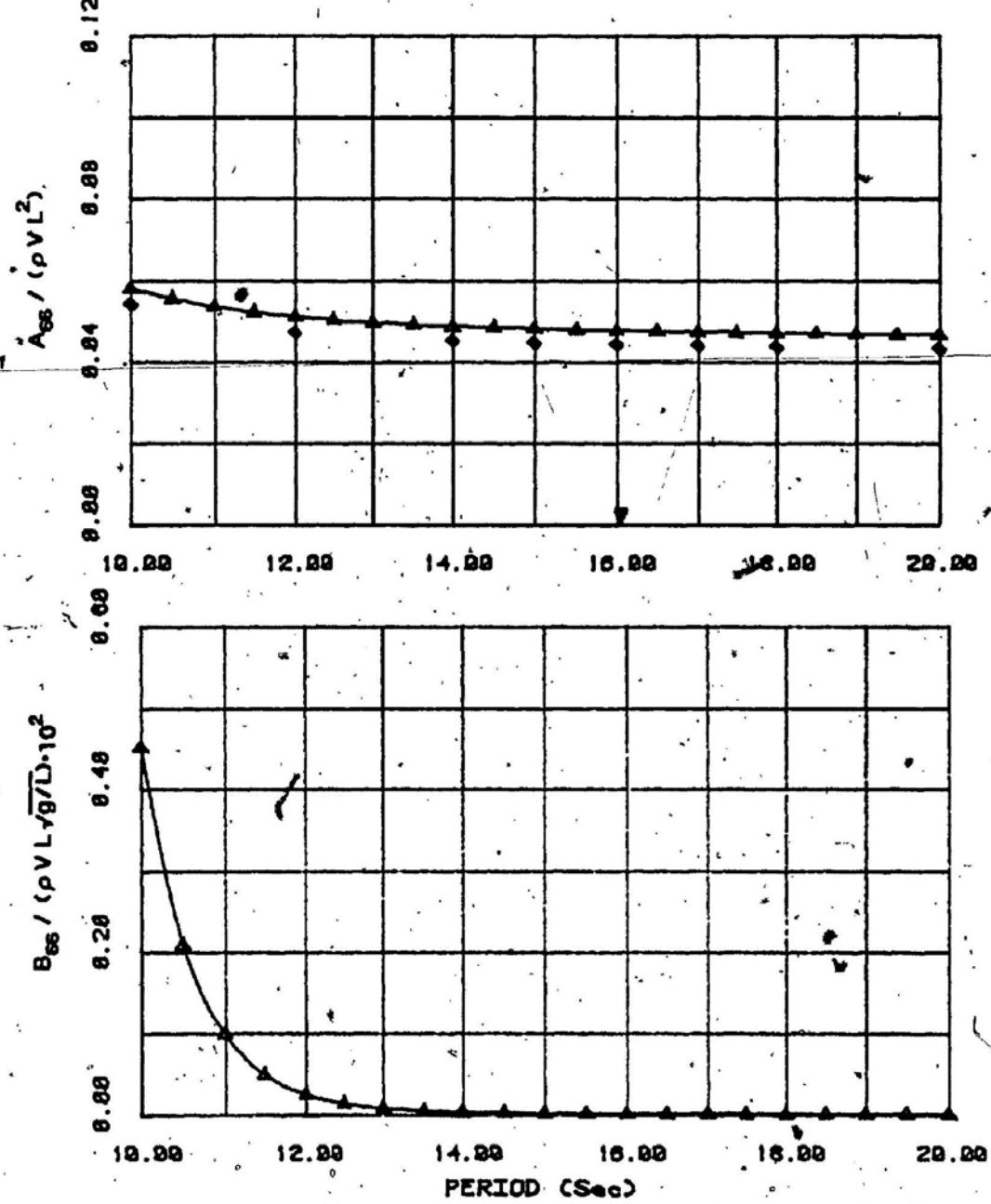


Figure (18) Added mass and damping in yaw for rectangular box
($L \times B \times D = 90 \times 90 \times 40$ m, water depth = 500m)

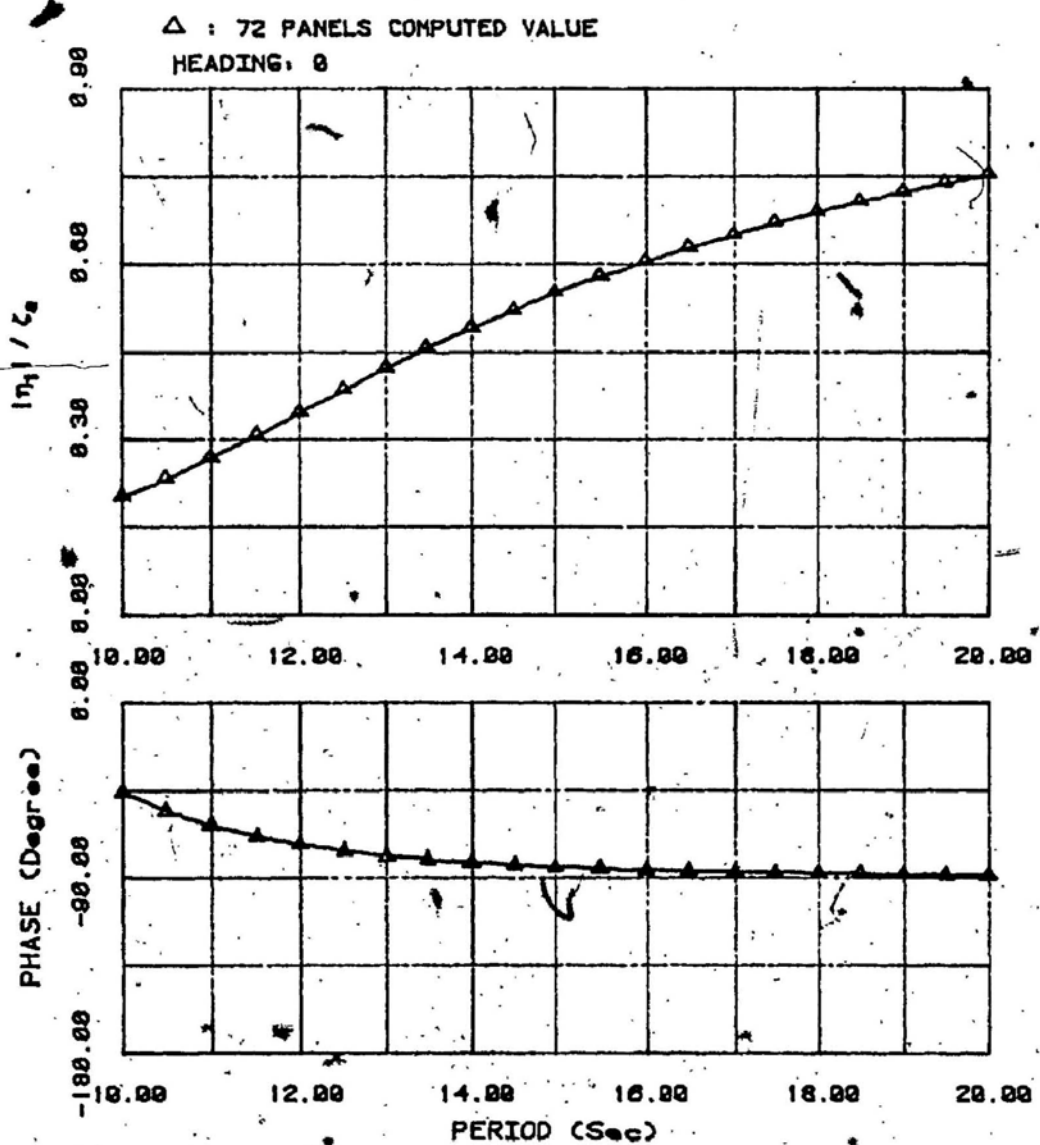


Figure (14-a) Surge motion and phase for rectangular box
($L \times B \times D = 90^{\circ}90^{\circ}40m$, water depth = 500m, heading = 0 Deg.)

- 69 -

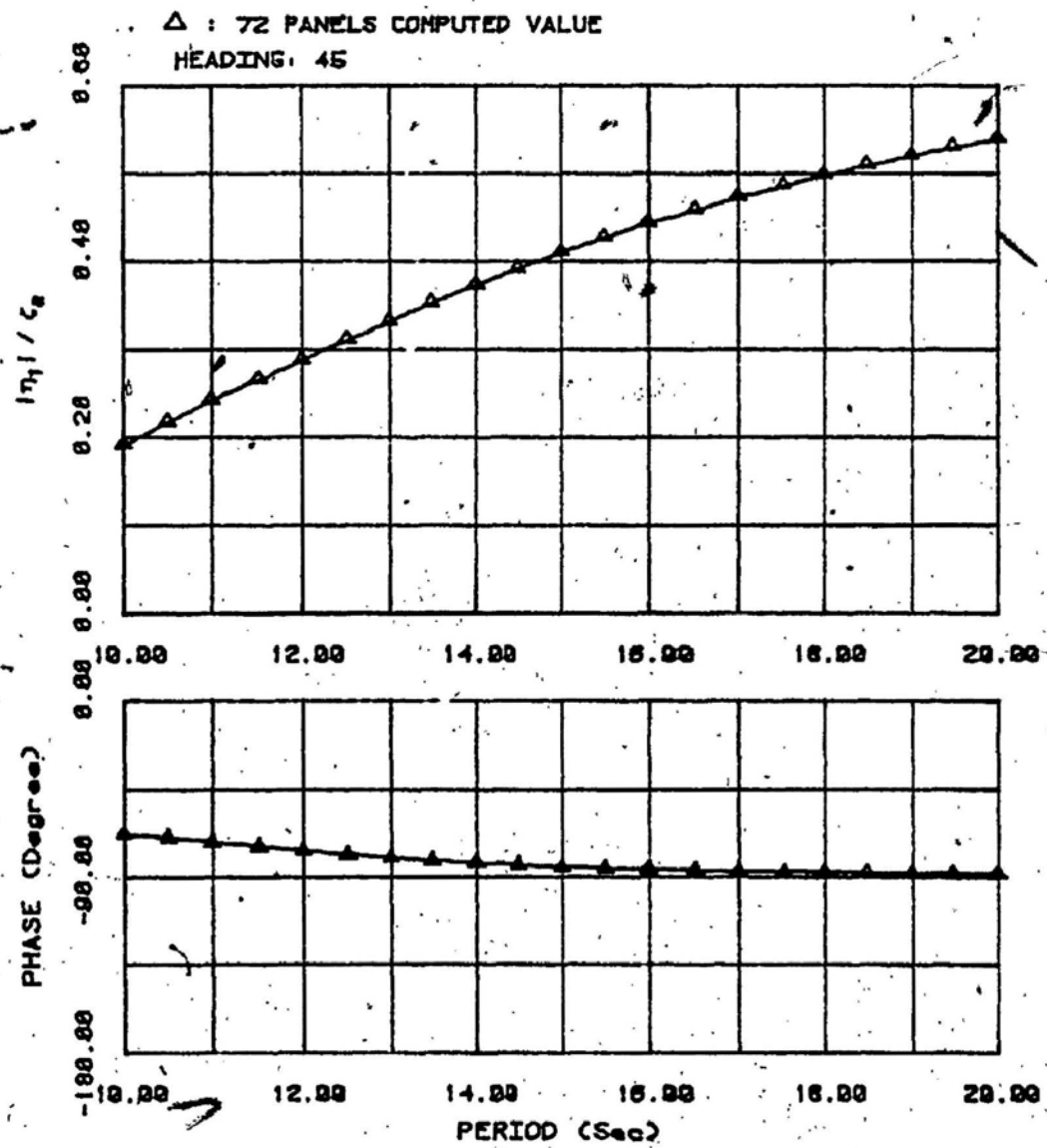


Figure (14.b) Surge motion and phase for rectangular box
($L \times B \times D = 90 \times 90 \times 40$ m, water depth = 500m, heading = 45 Deg.)

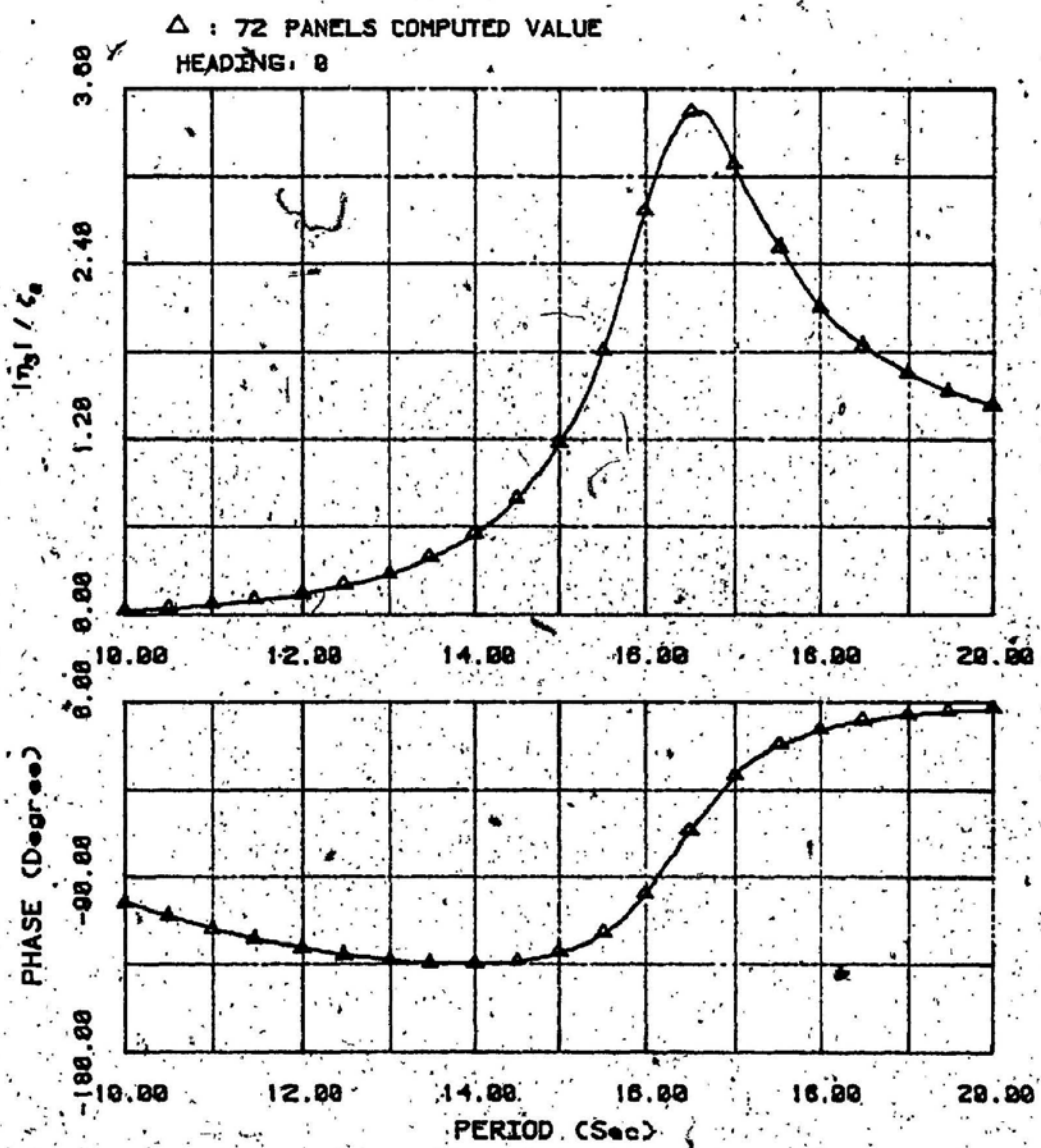


Figure (15.a) Heave motion and phase for rectangular box
($L^*B^*D = 90^*90^*40$ m, water depth = 500m, heading = 0 Deg.)

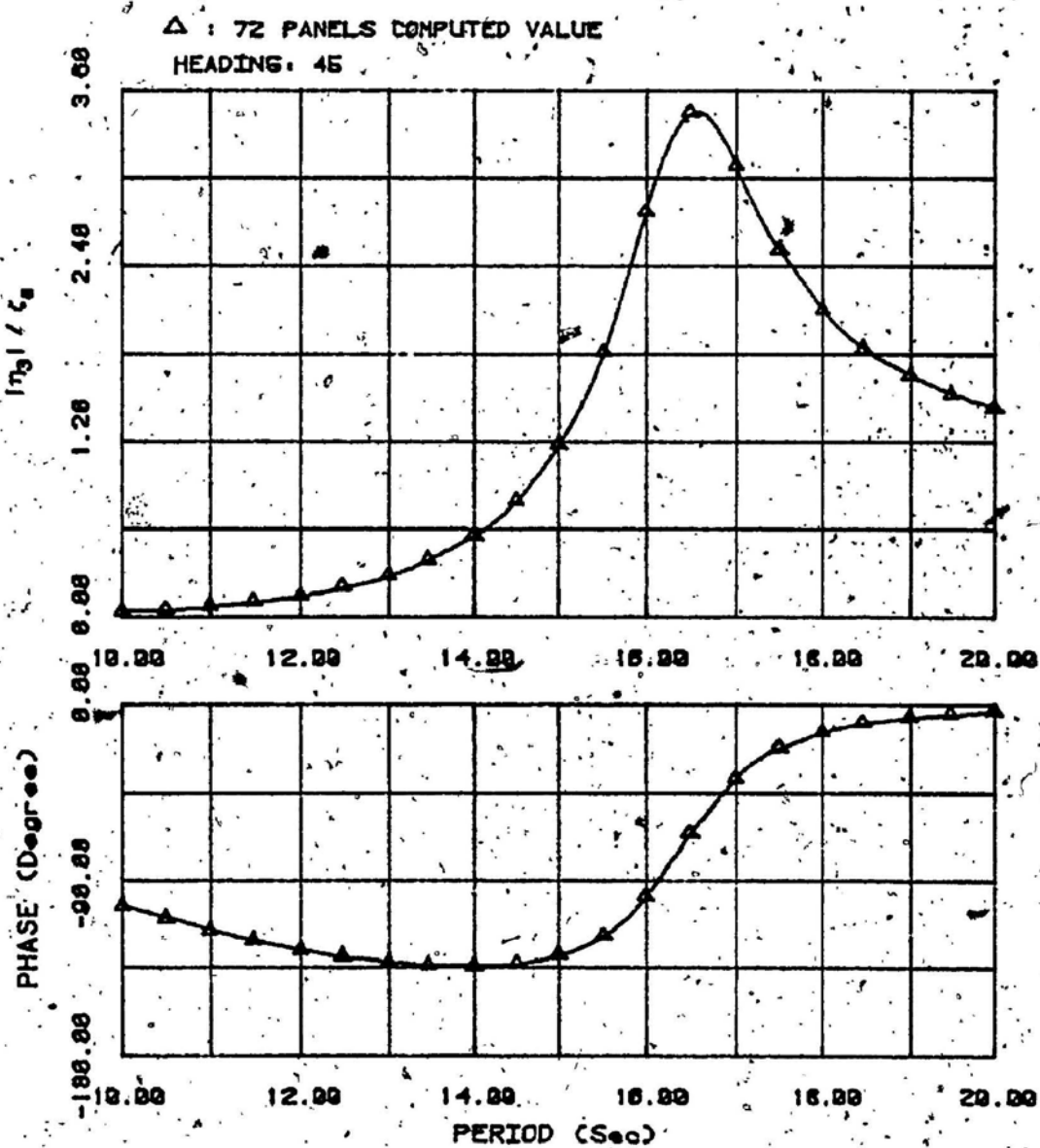


Figure (15.b) Heave motion and phase for rectangular box
($L^*B^*D = 90^*90^*40\text{m}$; water depth = 500m; heading = 45 Deg.)

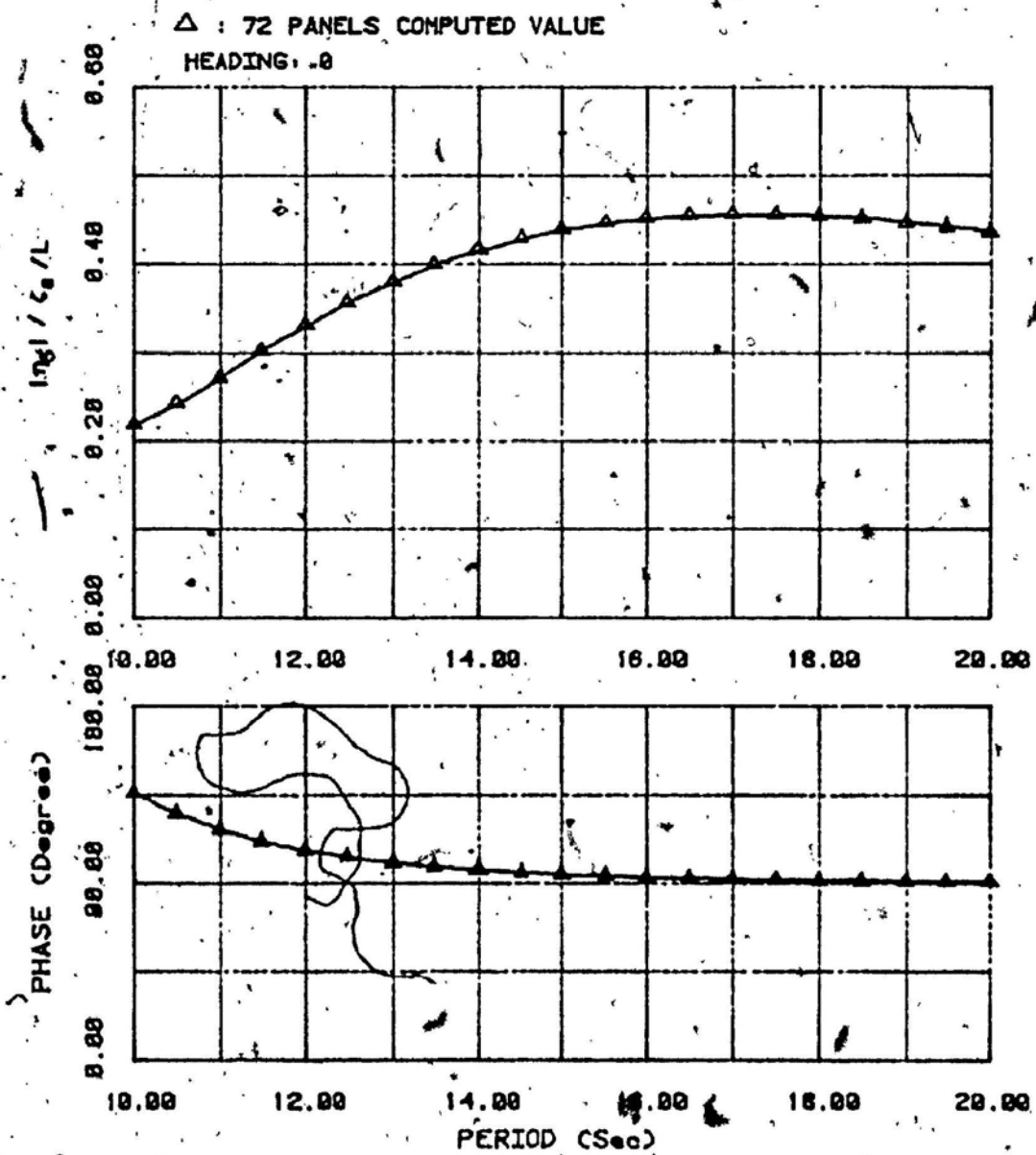


Figure (16.a) Pitch motion and phase for rectangular box
($L^*B^*D = 90^*90^*40$ m, water depth = 500m, heading = 0 Deg.)

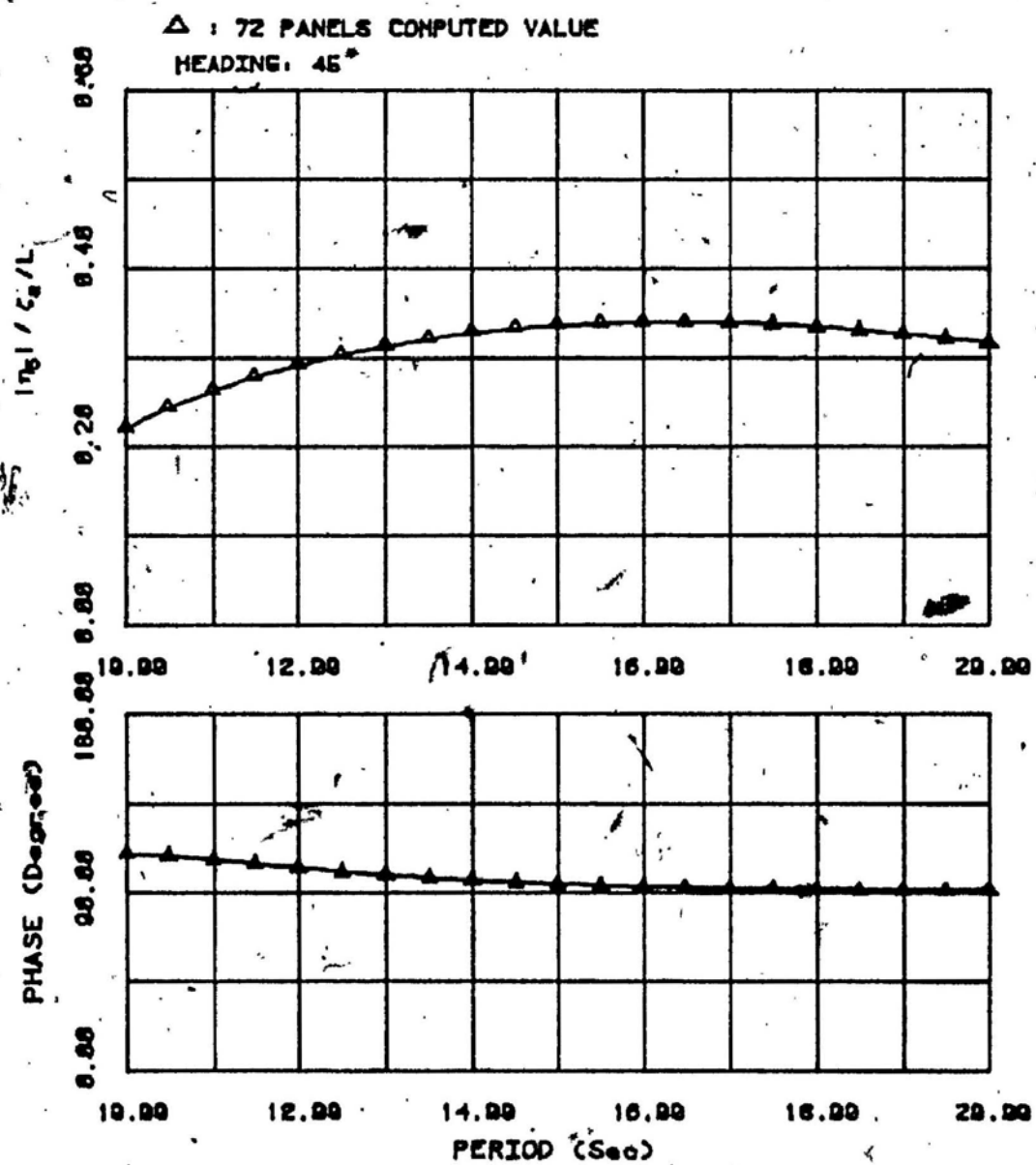


Figure (16.b) Pitch motion and phase for rectangular box
($L^aB^aD = 90^a90^a40$ m, water depth = 500m, heading = 45 Deg.)

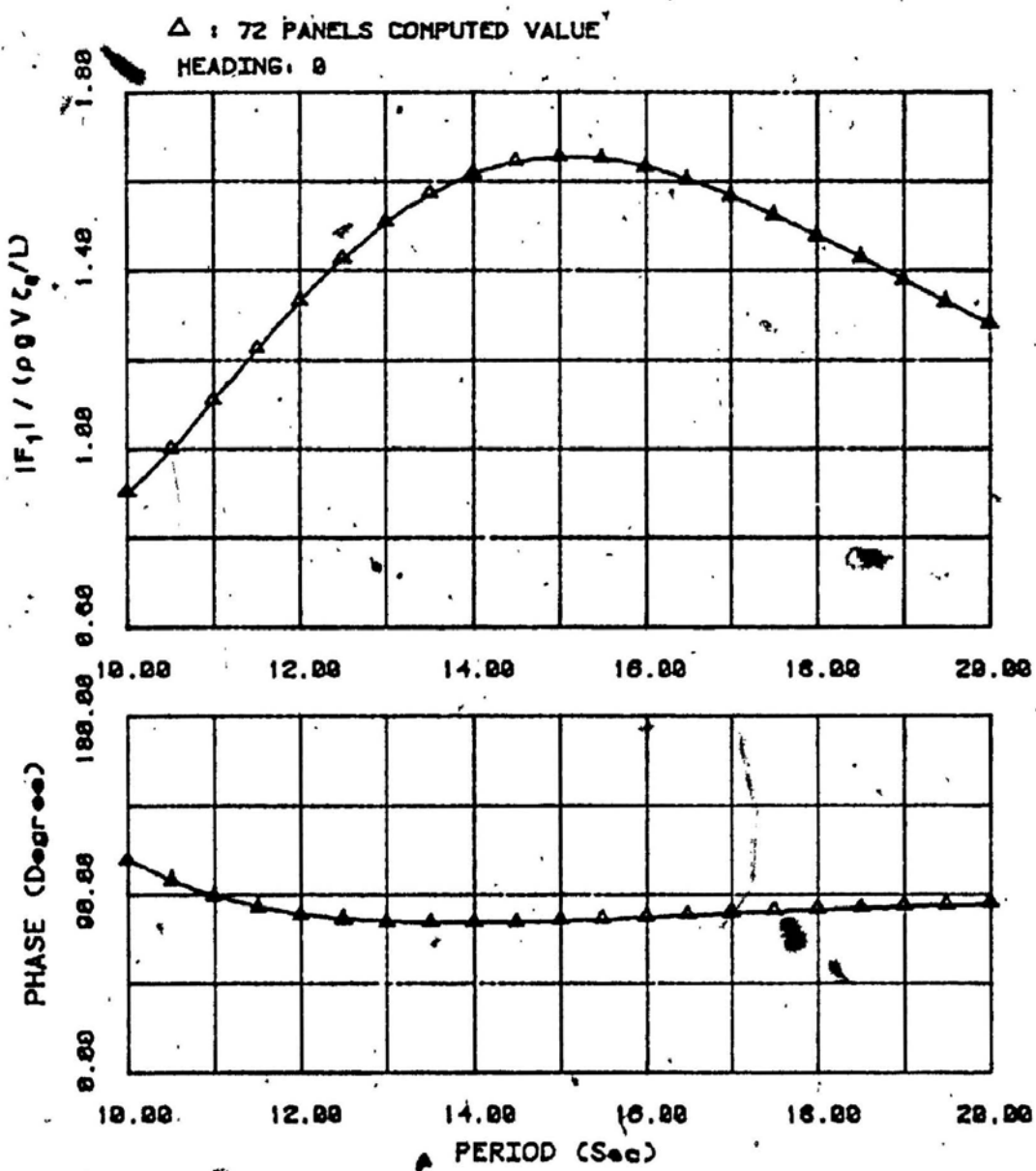


Figure (17.a) Surge exciting force and phase for rectangular box
($L^*B^*D = 90^*90^*40\text{m}$, water depth = 500m, heading = 0 Deg.)

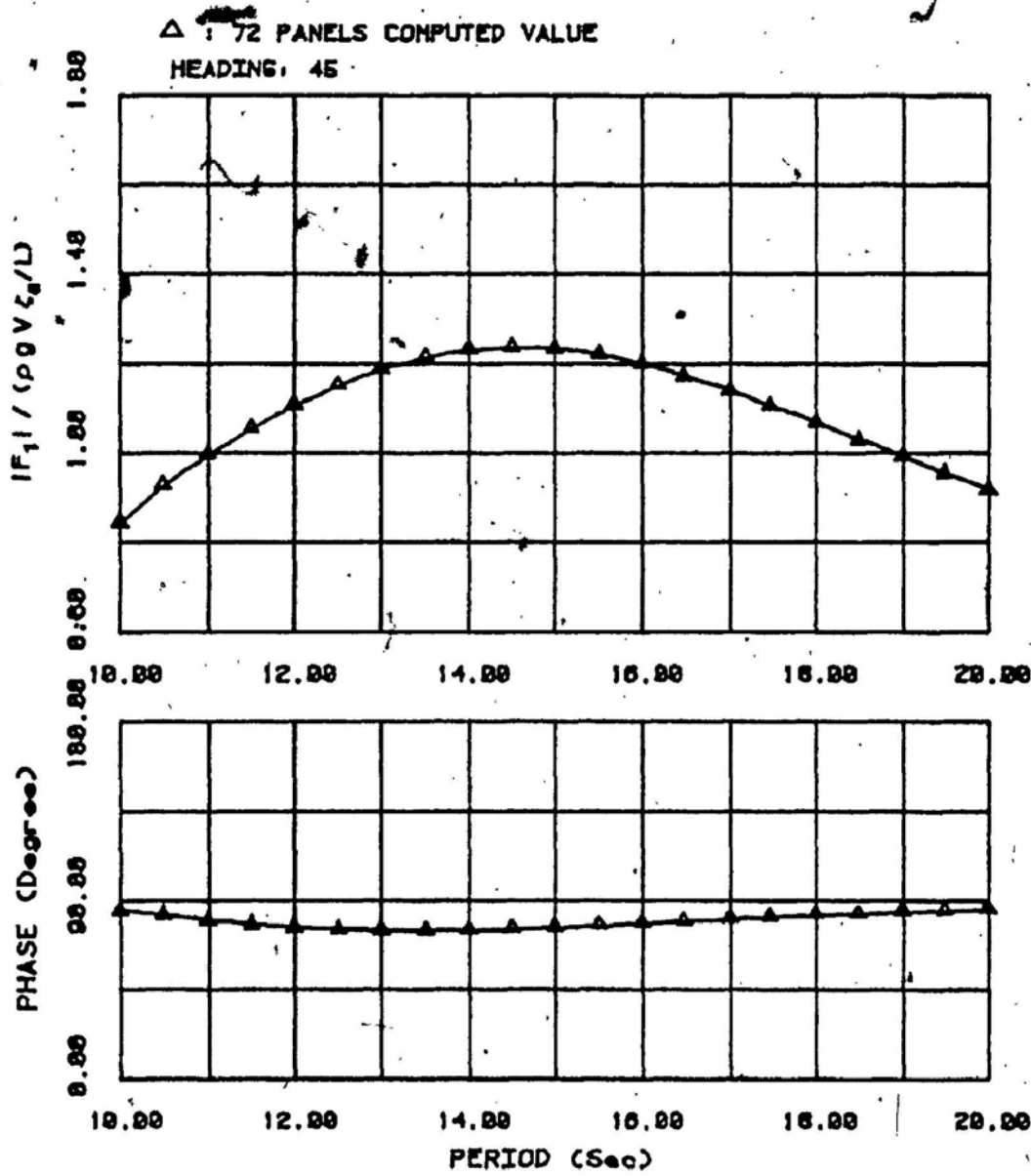


Figure (17.b) Surge exciting force and phase for rectangular box
($L^aB^aD = 90^a90^a40m$, water depth = 500m, heading = 45 Deg.)

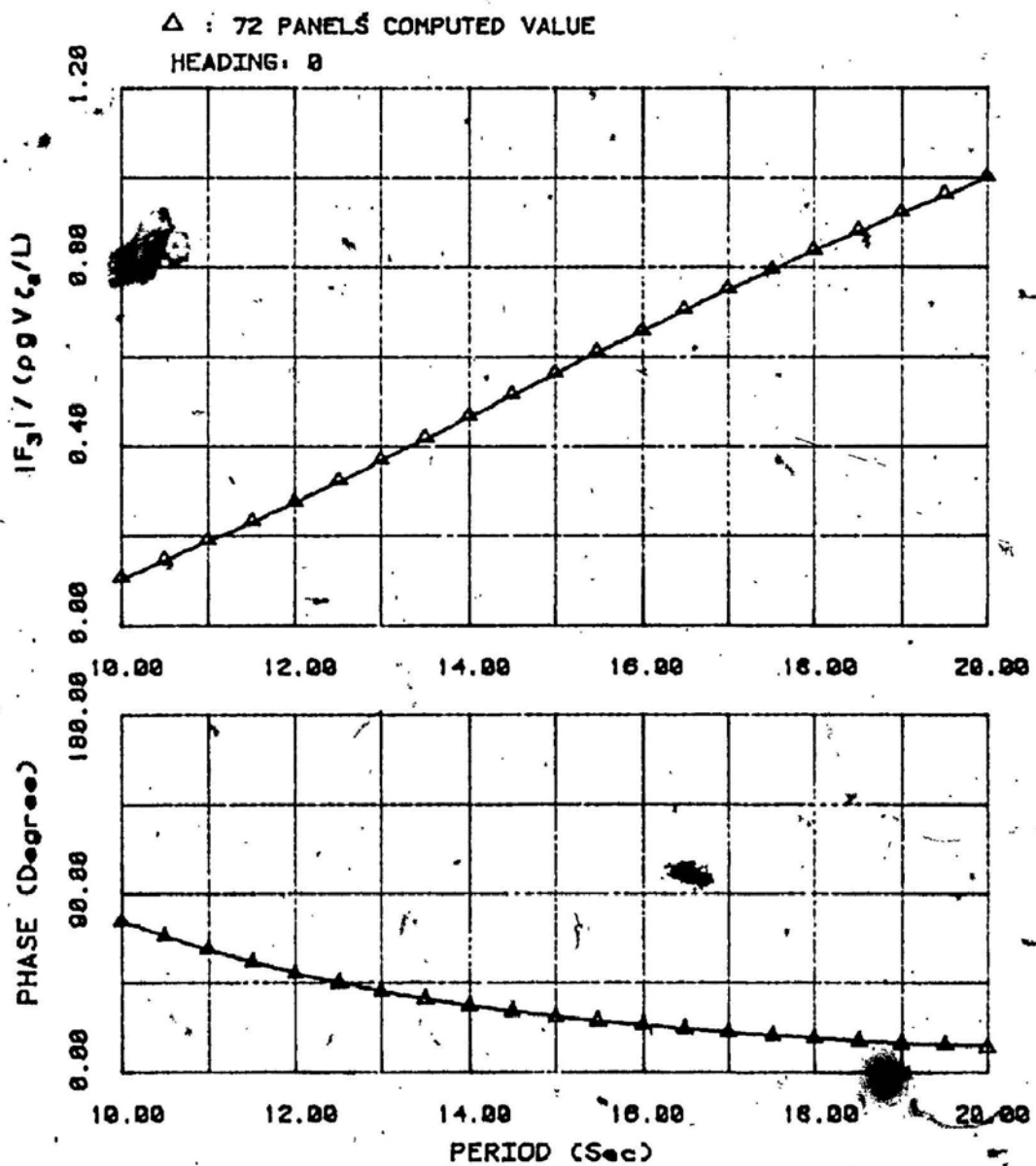


Figure (18.a) Heave exciting force and phase for rectangular box.
($L \times B \times D = 90 \times 90 \times 40$ m, water depth = 500m, heading = 0 Deg.)

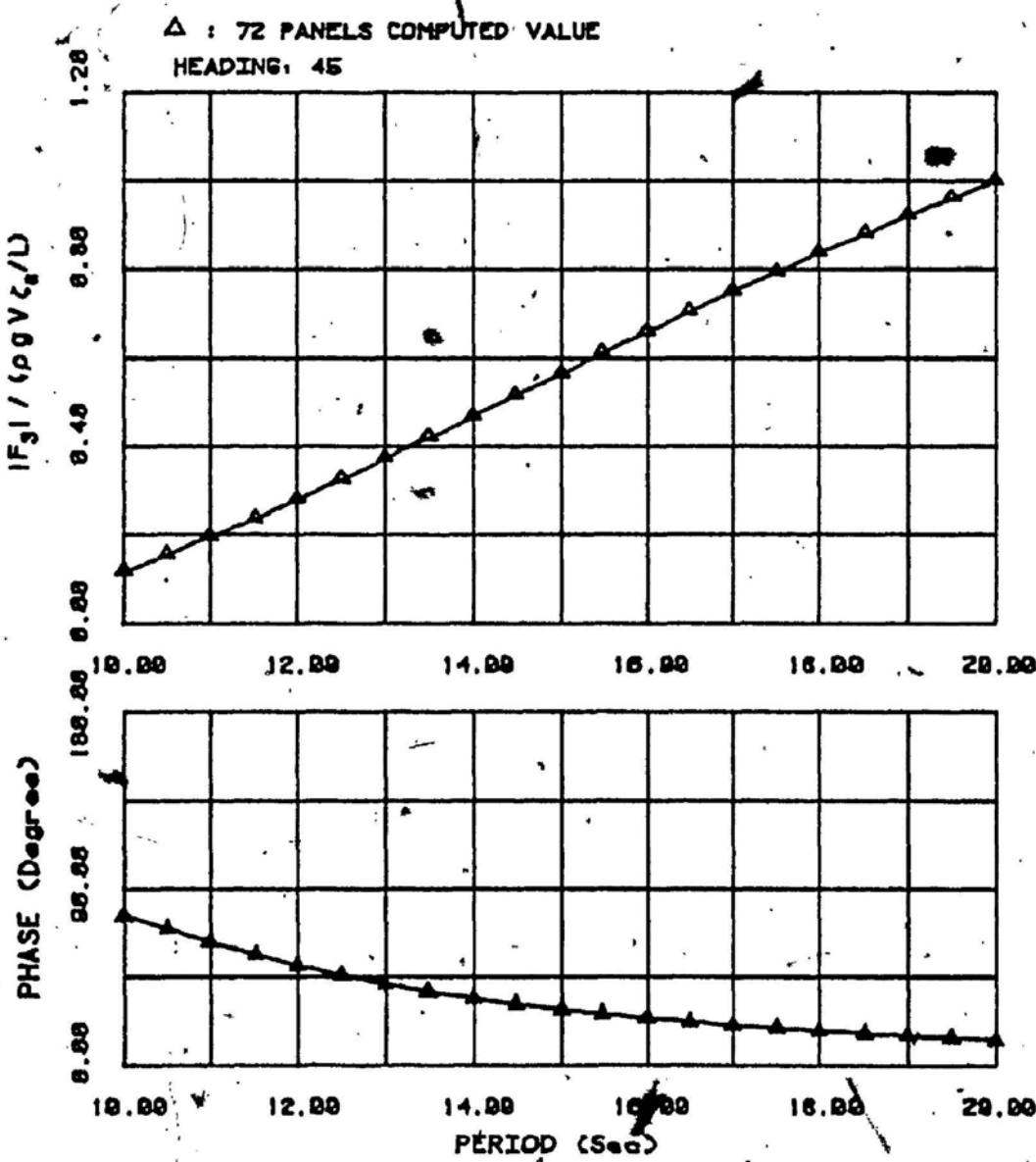


Figure (18.b) Heave exciting force and phase for rectangular box
($L^*B^*D = 90^*90^*40$ m, water depth = 500m, heading = 45 Deg.)

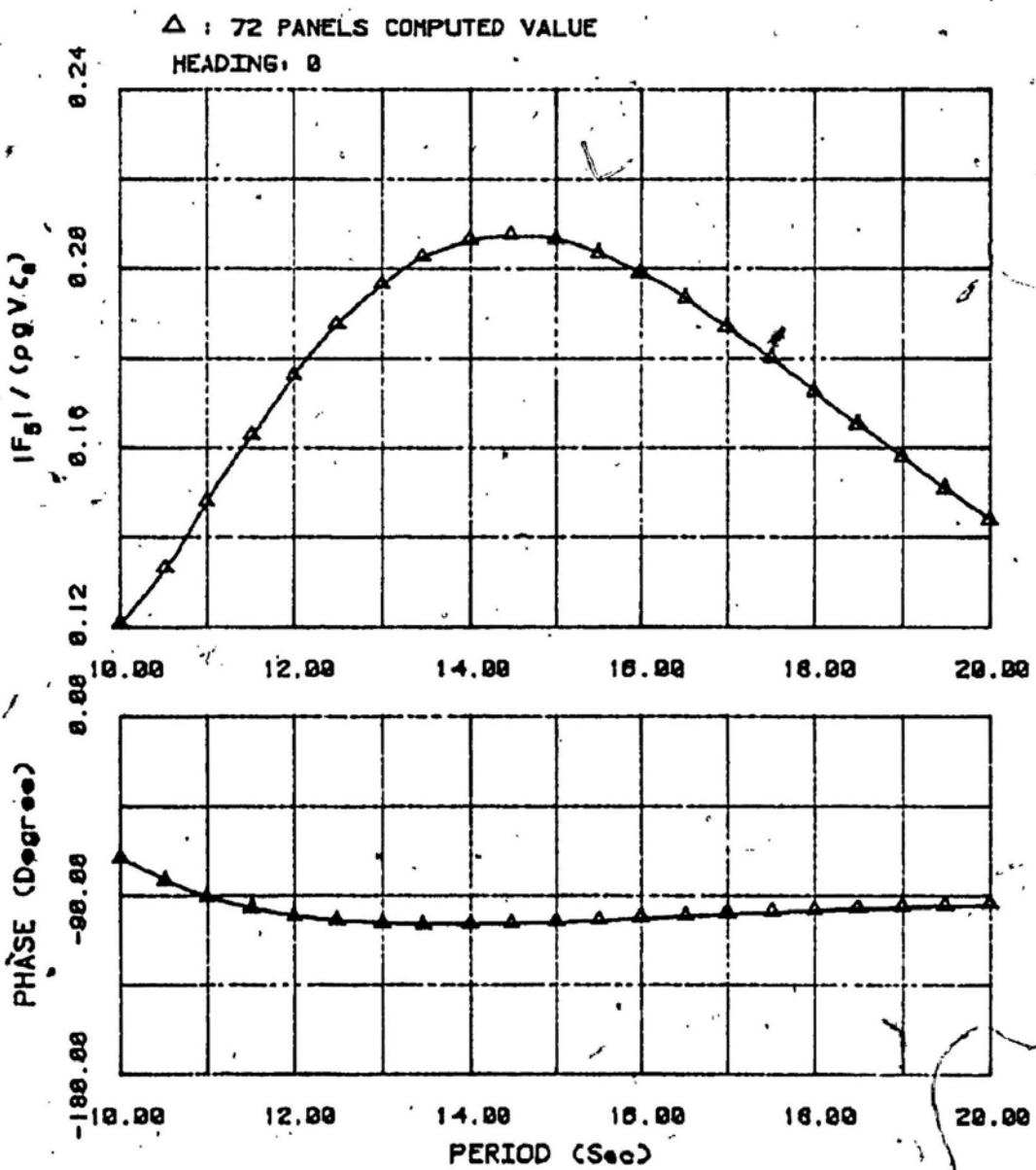


Figure (19.a) Pitch exciting force and phase for rectangular box
($L^*B^*D = 90^*90^*40$ m, water depth = 500m, heading = 0 Deg.)

- 79 -

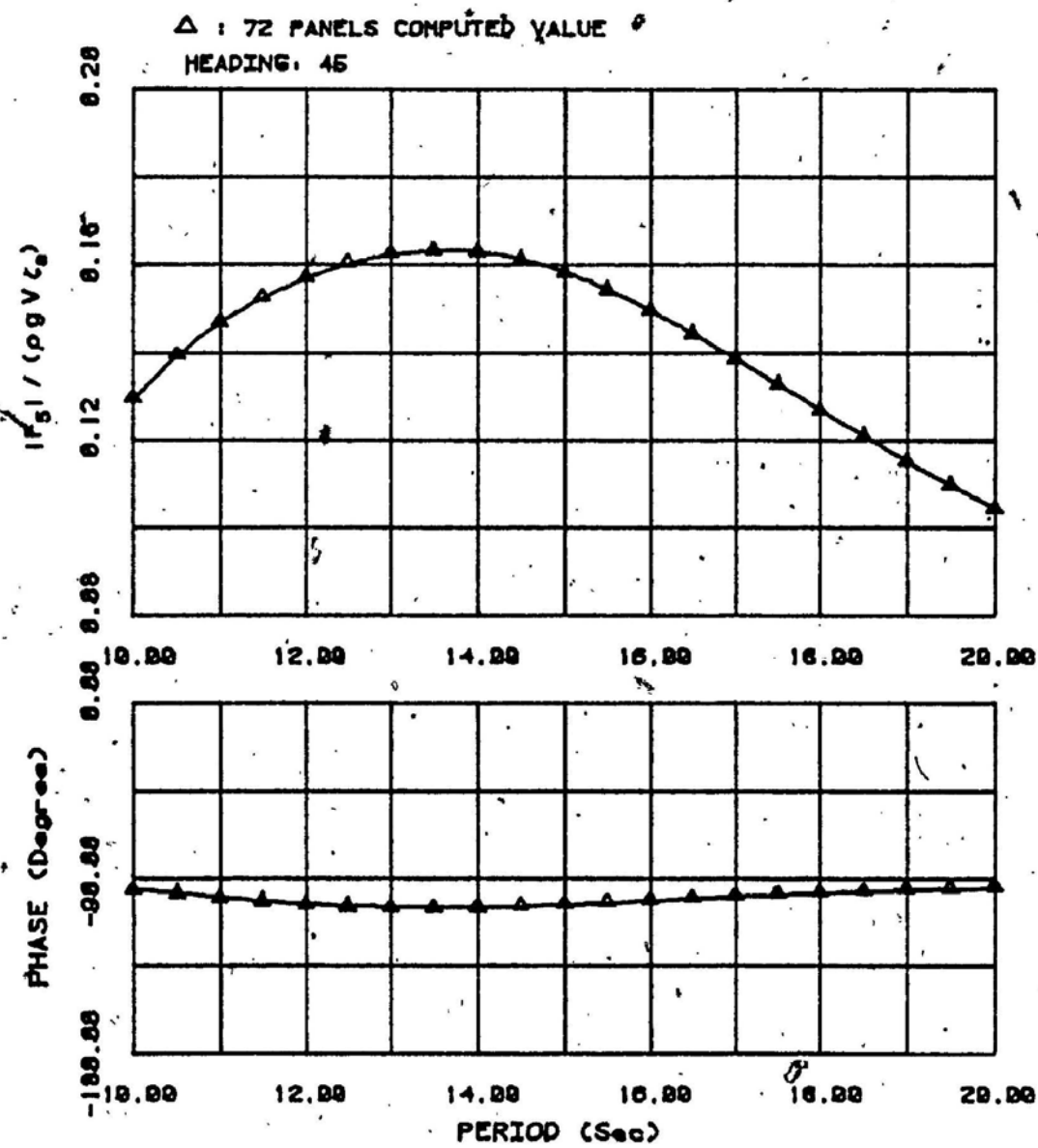


Figure (19.b) Pitch exciting force and phase for rectangular box.
($L^*B^*D = 90^*90^*40\text{m}$, water depth = 500m, heading = 45 Deg.)

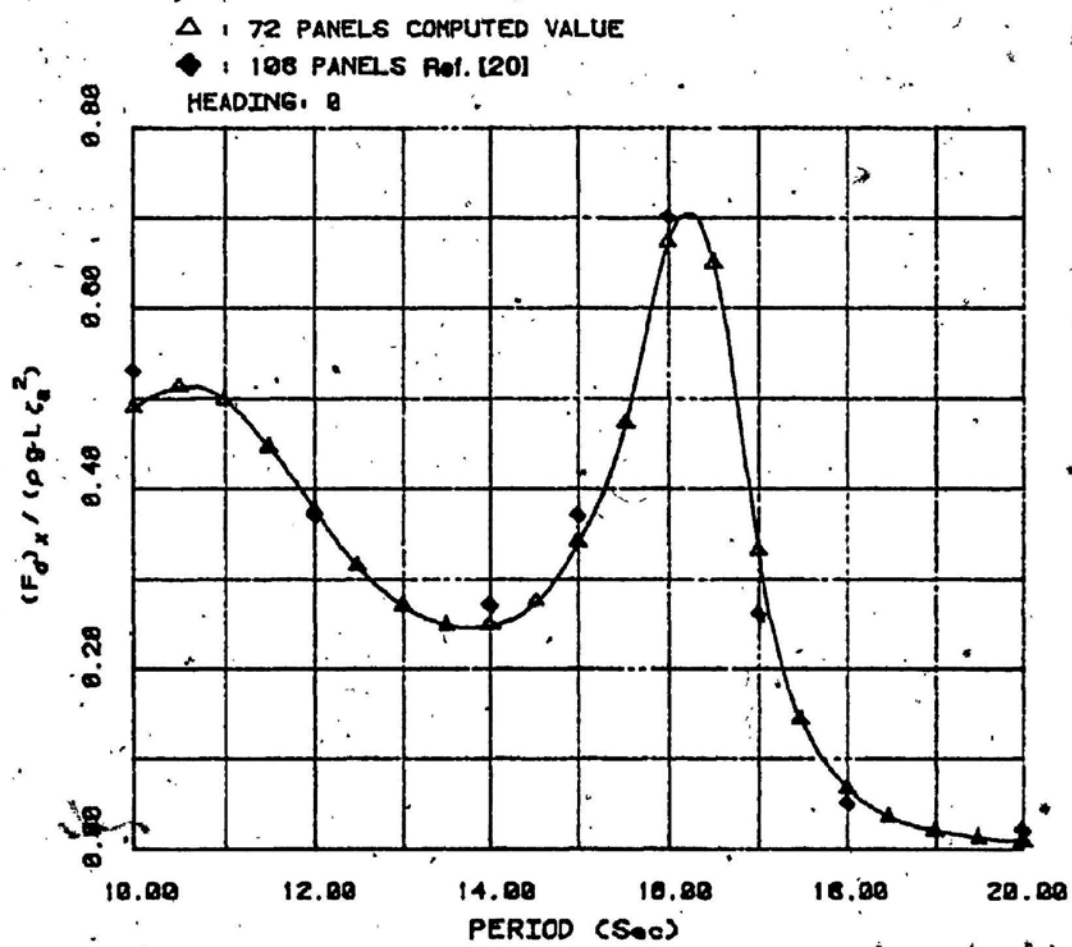


Figure (20.a) Drift force in x-component for rectangular box
($L^aB^aD = 90^a90^a40m$, water depth = 500m, heading = 0 Deg.)

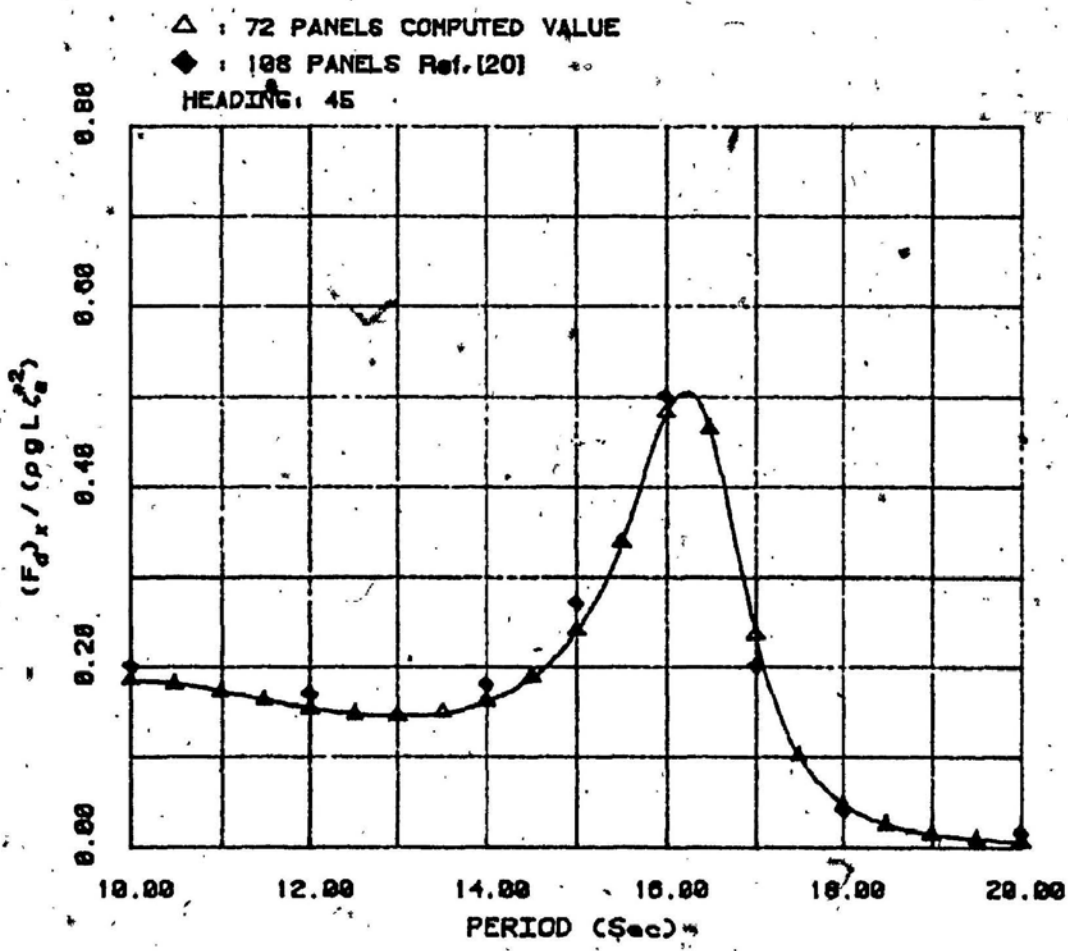


Figure (20.b) Drift force in x-component for rectangular box
($L^2B^2D = 90^2 \cdot 90 \cdot 40 \text{ m}^3$, water depth = 500m, heading = 45 Deg.)

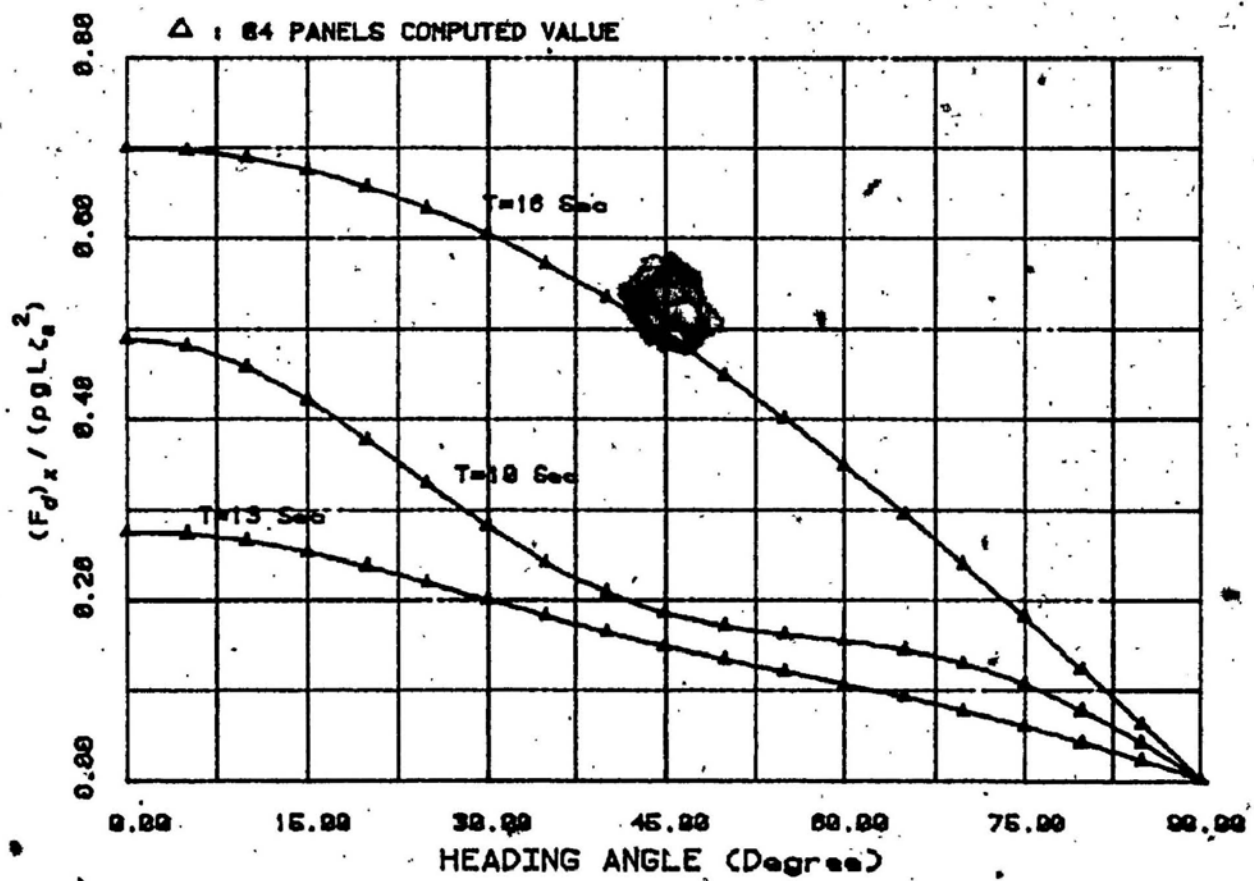


Figure (21) Drift force in x-component for rectangular box
at various heading angles ($L^*B^*D = 90^*90^*40\text{m}$, water depth = 500m)

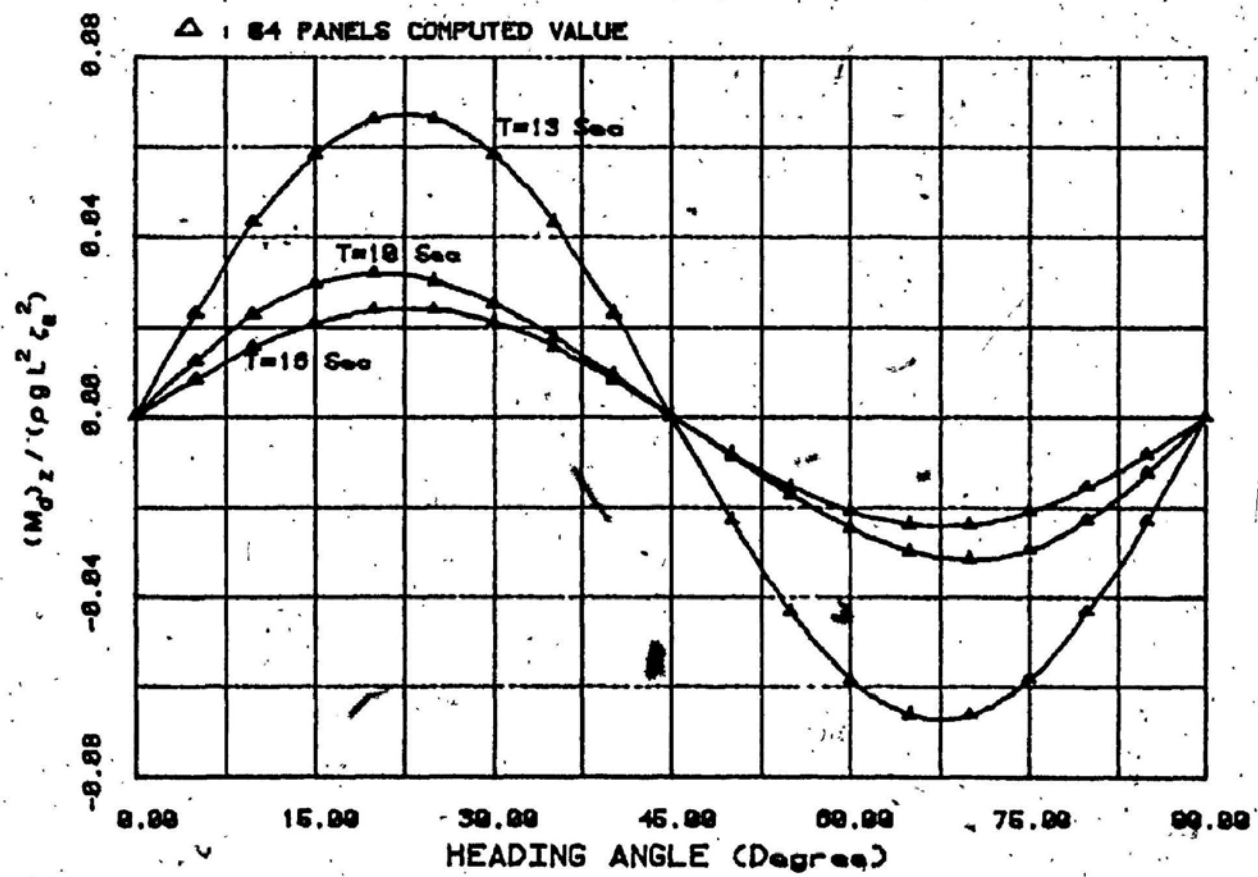


Figure (22) Vertical Drift moment for rectangular box
at various heading angles ($L^*B^*D = 90^*90^*40m$, water depth = 500m)

APPENDIX A

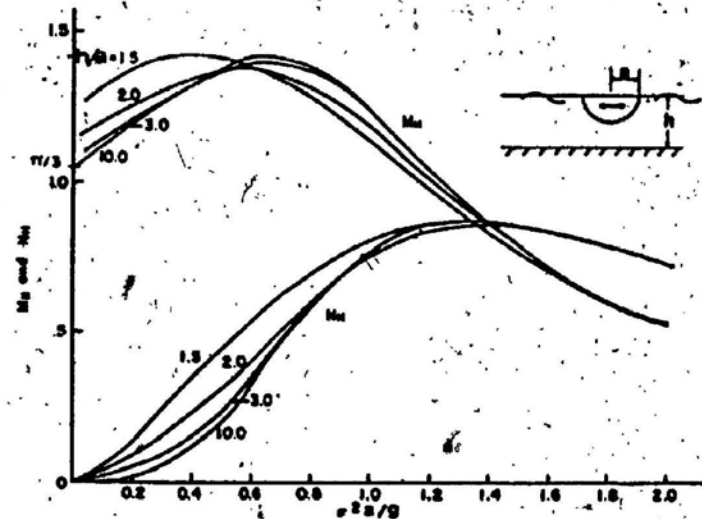


Figure 3.19 Added mass and damping in surge for a hemisphere

Figure (A-1)

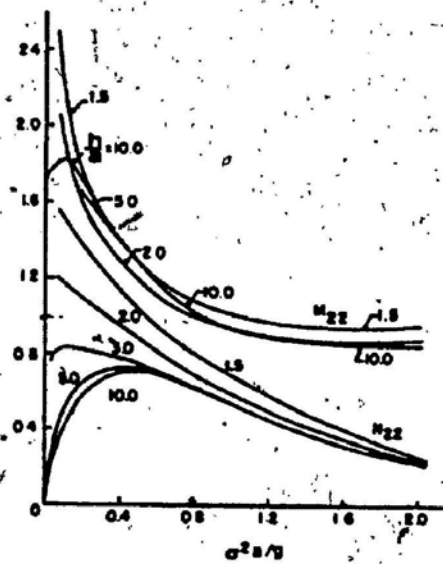


Figure 3.18 Added mass and damping in heave for a hemisphere

Figure (A-2)

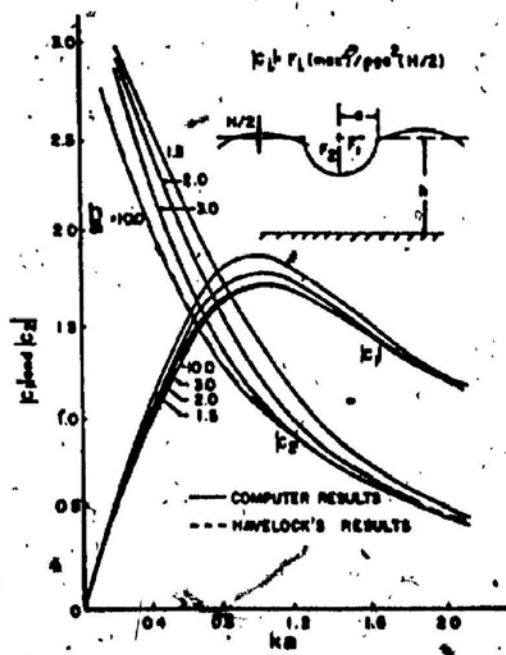


Figure 3.17 Surge and heave forces on a hemisphere

Figure (A-3)

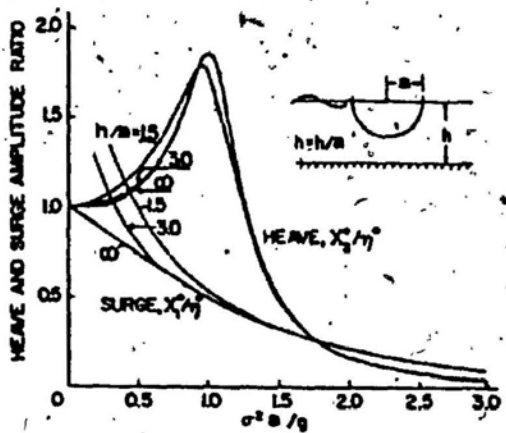
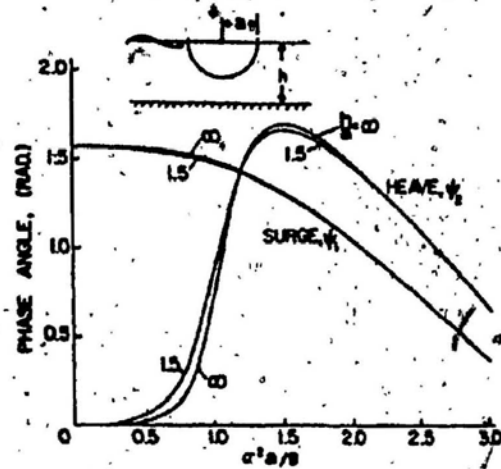


Figure (A-4)



Figures 3.20 Heave and surge response of a floating sphere

Figure (A-5)

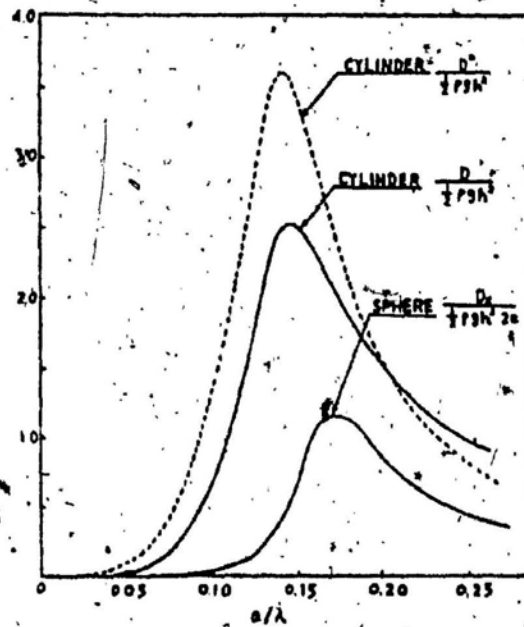


Fig. 2 Drifting force on circular cylinder and sphere floating on waves

Figure (A-6)

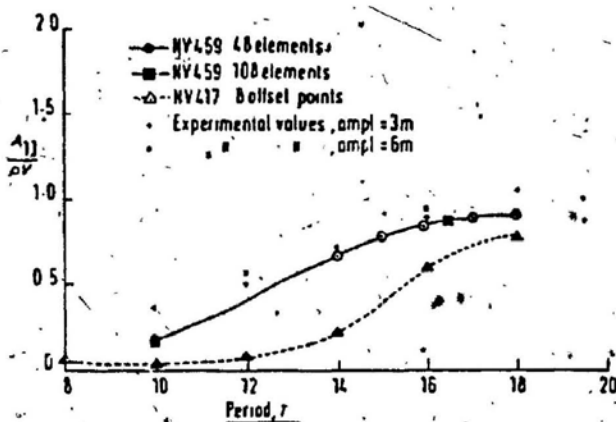


Fig. 4. Surge added-mass coefficients for floating box ($L \times B \times d = 90\text{m} \times 90\text{m} \times 40\text{m}$). Infinite water depth

Figure (A-7.a)

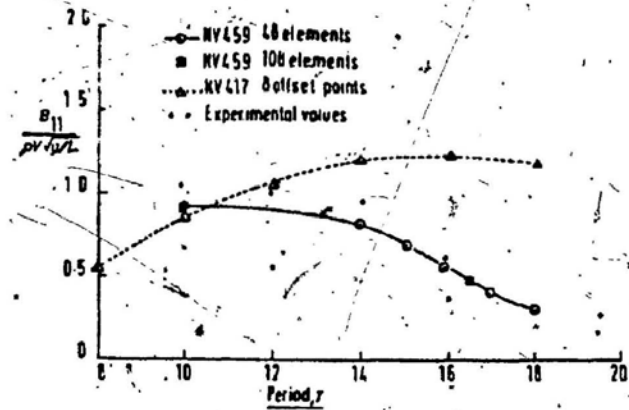


Fig. 12. Surge damping coefficients for floating box ($L \times B \times d = 90\text{m} \times 90\text{m} \times 40\text{m}$). Infinite water depth

Figure (A-7.b)

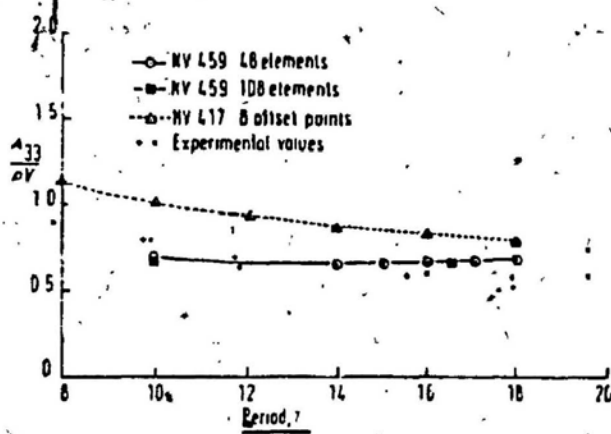


Fig. 6. Heave added-mass coefficients for floating box ($L \times B \times d = 90\text{m} \times 90\text{m} \times 40\text{m}$). Infinite water depth

Figure (A-8.a)

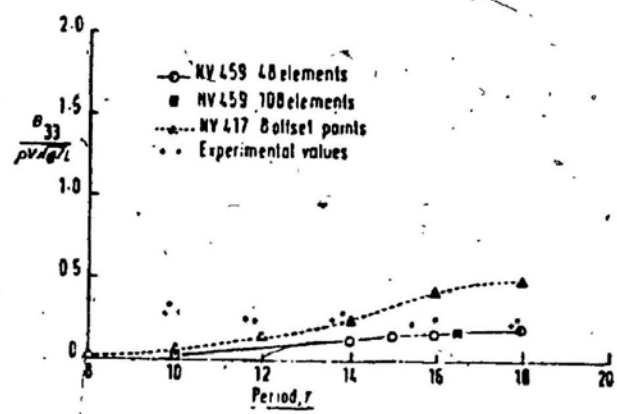


Fig. 14. Heave damping coefficients for floating box ($L \times B \times d = 90\text{m} \times 90\text{m} \times 40\text{m}$). Infinite water depth

Figure (A-8.b)

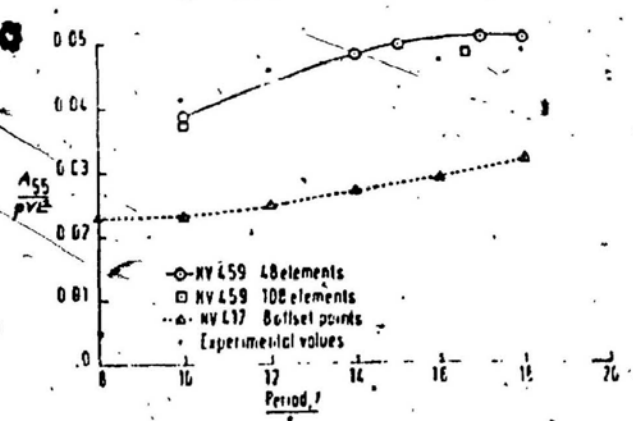


Fig. 8. Pitch added mass and damping coefficients for floating box ($L \times B \times d = 90\text{m} \times 90\text{m} \times 40\text{m}$). Infinite water depth

Figure (A-9.a)

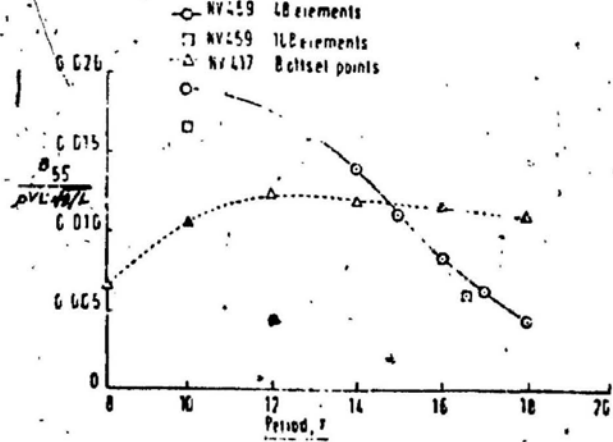


Fig. 16. Pitch added-mass and damping coefficients for floating box ($L \times B \times d = 90\text{m} \times 90\text{m} \times 40\text{m}$). Infinite water depth

Figure (A-9.b)

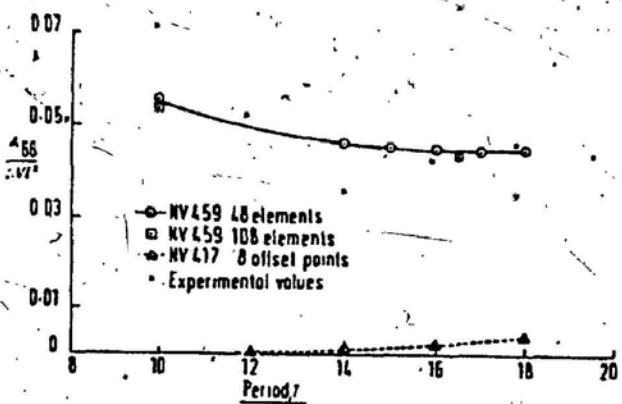


Fig. 10. Yaw added-mass coefficients for floating box.
($L \times B \times d = 90\text{m} \times 90\text{m} \times 40\text{m}$). Infinite water depth.

Figure (A-10.a)

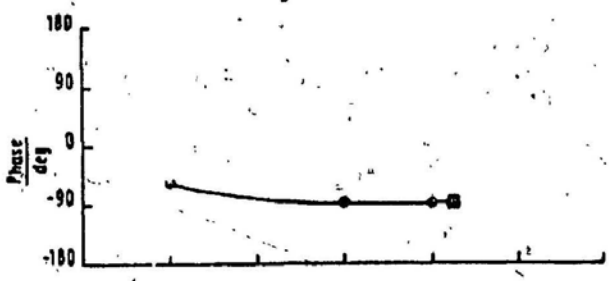
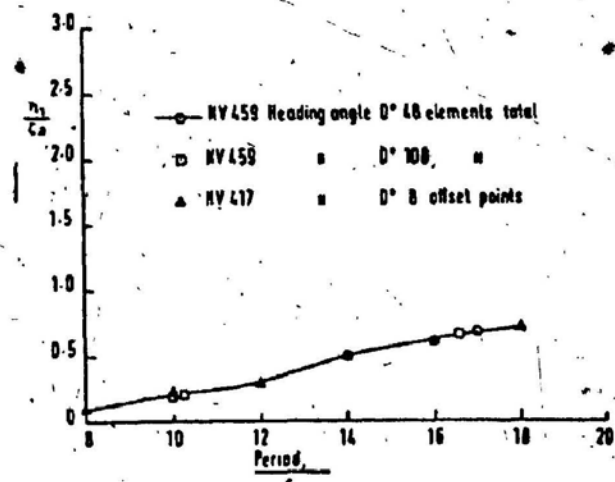


Fig. 32. Motions of floating box ($L \times B \times d = 90\text{m} \times 90\text{m} \times 40\text{m}$). Infinite water depth, amplitudes and phases

Figure (A-11.a)

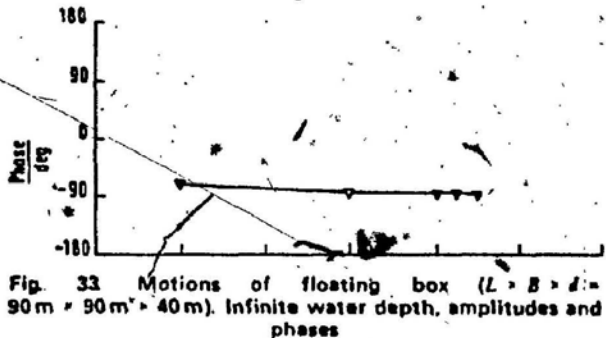
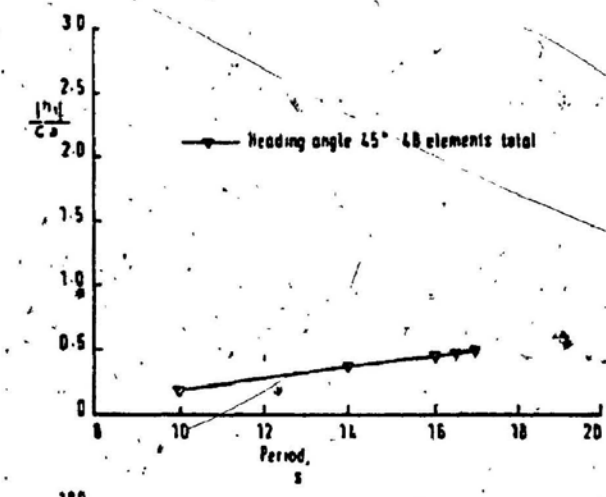


Fig. 33. Motions of floating box ($L \times B \times d = 90\text{m} \times 90\text{m} \times 40\text{m}$). Infinite water depth, amplitudes and phases

Figure (A-11.b)

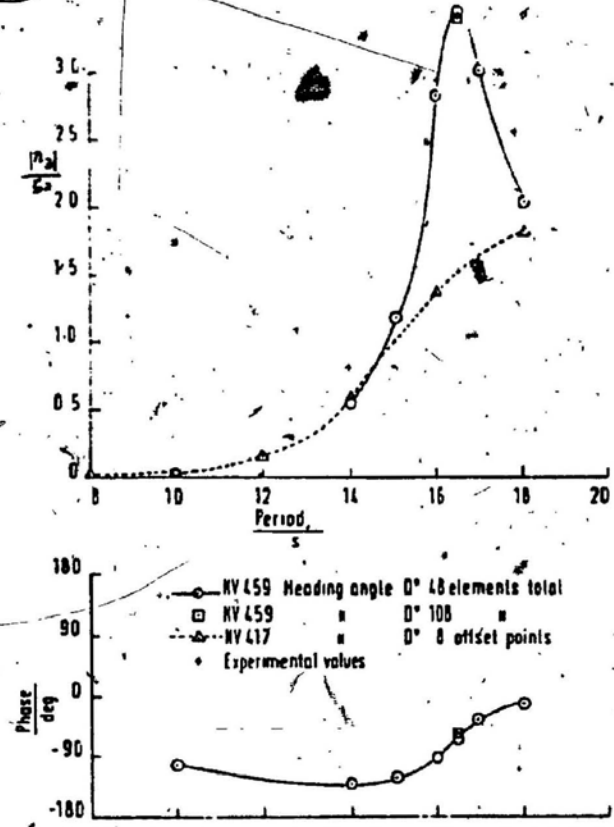


Fig. 35 Motions of floating box ($L \times B \times d = 90m \times 90m \times 40m$). Infinite water depth, amplitudes and phases

Figure (A-12.a)

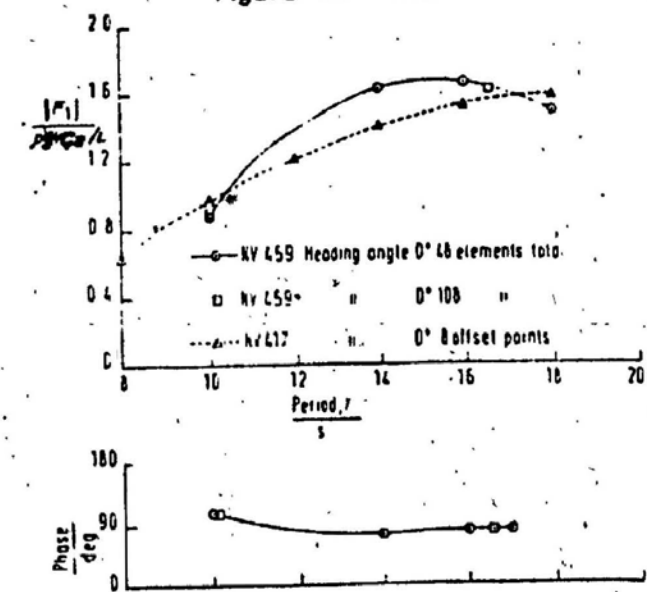


Fig. 1B Exciting force on floating box ($L \times B \times d = 90m \times 90m \times 40m$). Infinite water depth, amplitudes and phases

Figure (A-14.a)

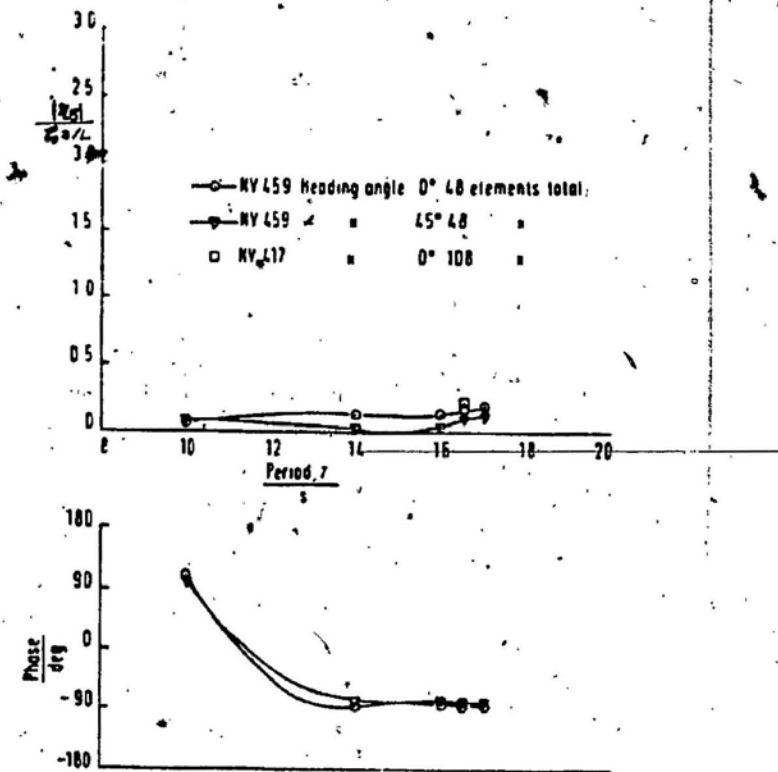


Fig. 37 Motions of floating box ($L \times B \times d = 90m \times 90m \times 40m$). Infinite water depth, amplitudes and phases

Figure (A-13.a)

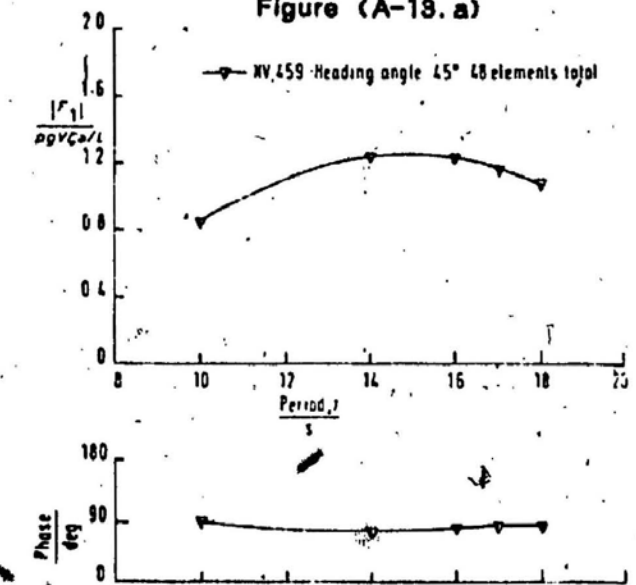


Fig. 20 Exciting force on floating box ($L \times B \times d = 90m \times 90m \times 40m$). Infinite water depth, amplitudes and phases

Figure (A-14.b)

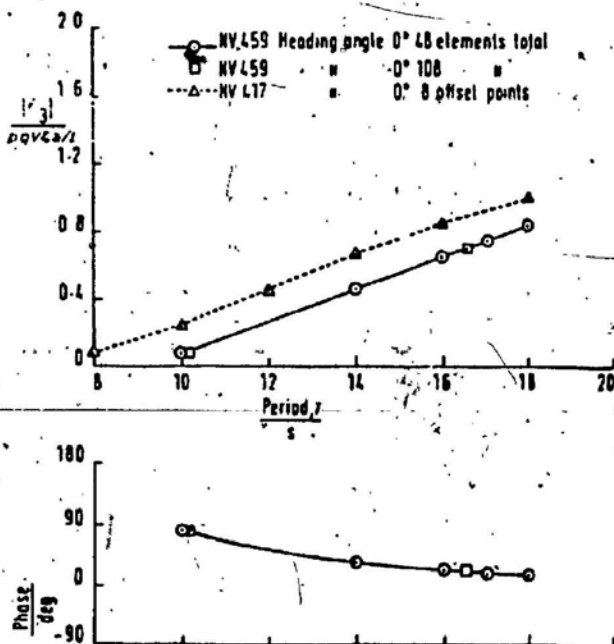


Fig. 22 Exciting force on floating box ($L = B = d = 90 \text{ m} > 90 \text{ m} \times 40 \text{ m}$). Infinite water depth, amplitudes and phases.

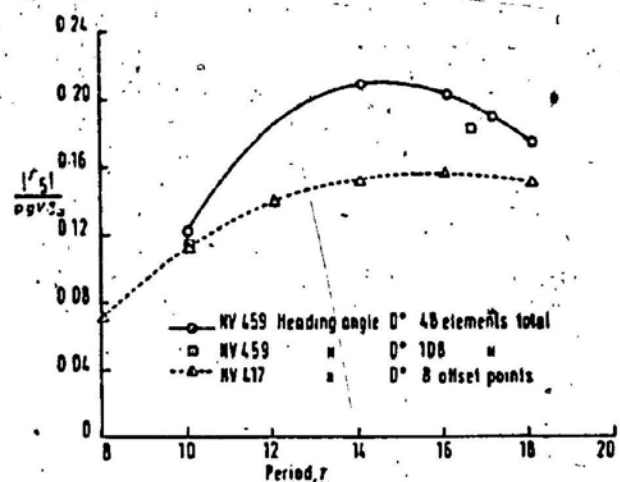


Fig. 25 Exciting moment on floating box ($L = B = d = 90 \text{ m} > 90 \text{ m} \times 40 \text{ m}$) Infinite water depth, amplitudes and phases

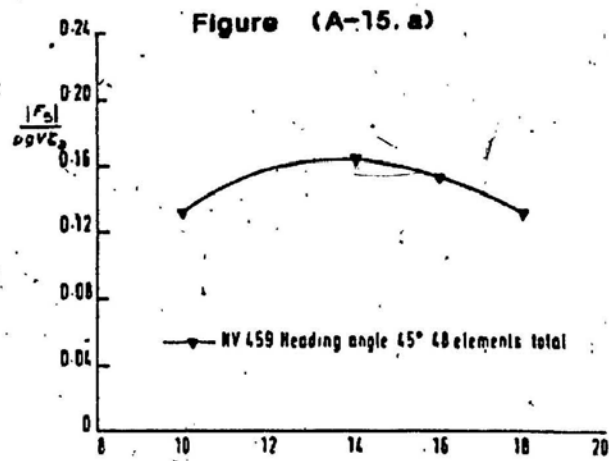


Fig. 26 Exciting moment on floating box ($L = B = d = 90 \text{ m} > 90 \text{ m} \times 40 \text{ m}$). Infinite water depth, amplitudes and phases



Figure (A-16. b)

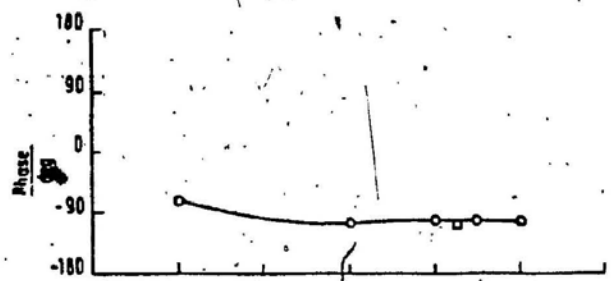


Figure (A-16. b)

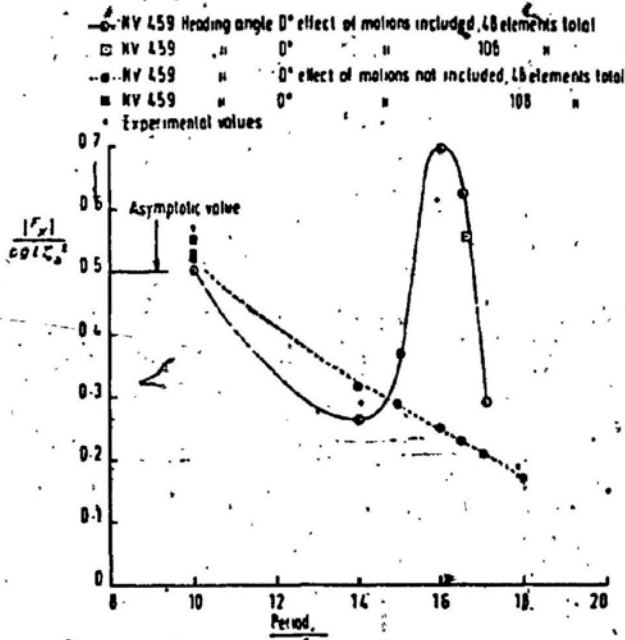


Fig. 28. Drift forces on floating box ($L \times B \times d = 90 \text{ m} \times 90 \text{ m} \times 40 \text{ m}$). Infinite water depth

Figure (A-17.a)

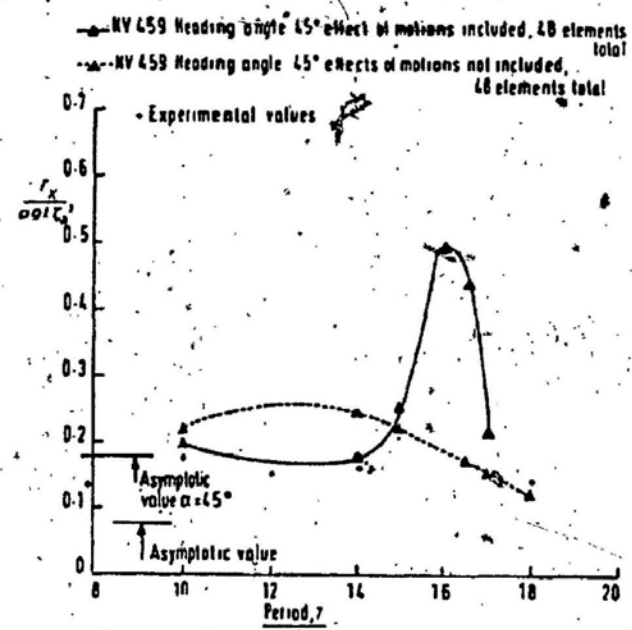


Fig. 28. Drift forces on floating box ($L \times B \times d = 90 \text{ m} \times 90 \text{ m} \times 40 \text{ m}$). Infinite water depth

Figure (A-17.b)

APPENDIX B
SAMPLE COMPUTER PROGRAM

PROGRAM MAIN

```
DIMENSION PAN(36,3),UN(36,3),UNN(36,3),SUR(36),
1           DG11R(36,36),DG11I(36,36),DG12R(36,36),DG12I(36,36),
2           • G11R(36,36),G11I(36,36),G12R(36,36),G12I(36,36),
3           PHI7R(36),PHI7I(36),PHI8R(36),PHI8I(36),QDF1(72),QDF2(72),
4           • POT135(72,4),POT246(72,4),Q135(72,4),Q246(72,4),
5           AM(6,6),DEMP(6,6),RM(6,6),C(6,6),FOR(12),AMP(12)
DIMENSION DA(72,72),DN(72,4),TTUN(36,6),PO1R(36),POLI(36),
1           PO2R(36),PO2I(36),TPR(36,6),TPI(36,6),
2           VA(3),VB(3),VC(3),VD(3),VE(3),VF(3)

COMMON /C2/ GRAV,DEN,FREQ,DEPTH,MNUM,ANU,HEAD
COMMON /C3/ VOL,XB,YB,ZB,AREA,AREAMP,XG,YG,ZG
COMMON /CC/ RI44,RI55,RI66
COMMON /SER/ UK(1000),GAMMA(1000),ALPHA
DATA NSP/36/
DATA GRAV,DEN/9.8,1000.0/
DATA XG,YG,ZG/0.0,0.0,10.62/
DATA RI44,RI55,RI66/33.04,32.09,32.92/
DATA DEPTH,HEAD/500.0,0.0/
```

C*****

C.....DEFINITION

C.....PAN	COORDINATE OF CENTROID OF PANEL (X,Y,Z) (INPUT)
C.....UN	UNIT OUTWARD NORMAL OF PANEL (N1,N2,N3) (INPUT)
C.....UNN	(N4,N5,N6)
C.....SUR	SURFACE AREA OF PANEL (INPUT)
C.....NSP	NUMBER OF PANELS (0.5*TOTAL PANELS)
C.....VOL	VOLUME
C.....XB,YB,ZB	CENTER OF BUOYANCY
C.....AREA	NETTED SURFACE AREA
C.....AREAMP	WATER PLANE AREA
C.....XG,YG,ZG	CENTER OF GRAVITY (INPUT)
C.....RI44,...	MOMENT OF INERTIA (INPUT)
C.....GRAV	GRAVITATION CONSTANT (INPUT)
C.....DEN	FLUID DENSITY (INPUT)
C.....FREQ	FREQUENCY (INPUT **)
C.....DEPTH	WATER DEPTH (INPUT)
C.....MNUM	WAVE NUMBER (INPUT **)
C.....ANU	FREQ*FREQ/GRAV
C.....HEAD	HEADING ANGLE (INPUT)
C.....POT135	POTENTIAL OF SYMMETRIC PART
C.....POT246	POTENTIAL OF ANTI-SYMM. PART
C.....Q135	SOURCE DENSITY OF SYM. PART
C.....Q246	SOURCE DENSITY OF ANTI-SYMM. PART
C.....AM	ADDED MASS
C.....DEMP	DAMPING COEFFICIENT

C.....RM REAL MASS TENSOR
C.....C RESTORING COEF.
C.....FOR EXCITING FORCE, (1-6 REAL, 7-12 IMAG)
C.....AMP MOTION AMPLITUDE (1-6 REAL, 7-12 IMAG)
C.....DRIFX DRIFT FORCE (X-COMP)
C.....DRIFY DRIFT FORCE (Y-COMP)
C.....DRMZ DRIFT MOMENT (Z-COMP)

C*****

```
CALL ASSIGN (1,'PRNT1.DAT')
CALL ASSIGN (2,'COM.DAT')
HEAD=HEAD/180.0*3.14159
CALL CHART(NSP,PAN,UN,UNN,SUR,C,RM)
CALL PRNT1(NSP,PAN,UN,UNN,SUR,C,RM)
DO 17 KI=1,6
TT=10.+2.0*(KI-1.0)
WNUM=4.0*3.14159*3.14159/(GRAV*TT*TT)
CALL LINK1(NSP,PAN,UN,SUR,DG11R,DG11I,DG12R,DG12I,G11R,G11I,
1 G12R,G12I)
C DO 17 JJ=1,19
C HEAD=(JJ-1)*5.0
C HEAD=HEAD/180.0*3.14159
CALL PHI78(NSP,PAN,UN,PHI7R,PHI7I,PHI8R,PHI8I)
CALL GINVER(NSP,2*NSP,UN,UNN,PHI7R,PHI7I,PHI8R,PHI8I,DA,DN,
1 DG11R,DG11I,DG12R,DG12I,Q135,Q245)
CALL POTEN(NSP,2*NSP,G11R,G11I,G12R,G12I,Q135,Q246,DA,
1 POT135,POT246)
CALL AMASS(NSP,2*NSP,UN,UNN,SUR,POT135,POT246,TPR,TPI,TTUN,
1 AM,DEMP)
CALL EXPOR(NSP,2*NSP,PAN,UN,UNN,SUR,POT135,POT246,TTUN,PO1R,
1 PO1I,PO2R,PO2I,FOR)
CALL AMPL(AM,DEMP,RM,C,FOR,AMP)
CALL QTOTAL(NSP,2*NSP,Q135,Q246,AMP,QDF1,QDF2)
CALL DRIFT(NSP,2*NSP,PAN,SUR,QDF1,QDF2,DRIFX,DRIFY,DRMZ)
C WRITE (2)PAN,SUR,Q135,Q246,FOR,AMP,AM,DEMP,C,RM,
C 1 GRAV,DEN,FREQ,DEPTH,WNUM,ANU,HEAD,DRIFX,DRIFY,DRMZ
C WRITE (2)PAN,SUR,FOR,AMP,AM,DEMP,C,RM,
C 1 GRAV,DEN,FREQ,DEPTH,WNUM,ANU,HEAD,DRIFX,DRIFY,DRMZ
17 CONTINUE
STOP
END
```

SUBROUTINE CHART(NSP,PAN,UN,UNN,SUR,C,RM)
C...COMPUTE THE CHARACTERISTICS OF THE FLOATING RECTANGULAR BOX
C...OUTPUT: PAN,UN,UNN,SUR,C; ALSO, VOL,XB,AREA,AREAMP IN /C3/
DIMENSION PAN(NSP,3),UN(NSP,3),UNN(NSP,3),SUR(NSP),
1 C(6,6),RM(6,6)
DIMENSION VA(3),VB(3),VC(3),VD(3),VE(3),VF(3)
COMMON /C2/ GRAV,DEN,FREQ,DEPTH,WNUM,ANU,HEAD
COMMON /C3/ VOL,XB,YB,ZB,AREA,AREAMP,XG,YG,ZG
COMMON /CC/ RI44,RI55,RI66

```
CALL ASSIGN(5,'POR005.DAT')
N=NSP/2
DO 10 J=1,N
JJ=J+N
READ(5,*)I,X,Y,Z,UN1,UN2,UN3,S
PAN(J,1)=X
PAN(JJ,1)=X
PAN(J,2)=Y
PAN(JJ,2)=Y
PAN(J,3)=Z
PAN(JJ,3)=Z
UN(J,1)=UN1
UN(JJ,1)=UN1
UN(J,2)=UN2
UN(JJ,2)=UN2
UN(J,3)=UN3
UN(JJ,3)=UN3
SUR(J)=S
SUR(JJ)=S
CONTINUE
10
C...CALCULATE THE /C3/
XB=0.0
YB=0.0
ZB=0.0
AREA=0.0
AREAMP=0.0
VOL=0.0
TEMP2=0.0
TEMP3=0.0
TEMP4=0.0
DO 40 I=1,NSP
VA(1)=PAN(I,1)
VA(2)=PAN(I,2)
VA(3)=PAN(I,3)
URN(I,1)=VA(2)*UN(I,3)-VA(3)*UN(I,2)
URN(I,2)=VA(3)*UN(I,1)-VA(1)*UN(I,3)
URN(I,3)=VA(1)*UN(I,2)-VA(2)*UN(I,1)
VB(1)=UN(I,1)
VB(2)=UN(I,2)
VB(3)=UN(I,3)
CALL VDOT(VA,VB,TEMP1)
VOL=VOL+TEMP1*SUR(I)
XB=XB+VA(1)*VA(1)*VB(1)*SUR(I)
ZB=ZB+VA(3)*VA(3)*VB(3)*SUR(I)
AREA=AREA+SUR(I)
TEMP=VB(3)*SUR(I)
AREAMP=AREAMP+TEMP
TEMP2=TEMP2+VA(1)*TEMP
TEMP3=TEMP3+VA(1)*VA(1)*TEMP
TEMP4=TEMP4+VA(2)*VA(2)*TEMP
CONTINUE
DO 45 I=1,6
DO 45 J=1,6
```

45. C(I,J)=0.0
CONTINUE
VOL=2.0*(VOL/3.0)
XB=XB/VOL
ZB=ZB/VOL
AREA=2.0*AREA
AREAMP=-2.0*AREAMP
TEMP=DEN*GRAV
C(3,3)=TEMP*AREAMP
C(3,5)=TEMP*2.0*TEMP2
C(5,3)=C(3,5)
C(4,4)=TEMP*(VOL*(ZB-ZG)-2.0*TEMP4)
C(5,5)=TEMP*(VOL*(ZB-ZG)-2.0*TEMP3)
RM(1,1)=DEN*VOL
RM(2,2)=DEN*VOL
RM(3,3)=DEN*VOL
RM(4,4)=DEN*VOL*RI44*RI44
RM(5,5)=DEN*VOL*RI55*RI55
RM(6,6)=DEN*VOL*RI66*RI66
RM(1,5)=DEN*VOL*ZG
RM(5,1)=RM(1,5)
RM(2,4)=DEN*VOL*ZG
RM(4,2)=RM(2,4)
RETURN
END

SUBROUTINE PRNT1(NSP,PAN,UN,UNN,SUR,C,RM)
DIMENSION PAN(NSP,3),UN(NSP,3),UNN(NSP,3),SUR(NSP),
1 C(6,6),RM(6,6)
COMMON /C2/ GRAV,DEN,FREQ,DEPTH,WMUM,ANU,HEAD
COMMON /C3/ VOL,XB,YB,ZB,AREA,AREAMP,XG,YG,ZG

WRITE(1,*)"DATA FOR RECTANGULAR BOX"
WRITE(1,*)
WRITE(1,*)"VOL= ",VOL
WRITE(1,*)"AREA= ",AREA
WRITE(1,*)"CENTROID XB,YB,ZB : ",XB,YB,ZB
WRITE(1,*)"CENTER OF GRAVITY XG,YG,ZG : ",XG,YG,ZG
WRITE(1,*)"AREAMP= ",AREAMP
WRITE(1,*) 'PAN(I,K)'
DO 40 I=1,NSP
 WRITE(1,100) I,(PAN(I,K),K=1,3)
40 CONTINUE
WRITE(1,*) 'UN(I,K)'
DO 50 I=1,NSP
 WRITE(1,500) I,(UN(I,K),K=1,3)
50 CONTINUE
WRITE(1,*) 'UNN(I,K)'
DO 51 I=1,NSP
 WRITE(1,500) I,(UNN(I,K),K=1,3)
51 CONTINUE
WRITE(1,*) 'SUR(I)'
DO 60 I=1,NSP
 WRITE(1,600) I,SUR(I)

```
60      CONTINUE
100     FORMAT(1X,'( ',I2,',')',3F13.6)
500     FORMAT(1X,'( ',I2,',')',3F13.6)
600     FORMAT(1X,'( ',I2,',')',F13.6)
700     FORMAT(1X,6E14.5)
      WRITE(1,*)'RESTORING COEFFICIENT'
      DO 21 I=1,6
      WRITE(1,700) (C(I,J),J=1,6)
21      CONTINUE
      WRITE(1,*)
      WRITE(1,*)'REAL MASS MATRIX'
      DO 22 I=1,6
      WRITE(1,700) (RM(I,J),J=1,6)
22      CONTINUE
      CALL CLOSE(1)
      RETURN
      END

SUBROUTINE LINK1(N,PAN,UN,SUR,DG11R,DG11I,DG12R,DG12I,
1           G11R,G11I,G12R,G12I)
C...THIS PROGRAM COMPUTES THE ELEMENTS OF GREEN'S FUNCTION MATRIX
C...INPUT:N,PAN,UN,SUR
C...OUTPUT:DG11R,DG11I,DG12R,DG12I,G11R,G11I,G12R,G12I
      DIMENSION PAN(N,3),UN(N,3),SUR(N)
      DIMENSION DG11R(N,N),DG11I(N,N),DG12R(N,N),DG12I(N,N),
1           G11R(N,N),G11I(N,N),G12R(N,N),G12I(N,N)

      DIMENSION G(2),DGX(2),DGY(2),DGZ1(2),DGZ2(2),VA(3),VB(3),VC(3)
      COMMON /C2/ GRAV,DEN,FREQ,DEPTH,WNUM,ANU,HEAD
      COMMON /SER/ UK(1000),GAMMA(1000),ALPHA

      ANU=WNUM*TANH(WNUM*DEPTH)
      FREQ=SQRT(GRAV*ANU)
      CALL ROOTUK(1000)
      ALPHA=6.283185/(4.0*DEPTH*EXP(-2.0*WNUM*DEPTH)+ANU*
1 ((1.0+EXP(-2.0*WNUM*DEPTH))/WNUM)**2.0)
      DO 10 I=1,N
      VA(1)=PAN(I,1)
      VA(2)=PAN(I,2)
      VA(3)=PAN(I,3)
      DO 20 J=1,N
      VB(1)=PAN(J,1)
      VB(2)=PAN(J,2)
      VB(3)=PAN(J,3)
      CALL VSUB(VA,VB,VC)
      IF(I.EQ.J)GO TO 11
      R1=SQRT(VC(1)*VC(1)+VC(2)*VC(2))
      IF(R1.EQ.0.0)GO TO 11
      TEMP=2.0+10.0*DEPTH/(3.1416*R1)
      IF(TEMP.GT.1000.)GO TO 11
      NTERM=TEMP
      CALL GS2(VA,VB,G,DGX,DGY,DGZ1,DGZ2,NTERM)
      GO TO 12
11      UNMAX=-10.0/(VA(3)+VB(3))
```

```
CALL GI2(VA,VB,G,DGX,DGY,DGZ1,DGZ2,UMAX)
12 CONTINUE
    G11R(I,J)=G(1)
    G11I(I,J)=G(2)
    DG11R(I,J)=DGX(1)*UN(I,1)+DGY(1)*UN(I,2)+(DGZ1(1)+DGZ2(1))
    1           *UN(I,3)
    DG11I(I,J)=DGX(2)*UN(I,1)+DGY(2)*UN(I,2)+(DGZ1(2)+DGZ2(2))
    1           *UN(I,3)
    IF ( I .EQ. J)GO TO 20
    G11R(J,I)=G(1)
    G11I(J,I)=G(2)
    DG11R(J,I)=DGX(1)*UN(J,1)-DGY(1)*UN(J,2)+(DGZ1(1)-DGZ2(1))
    1           *UN(J,3)
    DG11I(J,I)=DGX(2)*UN(J,1)-DGY(2)*UN(J,2)+(DGZ1(2)-DGZ2(2))
    1           *UN(J,3)
20 CONTINUE
DO 30 J=1,N
    VB(1)=PAN(J,1)
    VB(2)=PAN(J,2)
    VB(3)=PAN(J,3)
    CALL VSUB(VA,VB,VC)
    R1=SQRT(VC(1)*VC(1)+VC(2)*VC(2))
    TEMP=2.0+10.0*DEPTH/(3.1416*R1)
    IF(TEMP .GT. 1000.) GO TO 31
    NTERM=TEMP
    CALL GS2(VA,VB,G,DGX,DGY,DGZ1,DGZ2,NTERM)
    GO TO 32
31 UMAX=-10.0/(VA(3)+VB(3))
    CALL GI2(VA,VB,G,DGX,DGY,DGZ1,DGZ2,UMAX)
32 CONTINUE
    G12R(I,J)=G(1)
    G12I(I,J)=G(2)
    DG12R(I,J)=DGX(1)*UN(I,1)+DGY(1)*UN(I,2)+(DGZ1(1)+DGZ2(1))
    1           *UN(I,3)
    DG12I(I,J)=DGX(2)*UN(I,1)+DGY(2)*UN(I,2)+(DGZ1(2)+DGZ2(2))
    1           *UN(I,3)
    IF(I .EQ. J)GO TO 30
    G12R(J,I)=G(1)
    G12I(J,I)=G(2)
    DG12R(J,I)=DGX(1)*UN(J,1)+DGY(1)*UN(J,2)+(DGZ1(1)-DGZ2(1))
    1           *UN(J,3)
    DG12I(J,I)=DGX(2)*UN(J,1)+DGY(2)*UN(J,2)+(DGZ1(2)-DGZ2(2))
    1           *UN(J,3)
30 CONTINUE
10 CONTINUE
C...COMBINE DG11 AND DG12 TO BE DG11 FOR DG135 MODE,
C...AND DG12 FOR DG246 MODE
DO 40 I=1,N
DO 40 J=1,N
    TEMP1=DG11R(I,J)+DG12R(I,J)
    TEMP2=DG11I(I,J)+DG12I(I,J)
    TEMP3=DG11R(I,J)-DG12R(I,J)
    TEMP4=DG11I(I,J)-DG12I(I,J)
    DG11R(I,J)=TEMP1*SUR(J)
```

```
DG11I(I,J)=TEMP2*SUR(J)
DG12R(I,J)=TEMP3*SUR(J)
DG12I(I,J)=TEMP4*SUR(J)
40    CONTINUE
C...ADDING THE DIAGONAL TERM OF DG MATRIX
DO 50 I=1,N
DG11R(I,I)=DG11R(I,I)-6.28318
DG12R(I,I)=DG12R(I,I)-6.28318
50    CONTINUE
C...COMBINE G11 AND G12 TO BE G11 FOR G135 MODE,AND G12 FOR G246 MODE
DO 60 I=1,N
DO 60 J=1,N
TEMP1=G11R(I,J)+G12R(I,J)
TEMP2=G11I(I,J)+G12I(I,J)
TEMP3=G11R(I,J)-G12R(I,J)
TEMP4=G11I(I,J)-G12I(I,J)
G11R(I,J)=TEMP1*SUR(J)
G11I(I,J)=TEMP2*SUR(J)
G12R(I,J)=TEMP3*SUR(J)
G12I(I,J)=TEMP4*SUR(J)
60    CONTINUE
C...ADDING THE DIAGONAL TERM OF G MATRIX
DO 70 I=1,N
TEMP=2.0*SQRT(SUR(I)*3.14159)
G11R(I,I)=G11R(I,I)+TEMP
G12R(I,I)=G12R(I,I)+TEMP
70    CONTINUE
RETURN
END

SUBROUTINE PHI78(N,PAN,UN,PHI7R,PHI7I,PHI8R,PHI8I)
C...THIS PROGRAM CALCULATE THE PHI7:SYMMETRIC PART,PHI8:ANTI-SYM PART
DIMENSION PAN(N,3),UN(N,3)
DIMENSION PHI7R(N),PHI7I(N),PHI8R(N),PHI8I(N)
COMMON /C2/ GRAV,DEN,FREQ,DEPTH,MNUM,ANU,HEAD
APHI=GRAV/(FREQ*(1.0+EXP(-2.0*MNUM*DEPTH)))
AK1=MNUM*COS(HEAD)
AK2=MNUM*SIN(HEAD)
DO 10 I=1,N
V1=PAN(I,1)
V2=PAN(I,2)
V3=PAN(I,3)
XK1=V1*AK1
YK2=V2*AK2
ZK=V3+DEPTH
XN=UN(I,1)
YN=UN(I,2)
ZN=UN(I,3)
TEMPA=APHI*EXP(MNUM*V3)*(1.0+EXP(-2.0*MNUM*ZK))
TEMPB=APHI*EXP(MNUM*V3)*(1.0-EXP(-2.0*MNUM*ZK))
AKNX=TEMPA*AK1*XN
AKNY=TEMPA*AK2*YN
AKNZ=TEMPB*MNUM*ZN
```

```
CY2=COS(YK2)
SY2=SIN(YK2)
CX1=COS(XK1)
SX1=SIN(XK1)
PHI7R(I)=(-AKNX*CY2*SX1-ARNY*SY2*CX1+AKNZ*CY2*CX1)
PHI7I(I)=(-AKNX*CY2*CX1-ARNY*SY2*SX1+AKNZ*CY2*SX1)
PHI8R(I)=(-AKNX*SY2*CX1-ARNY*CY2*SX1-AKNZ*SY2*SX1)
PHI8I(I)=(-AKNX*SY2*SX1+ARNY*CY2*CX1+AKNZ*SY2*CX1)
10 CONTINUE
RETURN
END
```

```
SUBROUTINE GINVER(N,NN,UN,UNN,PHI7R,PHI7I,PHI8R,PHI8I,DA,DN,
1 DG135R,DG135I,DG246R,DG246I,Q135,Q246)
C... THIS PROGRAM COMPUTES THE INVERSE OF MATRIX DG AND SOURCE Q
C... INPUT:N,NN,UN,UNN,PHI,DG135,DG246
C... OUTPUT:Q135,Q246
C... DA AND DN IS FOR TEMPORARY USE, NN=2*N=2*NSP
```

```
DIMENSION UN(N, 3),UNN(N, 3),PHI7R(N),PHI7I(N),PHI8R(N),PHI8I(N),
1 DG135R(N,N),DG135I(N,N),DG246R(N,N),DG246I(N,N),
2 DA(NN,NN),DN(NN,4)
DIMENSION Q135(NN,4),Q246(NN,4)
```

C... FORMATION OF THE REAL MATRIX DA*Q-UN FOR THE SYMMETRIC PART

```
DO 10 I=1,N
DN(I,1)=UN(I,1)
DN(I,2)=UN(I,3)
DN(I,3)=UNN(I,2)
DN(I,4)=PHI7R(I)
DN(I+N,1)=0.0
DN(I+N,2)=0.0
DN(I+N,3)=0.0
DN(I+N,4)=PHI7I(I)
DO 10 J=1,N
DA(I,J)=DG135R(I,J)
DA(I+N,J)=DG135I(I,J)
DA(I,J+N)=DG135I(I,J)
DA(I+N,J+N)=DG135R(I,J)
```

10 CONTINUE
C... SOLVING Q BY INVERSION A*X=R, A(M*N), R(M*N), X(M*N) STORED IN R

```
CALL INV(DN,DA,NN,4)
DO 20 I=1,NN
DO 20 J=1,4
Q135(I,J)=DN(I,J)
```

20 CONTINUE
C... SOLVING Q246 (ANTISYMMETRIC PART) BY THE SIMILAR PROCESS AS ABOVE

```
DO 30 I=1,N
DN(I,1)=UN(I,2)
DN(I,2)=UNN(I,1)
DN(I,3)=UNN(I,3)
DN(I,4)=PHI8R(I)
DN(I+N,1)=0.0
DN(I+N,2)=0.0
```

```
DN(I+N,3)=0.0
DN(I+N,4)=PHI8I(I)
DO 30 J=1,N
DA(I,J)=DG246R(I,J)
DA(I+N,J)=DG246I(I,J)
DA(I,J+N)=DG246I(I,J)
DA(I+N,J+N)=DG246R(I,J)
30 CONTINUE
CALL INV(DN,DA,NN,4)
DO 40 I=1,NN
DO 40 J=1,4
Q246(I,J)=DN(I,J)
40 CONTINUE
RETURN
END

SUBROUTINE POTEN(N,NN,GL35R,GL35I,G246R,G246I,Q135,Q246,DA,
1 POT135,POT246).
C...COMPUTE THE POTENTIAL
C...INPUT:N,NN,GL35,G246,Q135,Q246
C...OUTPUT:POT135,POT246
C...DA IS FOR TEMPORARY USE
DIMENSION GL35R(N,N),GL35I(N,N),G246R(N,N),G246I(N,N),Q135(NN,4),
1 Q246(NN,4),DA(NN,NN)
DIMENSION POT135(NN,4),POT246(NN,4)

DO 10 I=1,N
DO 10 J=1,N
DA(I,J)=GL35R(I,J)
DA(I+N,J)=GL35I(I,J)
DA(I,J+N)=GL35I(I,J)
DA(I+N,J+N)=GL35R(I,J)
10 CONTINUE
CALL MPRD(DA,Q135,POT135,NN,NN,4)
DO 20 I=1,N
DO 20 J=1,N
DA(I,J)=G246R(I,J)
DA(I+N,J)=G246I(I,J)
DA(I,J+N)=G246I(I,J)
DA(I+N,J+N)=G246R(I,J)
20 CONTINUE
CALL MPRD(DA,Q246,POT246,NN,NN,4)
RETURN
END

SUBROUTINE AMASS(N,NN,UN,UNN,SUR,POT135,POT246,TPR,TPI,TTUN,
1 AM,DEMP)
C...COMPUTE THE ADDED MASS AND DEMPING COEFFICIENT
C...INPUT:N,NN,UN,UNN,SUR,POT135,POT246
C...OUTPUT:AM,DEMP
C...TPR,TPI,TTUN IS FOR TEMPORARY USE
DIMENSION UN(N,3),UNN(N,3),SUR(N),POT135(NN,4),POT246(NN,4),
1 TPR(N,6),TPI(N,6),TTUN(N,6),AM(6,6),DEMP(6,6)
COMMON /C2/ GRAV,DEN,FREQ,DEPTH,NNUM,ANU,HEAD
```

```
DO 5 I=1,N
DO 5 K=1,3
TTUN(I,K)=UN(I,K)
TTUN(I,K+3)=UNN(I,K)
5 CONTINUE
DO 10 J=1,N
JJ=J+N
DO 10 K=1,3
TPR(J,2*K-1)=POT135(J,K)
TPR(J,2*K) =POT246(J,K)
TPI(J,2*K-1)=POT135(JJ,K)
TPI(J,2*K) =POT246(JJ,K)
10 CONTINUE
DO 20 J=1,5,2
JJ=J+1
DO 20 K=1,5,2
KK=K+1
S1R=0.0
S1I=0.0
S2R=0.0
S2I=0.0
DO 25 I=1,N
S1R=S1R+TPR(I,J)*TTUN(I,K)*SUR(I)
S1I=S1I+TPI(I,J)*TTUN(I,K)*SUR(I)
S2R=S2R+TPR(I,JJ)*TTUN(I,KK)*SUR(I)
S2I=S2I+TPI(I,JJ)*TTUN(I,KK)*SUR(I)
25 CONTINUE
AM(J,K) --2.0*DEN*S1R
AM(JJ,KK) --2.0*DEN*S2R
DEMP(J,K) --2.0*DEN*FREQ*S1I
DEMP(JJ,KK)--2.0*DEN*FREQ*S2I
20 CONTINUE
RETURN
END

SUBROUTINE EXFOR(N,NN,PAN,UN,UNN,SUR,POT135,POT246,TTUN,PO1R,PO1I,
1 PO2R,PO2I,FOR)
C...COMPUTE THE EXCITING FORCE
C...INPUT:N,UN,UNN,SUR,POT135,POT246
C...OUTPUT:FOR
C...TTUN,PO1R,PO1I,PO2R,PO2I IS FOR TEMPERARY USE
DIMENSION PAN(N,3),UN(N,3),UNN(N,3),SUR(N),POT135(NN,4),POT246(NN,4),
1 TTUN(N,6),PO1R(N),PO1I(N),PO2R(N),PO2I(N),FOR(12)
COMMON /C2/ GRAV,DEN,FREQ,DEPTH,MNUM,ANU,HEAD

DO 5 I=1,N
DO 5 K=1,3
TTUN(I,K)=UN(I,K)
TTUN(I,K+3)=UNN(I,K)
5 CONTINUE
DO 10 I=1,5,2
II=I+1
S7R=0.0
```

- 101 -

```
S7I=0.0
S8R=0.0
S8I=0.0
DO 20 J=1,N
JJ=J+N
S7R=S7R+POT135(J,4)*TTUN(J,I)*SUR(J)
S7I=S7I+POT135(JJ,4)*TTUN(J,I)*SUR(J)
S8R=S8R+POT246(J,4)*TTUN(J,II)*SUR(J)
S8I=S8I+POT246(JJ,4)*TTUN(J,II)*SUR(J)
20 CONTINUE
TEMP=2.0*FREQ*DEN
POR(I)=TEMP*S7R
POR(II)=TEMP*S8R
POR(I+6)=TEMP*S7I
POR(II+6)=TEMP*S8I
10 CONTINUE
APHI=GRAV/(FREQ*(1.0+EXP(-2.0*WNUM*DEPTH)))
AK1=WNUM*COS(HEAD)
AK2=WNUM*SIN(HEAD)
DO 30 J=1,N
X=PAN(J,1)
Y=PAN(J,2)
Z=PAN(J,3)
TEMP1=APHI*EXP(WNUM*Z)*(1.0+EXP(-2.0*WNUM*(Z+DEPTH)))*SUR(J)
TEMP2=AK1*X+AK2*Y
TEMP3=AK1*X-AK2*Y
PO1R(J)=TEMP1*COS(TEMP2)
PO1I(J)=TEMP1*SIN(TEMP2)
PO2R(J)=TEMP1*COS(TEMP3)
PO2I(J)=TEMP1*SIN(TEMP3)
30 CONTINUE
DO 40 I=1,6
II=I+6
SR=0.0
SI=0.0
TB=1.0
IF((I/2)*2.EQ.I) TB=-1.0
DO 50 J=1,N
SR=SR+PO1R(J)*TTUN(J,I)+TB*PO2R(J)*TTUN(J,I)
SI=SI+PO1I(J)*TTUN(J,I)+TB*PO2I(J)*TTUN(J,I)
50 CONTINUE
POR(I)=POR(I)+FREQ*DEN*SR
POR(II)=POR(II)+FREQ*DEN*SI
TEMP=POR(I)
POR(I)=+POR(II)
POR(II)=+TEMP
40 CONTINUE
RETURN
END
```

SUBROUTINE AMPL(AM,DEMP,RM,C,POR,AMP)

C...COMPUTE THE RESPONSE AMPLITUDE
C...INPUT:AM,DEMP,RM,C,POR
C...OUTPUT:AMP

C...DC AND DF IS FOR TEMPERARY USE

```
DIMENSION AM(6,6),DEMP(6,6),RM(6,6),C(6,6),FOR(12),AMP(12),
1           DC(12,12),DF(12)
COMMON /C2/ GRAV,DEN,FREQ,DEPTH,VNUM,ANU,HEAD
```

```
DO 10 I=1,6
II=I+6
DF(I)=FOR(I)
DF(II)=FOR(II)
DO 10 J=1,6
JJ=J+6
TEMP1=FREQ*FREQ*(AM(I,J)+RM(I,J))+C(I,J)
TEMP2=FREQ*DEMP(I,J)
DC(I,J)= TEMP1
DC(II,JJ)=TEMP1
DC(II,J)=TEMP2
DC(I,JJ)=TEMP2
10 CONTINUE
CALL INV(DF,DC,12,1)
DO 20 I=1,12
AMP(I)=DF(I)
20 CONTINUE
RETURN
END
```

```
SUBROUTINE GI2(VX,VXX,G,DGX,DGY,DGZ1,DGZ2,UMAX)
EXTERNAL PG1,PGE,PGK1,PGKE,PGZ11,PGZ1E,PGZ21,PGZ2E
DIMENSION VX(3),VXX(3),G(2),DGX(2),DGY(2),DGZ1(2),DGZ2(2)
COMMON /C2/ GRAV,DEN,FREQ,DEPTH,VNUM,ANU,HEAD
COMMON /SER/ UK(1000),GAMMA(1000),ALPHA
COMMON /G1/ ZH,ZZH,R1
```

C....THIS PROGRAM CALCULATE THE GREEN'S FUNCTION BY INTEGRAL FORM

C....F1 IS THE INTEGRAND; F2 IS THE SYMMETRIC PART OF THE INTEGRAND

```
FZ1(X)=X*(EXP(X*(ZH+ZZH-2.0*DEPTH))-EXP(-X*(ZH+ZZH+2.0*DEPTH)))
FZ2(X)=X*(EXP(-X*(ZZH-ZH+2.0*DEPTH))-EXP(-X*(ZH-ZZH+2.0*DEPTH)))
TEMP1=VX(1)-VXX(1)
TEMP2=VX(2)-VXX(2)
TEMP3=VX(3)-VXX(3)
R1=SQRT(TEMP1*TEMP1+TEMP2*TEMP2)
IF (R1 .LE. 1.0E-6) R1=0.0
TEMP4=R1*VNUM
ZH=VX(3)+DEPTH
ZZH=VXX(3)+DEPTH
R=SQRT(R1*R1+TEMP3*TEMP3)
IF (R .LE. 1.0E-6) R=0.0
R2H=SQRT(R1*R1+(ZH+ZZH)*(ZH+ZZH))
BJ0=BJ(TEMP4,0)
BJ1=BJ(TEMP4,1)
EZH=EXP(-2.0*VNUM*ZH)
EZZH=EXP(-2.0*VNUM*ZZH)
G(1)=1.0/R2H
IF(R .NE. 0.0)G(1)=G(1)+1.0/R
G(2)=ALPHA*(1.0+EZH)*(1.0+EZZH)*BJ0*EXP(VNUM*(VX(3)+VXX(3)))
DGX(1)=-1.0/R2H**3.0
```

```
IF(R .NE. 0.0)DGX(1)=DGX(1)-1.0/R**3.0
IF(R1 .EQ. 0.0) GO TO 1
DGX(2)=ALPHA*(1.0+EZH)*(1.0+ZZH)*EXP(WNUM*(VX(3)+VXX(3)))
1      *BJ(TEMP4,1)*WNUM/R1
GO TO 2
1. DGX(2)=ALPHA*(1.0+EZH)*(1.0+ZZH)*EXP(WNUM*(VX(3)+VXX(3)))
1.      *0.5*WNUM*WNUM
2. DGZ1(1)=(ZZH+ZH)/R2H**3.0
DGZ1(2)=ALPHA*FZ1(WNUM)*BJ0
DGZ2(1)=0.0
IF(R .NE. 0.0)DGZ2(1)=DGZ2(1)-(ZH-ZZH)/R**3.0
DGZ2(2)=ALPHA*FZ2(WNUM)*BJ0
UINT=0.01*WNUM
CALL DG16(UINT,WNUM,PGE,SMG1)
CALL DG16(2.0*WNUM,UMAX,PG1,SMG2)
G(1)=G(1)+SMG1+UINT*PGE(UINT)
CALL DG16(UINT,WNUM,PGE,SMG1)
CALL DG16(2.0*WNUM,UMAX,PG1,SMG2)
DGK(1)=DGK(1)+SMG1+SMG2+UINT*PGE(UINT)
CALL DG16(UINT,WNUM,PGZ1,E,SMG1)
CALL DG16(2.0*WNUM,UMAX,PGZ11,SMG2)
DGZ1(1)=DGZ1(1)+SMG1+SMG2+UINT*PGZ1(E)
CALL DG16(UINT,WNUM,PGZ2,E,SMG1)
CALL DG16(2.0*WNUM,UMAX,PGZ21,SMG2)
DGZ2(1)=DGZ2(1)+SMG1+SMG2+UINT*PGZ2(E)
DGY(1)=DGK(1)*TEMP2
DGY(2)=DGK(2)*TEMP2
DGK(1)=DGK(1)*TEMP1
DGK(2)=DGK(2)*TEMP1
RETURN
END

FUNCTION PG1(X)
COMMON /C2/ GRAV,DEN,FREQ,DEPTH,WNUM,ANU,HEAD
COMMON /G1/ ZH,ZZH,R1
B=1.0/((X-ANU)/(X+ANU)-EXP(-2.0*X*DEPTH))
PG1=B*EXP(X*(ZH+ZZH-2.0*DEPTH))*(1.0+EXP(-2.0*X*ZH))*  

1  (1.0+EXP(-2.0*X*ZZH))*BJ(X*R1,0)
RETURN
END

FUNCTION PGE(X)
COMMON /C2/ GRAV,DEN,FREQ,DEPTH,WNUM,ANU,HEAD
COMMON /G1/ ZH,ZZH,R1
PGE=PG1(X+WNUM)+PG1(-X+WNUM)
RETURN
END

FUNCTION PGK1(X)
COMMON /C2/ GRAV,DEN,FREQ,DEPTH,WNUM,ANU,HEAD
COMMON /G1/ ZH,ZZH,R1
B=1.0/((X-ANU)/(X+ANU)-EXP(-2.0*X*DEPTH))
1  *EXP(X*(ZH+ZZH-2.0*DEPTH))*(1.0+EXP(-2.0*X*ZH))*  

2  (1.0+EXP(-2.0*X*ZZH))
```

```
IF (R1 .EQ. 0.0) GO TO 10
PGKL=B*BJ(X*R1,1)*X/R1
RETURN
10 PGKL=B*0.5*X*X
RETURN
END

FUNCTION PGKE(X)
COMMON /C2/ GRAV,DEN,FREQ,DEPTH,MNUM,ANU,HEAD
COMMON /G1/ ZH,ZZH,R1
PGKE=PGKL(X+MNUM)+PGKL(-X+MNUM)
RETURN
END

FUNCTION PGZ11(X)
COMMON /C2/ GRAV,DEN,FREQ,DEPTH,MNUM,ANU,HEAD
COMMON /G1/ ZH,ZZH,R1
B=1.0/((X-ANU)/(X+ANU)-EXP(-2.0*X*DEPTH))
PGZ11=B*X*(EXP(X*(ZH+ZZH-2.0*DEPTH))-EXP(-X*(ZH+ZZH+2.0*DEPTH)))
1    *BJ(X*R1,0)
RETURN
END

FUNCTION PGZ1E(X)
COMMON /C2/ GRAV,DEN,FREQ,DEPTH,MNUM,ANU,HEAD
COMMON /G1/ ZH,ZZH,R1
PGZ1E=PGZ11(X+MNUM)+PGZ11(-X+MNUM)
RETURN
END

FUNCTION PGZ21(X)
COMMON /C2/ GRAV,DEN,FREQ,DEPTH,MNUM,ANU,HEAD
COMMON /G1/ ZH,ZZH,R1
B=1.0/((X-ANU)/(X+ANU)-EXP(-2.0*X*DEPTH))
PGZ21=B*X*(EXP(-X*(ZZH-ZH+2.0*DEPTH))-EXP(-X*(ZH-ZZH+2.0*DEPTH)))
1    *BJ(X*R1,0)
RETURN
END

FUNCTION PGZ2E(X)
COMMON /C2/ GRAV,DEN,FREQ,DEPTH,MNUM,ANU,HEAD
COMMON /G1/ ZH,ZZH,R1
PGZ2E=PGZ21(X+MNUM)+PGZ21(-X+MNUM)
RETURN
END

SUBROUTINE GS2(VX,VXX,G,DGX,DGY,DGZ1,DGZ2,INTERM)
DIMENSION VX(3),VXX(3),G(2),DGX(2),DGY(2),DGZ1(2),DGZ2(2)
COMMON /C2/ GRAV,DEN,FREQ,DEPTH,MNUM,ANU,HEAD
COMMON /SER/ UK(1000),GAMMA(1000),ALPHA
C....THIS PROGRAM CALCULATE THE GREEN'S FUNCTION BY SERIES FORM
TEMP1=VX(1)-VXX(1)
TEMP2=VX(2)-VXX(2)
TEMP3=VX(3)-VXX(3)
```

```
R1=SQRT(TEMP1*TEMP1+TEMP2*TEMP2)
ZH=VX(3)+DEPTH
ZZH=VXX(3)+DEPTH
TEMP4=ALPHA*(1.0+EXP(-2.0*WNUM*ZH))*(1.0+EXP(-2.0*WNUM*ZZH))
1 *EXP(WNUM*(ZH+ZZH-2.0*DEPTH))
TEMP5=WNUM*R1
TEMP6=TEMP4*WNUM/R1
BYO=BY(TEMP5,0)
BJO=BJ(TEMP5,0)
G(1)=TEMP4*BYO
G(2)=TEMP4*BJO
DGX(1)=TEMP6*BY(TEMP5,1)
DGX(2)=TEMP6*BJ(TEMP5,1)
TZ1=ALPHA*WNUM*EXP(WNUM*(ZH+ZZH-2.0*DEPTH))*  
1 *(1.0-EXP(-2.0*WNUM*(ZH+ZZH)))
TZ2=ALPHA*WNUM*(EXP(WNUM*(ZH-ZZH-2.0*DEPTH))*
1 -EXP(WNUM*(ZZH-ZH-2.0*DEPTH)))
DGZ1(1)=TZ1*BYO
DGZ1(2)=TZ1*BJO
DGZ2(1)=TZ2*BYO
DGZ2(2)=TZ2*BJO
SUMG=0.0
SUMGX=0.0
SUMGZ1=0.0
SUMGZ2=0.0
IF (NTERM .EQ. 0) GO TO 11
DO 10 I=1,NTERM
J=NTERM-I+1
TEMP7=UK(J)*R1
BKO=BK(TEMP7,0)
S1=GAMMA(J)*COS(UK(J)*ZH)*COS(UK(J)*ZZH)
S2=GAMMA(J)*UK(J)*BKO
SG=S1*BKO
SGX=S1*UK(J)*BK(TEMP7,1)
SGZ1=S2*0.5*SIN(UK(J)*(ZH+ZZH))
SGZ2=S2*0.5*SIN(UK(J)*(ZH-ZZH))
SUMG=SUMG+SG
SUMGX=SUMGX+SGX
SUMGZ1=SUMGZ1+SGZ1
SUMGZ2=SUMGZ2+SGZ2
10 CONTINUE
11 CONTINUE
G(1)=G(1)+SUMG
DGX(1)=DGX(1)+SUMGX/R1
DGY(1)=DGX(1)*TEMP2
DGY(2)=DGX(2)*TEMP2
DGX(1)=DGX(1)*TEMP1
DGX(2)=DGX(2)*TEMP1
DGZ1(1)=DGZ1(1)+SUMGZ1
DGZ2(1)=DGZ2(1)+SUMGZ2
RETURN
END

SUBROUTINE ROOTUK(N)
```

```
COMMON /C2/ GRAV, DLEN, FREQ, DEPTH, MNUM, ANU, HEAD
COMMON /SER/ UK(1000), GAMMA(1000), ALPHA
F(X)=X*TAN(X*1.570796327)+BETA
ERR=1.OE-6
BETA=ANU*DEPTH/1.570796327
DO 20 J=1,N
DELTA=1.OE-2
A2=2.0*N
5 A1=2*N-1+DELTA
Y1=F(A1)
Y2=F(A2)
IF(ABS(Y1).LE.ERR) GO TO 100
IF(ABS(Y2).LE.ERR) GO TO 200
IF(Y1).LT.13,100,12
12 DELTA=DELTA/10.
A2=A1
GO TO 5
13 A3=(A1+A2)*0.5
Y3=F(A3)
IF(ABS(Y3).LE.ERR) GO TO 101
IF(Y3 .LT. 0.0) A1=A3
IF(Y3 .GT. 0.0) A2=A3
RA=ABS((A2-A1)/A3)
IF(RA .LE. ERR) GO TO 101
GO TO 13
100 UK(J)=A1
GO TO 10
200 UK(J)=A2
GO TO 10
101 UK(J)=A3
10 UK(J)=UK(J)*1.570796327/DEPTH
20 CONTINUE
TEMP1=ANU*ANU
TEMP2=TEMP1*DEPTH-ANU
DO 50 J=1,N
TEMP3=UK(J)*UK(J)
GAMMA(J)=4.0*(TEMP3+TEMP1)/(TEMP3*DEPTH+TEMP2)
50 CONTINUE
RETURN
END

FUNCTION BJ(X,N)
BJ=0.0
IF (N .EQ. 1 .AND. X .EQ. 0.0)GO TO 1
IF (N .EQ. 0 .AND. X .EQ. 0.0)GO TO 2
D=1.OE-4
10 IF(N).LT.20,20,20
IER=1
TYPE *, 'SOMETHING WRONG IN BESJ IER = ', IER
1 RETURN
2 BJ=1.0
20 RETURN
30 IF(X).LT.30,30,31
30 IER=2
```

```
TYPE *, 'SOMETHING WRONG IN BESJ IER = ',IER
RETURN
31 IF(X<-15.)32,32,34
32 NTEST=20.+10.*X-X** 2/3
GO TO 36
34 NTEST=90.+X/2.
36 IF(N-NTEST)40,38,38
38 IER=4
TYPE *, 'SOMETHING WRONG IN BESJ IER = ',IER
RETURN
40 IER=0
N1=N+1
BPREV=.0
C...COMPUTE STARTING VALUE OF M
41 IF(X<-5.)50,60,60
50 MA=X+6.
GO TO 70
60 MB=1.4*X+60./X
70 MB=N+IFIX(X)/4+2
MZERO=MAXD(MA,MB)
C...SET UPPER LIMIT OF M
71 NMAX=NTEST
100 DO 190 M=MZERO,NMAX,3
C...SET F(M),F(M-1)
72 FM1=1.0E-28
FM=0.0
ALPHA=0.0
73 IF(M-(M/2)*2)120,110,120
110 JT=1
GO TO 130
120 JT=1
130 M2=M-2
DO 160 K=1,M2
MK=M-K
BK=2.*FLOAT(MK)*FM1/X-FM
FM=FM1
FM1=BK
74 IF(MK=N-1)150,140,150
140 BJ=BK
150 JT=-JT
S=1+JT
160 ALPHA=ALPHA+BK*S
BK=2.*FM1/X-FM
170 IF(N)180,170,180
BJ=BK
180 ALPHA=ALPHA+BK
BJ=BJ/ALPHA
190 IF(ABS(BJ-BPREV)-ABS(D*BJ))200,200,190
BPREV=BJ
IER=3
TYPE *, 'SOMETHING WRONG IN BESJ IER = ',IER
200 RETURN
END
```

```
FUNCTION BK(X,N)
DIMENSION T(12)
BK=0.0
IF(N)10,11,11
10 IER=1
TYPE *, 'SOMETHING WRONG IN BESK IER = ', IER
RETURN
11 IF(X)12,12,20
12 IER=2
TYPE *, 'SOMETHING WRONG IN BESK IER = ', IER
RETURN
20 IF(X-170.0)22,22,21
21 IER=3
C.....TYPE *, 'SOMETHING WRONG IN BESK IER = ', IER
RETURN
22 IER=0
IF(X-1.)36,36,25
25 A=EXP(-X)
B=1./X
C=SQRT(B)
T(1)=B
DO 26 L=2,12
26 T(L)=T(L-1)*B
IF(N-1)27,29,27
C...COMPUTE K0 USING POLYNOMIAL APPROXIMATION
27 G0=A*(1.25331414-.15666418*T(1)+0.088111278*T(2)-0.091390954*T(3)
2+.13445962*T(4)-.22998503*T(5)+.37924097*T(6)-.52472773*T(7)
3+.55753684*T(8)-.42626329*T(9)+.21845181*T(10)
4-.066809767*T(11)+0.009189383*T(12))*C
IF(N)20,28,29
28 BK=G0
RETURN
C...COMPUTE K1 USING POLYNOMIAL APPROXIMATION
29 G1=A*(1.2533141+.46999270*T(1)-.14685830*T(2)+.12804226*T(3)
2-.17364316*T(4)+.28476181*T(5)-.45943421*T(6)+.62633807*T(7)
3-.66322954*T(8)+.50502386*T(9)-.25813038*T(10)+.078800012*T(11)
4-.010824177*T(12))*C
IF(N-1)20,30,31
30 BK=G1
RETURN
C...FROM K0,K1 COMPUTE KN USING RECURRENCE RELATION
31 DO 35 J=2,N
GJ=2.*FLOAT(J)-1.)*G1/X+G0
IF(GJ-1.0E38)33,33,32
32 IER=4
TYPE *, 'SOMETHING WRONG IN BESK IER = ', IER
GO TO 34
33 G0=G1
34 G1=GJ
BK=GJ
RETURN
36 B=X/2.
A=.57721566+ ALOG(B)
C=B*B
```

IF(N-1)37,43,37
C...COMPUTE K0 USING SERIES EXPANSION
37 GO=-A
 X2J=1.
 FACT=1.
 HJ=0.0
 DO 40 J=1,6
 RJ=1./FLOAT(J)
 X2J=X2J*C
 FACT=FACT*RJ*RJ
 HJ=HJ+RJ
40 GO=GO+X2J*FACT*(HJ-A)
 IF(N)43,42,43
42 BK=GO
 RETURN
C...COMPUTE K1 USING SERIES EXPANSION
43 X2J=B
 FACT=1.
 HJ=1.
 G1=1./X+X2J*(.5+A-HJ)
 DO 50 J=2,8
 X2J=X2J*C
 RJ=1./FLOAT(J)
 FACT=FACT*RJ*RJ
 HJ=HJ+RJ
50 G1=G1+X2J*FACT*(.5+(A-HJ)*FLOAT(J))
 IF(N-1)31,52,31
52 BK=G1
 RETURN
END

FUNCTION BY(X,N)
C...CHECK FOR ERRORS IN N AND X
IF(N)180,10,10
10 IER=0
 IF(X)190,190,20
C...BRANCH IF X LESS THAN OR EQUAL 4
20 IF(X-.4)40,40,30
C...COMPUTE Y1 AND Y0 FOR X GREATER THAN 4.0
30 T1=4.0/X
 T2=T1*T1
 P0=(-(.0000037043*T2+.0000173565)*T2-.0000487613)*T2
 1+.00017343)*T2-.001753062)*T2+.3989423
 Q0=(-(.0000032312*T2-.0000142078)*T2+.0000342468)*T2
 1-.0000869791)*T2+.0004564324)*T2-.01246694
 P1=(-(.0000042414*T2-.0000200920)*T2+.0000580759)*T2
 1-.000223203)*T2+.002921826)*T2+.3989423
 Q1=(-(.0000036594*T2+.00001622)*T2-.0000398708)*T2
 1+.0001064741)*T2-.0006390400)*T2+.03740084
 A=2.0/SQRT(X)
 B=A*T1
 C=X-.7853982
 Y0=A*P0*SIN(C)+B*Q0*COS(C)
 Y1=A*P1*COS(C)+B*Q1*SIN(C)

- 110 -

GO TO 90
C...COMPUTE Y0 AND Y1 FOR X LESS OR EQUAL TO 4.0
40 XX=X/2.
 X2=XX*XX
 T=ALOG(XX)+.5772157
 SUM=0.0
 TERM=T
 Y0=T
 DO 70 L=1,15
 IF(L=1)50,60,50
 50 SUM=SUM+1./FLOAT(L-1)
 60 FL=L
 TS=T-SUM
 TERM=(TERM*(-X2)/FL**2)*(1.-1.)/(FL*TS))
 70 Y0=Y0+TERM
 TERM=XX*(T-.5)
 SUM=0.0
 Y1=TERM
 DO 80 L=2,16
 SUM=SUM+1./FLOAT(L-1)
 80 FL=L
 FLL=FL-1
 TS=T-SUM
 TERM=(TERM*(-X2)/(FLL*FL))*((TS-.5/FL)/(TS+.5/FLL))
 Y1=Y1+TERM
 PI2=.6366198
 Y0=PI2*Y0
 Y1=PI2/X+PI2*Y1
C...CHECK IF ONLY Y0 OR Y1 IS DESIRED
90 IF(N=1)100,100,130
C...RETURN EITHER Y0 OR Y1 AS REQUIRED
100 IF(N)110,120,110
110 BY=Y1
 GO TO 170
120 BY=Y0
 GO TO 170
C...PERFORM RECURRENCE OPERATIONS TO FIND YN(X)
130 YA=Y0
 YB=Y1
 K=1
140 T=FLOAT(2*K)/X
 YC=T*YB-YA
 IF(ABS(YC)-1.0E38)145,145,141
141 IER=3
 TYPE *, 'SOMETHING WRONG IN BESY IER= ', IER
 RETURN
145 K=K+1
 IF(K=N)150,160,150
150 YA=YB
 YB=YC
 GO TO 140
160 BY=YC
170 RETURN
180 IER=1

- 111 -

TYPE *, 'SOMETHING WRONG IN BESY IER = ',IER
RETURN
190 IER=2
TYPE *, 'SOMETHING WRONG IN BESY IER = ',IER
RETURN
END

SUBROUTINE DG16(XL,XU,PCT,SUM)
C....THIS PROGRAM COMPUTE INTEGRAL (PCT), SUMMED OVER X FROM
C....XL TO XU
C DOUBLE PRECISION XL,XU,Y,A,B,C,PCT
SUM=0.0
DO 10 I=1,50
DELT=A-(XU-XL)/I
SUM=0.0
DO 20 J=1,I
XL=XL+(J-1)*DELT
X2=XL+DELT
A=.5E0*(X2+XL)
B=DELT
C=.49470046749582497E0*B
Y=.13576229705877047E-1*(PCT(A+C)+PCT(A-C))
C=.47228751153661629E0*B
Y=Y+.31126761969323946E-1*(PCT(A+C)+PCT(A-C))
C=.43281560119391587E0*B
Y=Y+.47579255841246392E-1*(PCT(A+C)+PCT(A-C))
C=.37770220417750152E0*B
Y=Y+.62314485627766936E-1*(PCT(A+C)+PCT(A-C))
C=.30893812220132187E0*B
Y=Y+.7479799440828837E-1*(PCT(A+C)+PCT(A-C))
C=.22900838882861369E0*B
Y=Y+.8457825969750127E-1*(PCT(A+C)+PCT(A-C))
C=.14080177538962946E0*B
Y=Y+.9130170752246179E-1*(PCT(A+C)+PCT(A-C))
C=.47506254918818720E-1*B
Y=B*(Y+.9472530522753425E-1*(PCT(A+C)+PCT(A-C))),
SUM=SUM+Y
CONTINUE
IF(ABS(SUM-SUM0) .LE. ABS(SUM*1.0E-4)) GO TO 100
SUM0=SUM
CONTINUE
10 TYPE *, '***FAIL TO CONVERGE IN DG16***'
CONTINUE
100 RETURN
END

SUBROUTINE MPRD(A,B,R,N,M,L)
C....THIS PROGRAM COMPUTES R=A*B, WHERE A(N*M), B(M*L)
DIMENSION A(1),B(1),R(1)
IR=0
IK=M
DO 10 K=1,L
IK=IK+M
DO 10 J=1,N

```
IR=IR+1
JI=J-N
IB=IK
R(IR)=0.0
DO 10 I=1,M
JI=JI+N
IB=IB+1
10 R(IR)=R(IR)+A(JI)*B(IB)
RETURN.
END
```

```
SUBROUTINE INV(R,A,M,N)
DIMENSION A(1),R(1)
EPS=1.0E-4
IF(M)23,23,1
```

C...SEARCH FOR GREATEST ELEMENT IN MATRIX A

```
1    IER=0
     PIV=0.0E0
     MM=M*M
     NM=N*M
     DO 3 L=1,MM
       TB=ABS(A(L))
       IF(TB-PIV)3,3,2
2    PIV=TB
     I=L
     CONTINUE
     TOL=EPS*PIV
     LST=1
     DO 17 K=1,M
       IF(PIV)23,23,4
       IF(IER)7,5,7
       IF(PIV-TOL)6,6,7
       IER=K-1
       PIVI=1.0E0/A(I)
       J=(I-1)/M
       I=I-J*M-K
       J=J+1-K
       DO 8 L=K,MM,M
         LL=L+I
         TB=PIVI*R(LL)
         R(LL)=R(L)
         R(L)=TB
         IF(K-M)9,18,18
         LEND=LST+M-K
         IF(J)12,12,10
10   II=J*M
         DO 11 L=LST,LEND
           TB=A(L)
           LL=L+II
           A(L)=A(LL)
           A(LL)=TB
           DO 13 L=LST,MM,M
             LL=L+I
             TB=PIVI*A(LL)
```

13 A(LL)=A(L)
 A(L)=TB
 A(LST)=J
 PIV=0.0E0
 LST=LST+1
 J=0
 DO 16 II=LST,LEND
 PIVI=A(II)
 IST=II+M
 J=J+1
 DO 15 L=IST,MM,M
 LL=L-J
 A(L)=A(L)+PIVI*A(LL)
 TB=ABS(A(L))
 IF(TB-PIV)15,15,14
14 PIV=TB
 I=L
15 CONTINUE
 DO 16 L=K;NM,M
 LL=L+J
16 R(LL)=R(LL)+PIVI*R(L)
 LST=LST+M
17 IF(M-1)23,22,19
18 IST=MM+M
19 LST=M+1
 DO 21 I=2,M
 II=LST-I
 IST=IST-LST
 L=IST-M
 L=A(L)+0.5E0
 DO 21 J=II,NM,M
 TB=R(J)
 LL=J
 DO 20 K=IST,MM,M
 LL=LL+1
 TB=TB-A(K)*R(LL)
 K=J+L
 R(J)=R(K)
 R(K)=TB
 RETURN
 IER=-1
 TYPE *, '?????SOMETHING WRONG IN INV.FTNS!!!!'
 RETURN
 END

 SUBROUTINE VSUB(A,B,C)
 DIMENSION A(3),B(3),C(3)
 DO 10 I=1,3
 C(I)=A(I)-B(I)
 RETURN
 END

 SUBROUTINE VDOT(A,B,S)
 DIMENSION A(3),B(3)

```
S=0.0
DO 10 I=1,3
  S=S+A(I)*B(I)
RETURN
END

SUBROUTINE VCRO(A,B,C,S)
DIMENSION A(3),B(3),C(3)
C1=A(2)*B(3)-A(3)*B(2)
C2=A(3)*B(1)-A(1)*B(3)
C3=A(1)*B(2)-A(2)*B(1)
S=SQRT(C1*C1+C2*C2+C3*C3)
C(1)=C1
C(2)=C2
C(3)=C3
RETURN
END

SUBROUTINE VCOM(A,N1,N2,N3,C,I,J)
DIMENSION A(N1,N2,N3),C(N3)
DO 10 K=1,3
  C(K)=A(I,J,K)
RETURN
END

SUBROUTINE QTOTAL(NSP,NN,Q135,Q246,AMP,QDF1,QDF2)
C...THIS PROGRAM CALCULATE THE TOTAL Q FOR DRIFTING FORCE
C...INPUT: NSP,NN,Q135,Q246,AMP
C...OUTPUT: QDF1(SIDE 1),QDF2(SIDE 2)
DIMENSION Q135(NN,4),Q246(NN,4),QDF1(NN),QDF2(NN),AMP(12)
COMMON /C2/ GRAV,DEN,FREQ,DEPTH,VMOM,ANU,HEAD

DO 10 I=1,NSP
  II=I+NSP
  T1=0.0
  T2=0.0
  T3=0.0
  T4=0.0
  DO 20 J=1,3
    J1=2*J-1
    J2=J1+1
    T1=T1+Q135(I,J)*AMP(J1+6)+Q135(II,J)*AMP(J1)
    T2=T2+Q246(I,J)*AMP(J2+6)+Q246(II,J)*AMP(J2)
    T3=T3+Q135(I,J)*AMP(J1)-Q135(II,J)*AMP(J1+6)
    T4=T4+Q246(I,J)*AMP(J2)-Q246(II,J)*AMP(J2+6)
  CONTINUE
  QDF1(I)=Q135(I,4)+Q246(I,4)+FREQ*(T1+T2)
  QDF2(I)=Q135(I,4)-Q246(I,4)+FREQ*(T1-T2)
  QDF1(II)=Q135(II,4)+Q246(II,4)-FREQ*(T3+T4)
  QDF2(II)=Q135(II,4)-Q246(II,4)-FREQ*(T3-T4)
C...TOTAL SOURCE STRENGTH WHICH MOTION IS NOT INCLUDED
C  QDF1(I)=Q135(I,4)+Q246(I,4)
C  QDF2(I)=Q135(I,4)-Q246(I,4)
C  QDF1(II)=Q135(II,4)+Q246(II,4)
```

C QDP2(II)=Q135(II,4)-Q246(II,4)
10 CONTINUE
RETURN
END

SUBROUTINE SIR(N,NN,PAN,SUR,QDF1,QDF2,THETA,SR,SI,SCOS,SSIN,DSR,DSI,
1. DMENT)

C...THIS PROGRAM CALCULATE THE SR,SI...VALUES FOR DRIFTING FORCE
C...INPUT: N,NN,PAN,SUR,QDF1,QDF2,THETA
C...OUTPUT: SR,SI,SCOS,SSIN

DIMENSION PAN(N, 3), SUR(N), QDF1(NN), QDF2(NN)
COMMON /C2/ GRAV, DEN, FREQ, DEPTH, MNUM, ANU, HEAD
S1=0.0
S2=0.0
S3=0.0
S4=0.0
DS1=0.0
DS2=0.0
DS3=0.0
DS4=0.0
DO 10,I=1,N
II=I+N
CX=COS(THETA)*PAN(I,1)
SY=SIN(THETA)*PAN(I,2)
U1=MNUM*(CX+SY)+2.35619
U2=MNUM*(CX-SY)+2.35619
SX=SIN(THETA)*PAN(I,1)
CY=COS(THETA)*PAN(I,2)
DU1=MNUM*(SX-CY)
DU2=MNUM*(SX+CY)
Z=PAN(I,3)
TZ=EXP(MNUM*Z)*(1.0+EXP(-2.0*MNUM*(Z+DEPTH)))*SUR(I)
S1=S1+(QDF1(I)*COS(U1)+QDF1(II)*SIN(U1))*TZ
S2=S2+(QDF2(I)*COS(U2)+QDF2(II)*SIN(U2))*TZ
S3=S3+(QDF1(II)*COS(U1)-QDF1(I)*SIN(U1))*TZ
S4=S4+(QDF2(II)*COS(U2)-QDF2(I)*SIN(U2))*TZ
DS1=DS1+(QDF1(I)*SIN(U1)-QDF1(II)*COS(U1))*TZ*DU1
DS2=DS2+(QDF2(I)*SIN(U2)-QDF2(II)*COS(U2))*TZ*DU2
DS3=DS3+(QDF1(I)*COS(U1)+QDF1(II)*SIN(U1))*TZ*DU1
DS4=DS4+(QDF2(I)*COS(U2)+QDF2(II)*SIN(U2))*TZ*DU2

10 CONTINUE
SR=S1+S2
SI=S3+S4
DSR=DS1+DS2
DSI=DS3+DS4
SM=SR*SR+SI*SI
SCOS=SM*COS(THETA)
SSIN=SM*SIN(THETA)
DMENT=SR*DSI-SI*DSR
RETURN
END

SUBROUTINE DRIFT(NSP,NN,PAN,SUR,QDF1,QDF2,DRFX,DRFY,DRMZ)
C...CALCULATE THE DRIFTING FORCE

C...INPUT: NSP,NN,PAN,SUR,QDF1,QDF2
C...OUTPUT: DRFX,DRPY(DRIFTING FORCE IN X- AND Y-DIRECTION).
DIMENSION PAN(NSP,3),SUR(NSP),QDF1(NN),QDF2(NN)
COMMON /C2/ GRAV,DEN,FREQ,DEPTH,MNUM,ANU,HEAD

HK=MNUM*DEPTH
E2=EXP(-2.0*HK)
E4=EXP(-4.0*HK)
T1=(MNUM*MNUM-ANU*ANU)*DEPTH+ANU
T2=1.0+4.0*HK*E2/(1.0-E4)
TEMP1=4.44288*DEN*MNUM*FREQ*T2/(T1*(1.0+E2))
TEMP2=-6.28318*(1.0-E2)*DEN*(MNUM**4.0)*T2/(T1*T1*(1.0+E2)**3.0)

C...DRIFTING FORCE DUE TO THE INCOME WAVE EFFECT
CALL SIR(NSP,2*NSP,PAN,SUR,QDF1,QDF2,HEAD,SR,SI,SCOS,SSIN,DSR,DSI,TM)
DRFX=TEMP1*(SR-SI)*COS(HEAD)
DRFY=TEMP1*(SR-SI)*SIN(HEAD)
DRMZ=TEMP1*(DSR+DSI)/MNUM

C...USING GUASSIAN 16 POINTS FORMULAR TO INTEGRATE THE DRIFTING FORCE
C...DUE THE MOTION EFFECT
DELTA=6.28318/4.0
SUMX=0.0
SUMY=0.0.
SUMMEN=0.0
DO 20 J=1,4
X1=(J-1)*DELTA
X2=X1+DELTA
A=.5E0*(X2+X1)
B=DELTA
C=.49470046749582497E0*B
CALL SIR(NSP,2*NSP,PAN,SUR,QDF1,QDF2,A+C,SR,SI,APCC,APCS,TEM1,TEM2,DM1)
CALL SIR(NSP,2*NSP,PAN,SUR,QDF1,QDF2,A-C,SR,SI,AMCC,AMCS,TEM1,TEM2,DM2)
FX=.13576229705877047E-1*(APCC+AMCC)
FY=.13576229705877047E-1*(APCS+AMCS)
FMEN=.13576229705877047E-1*(DM1+DM2)
C=.47228751153661629E0*B
CALL SIR(NSP,2*NSP,PAN,SUR,QDF1,QDF2,A+C,SR,SI,APCC,APCS,TEM1,TEM2,DM1)
CALL SIR(NSP,2*NSP,PAN,SUR,QDF1,QDF2,A-C,SR,SI,AMCC,AMCS,TEM1,TEM2,DM2)
FX=FX+.31126761969323946E-1*(APCC+AMCC)
FY=FY+.31126761969323946E-1*(APCS+AMCS)
FMEN=FMEN+.31126761969323946E-1*(DM1+DM2)
C=.43281560119391587E0*B
CALL SIR(NSP,2*NSP,PAN,SUR,QDF1,QDF2,A+C,SR,SI,APCC,APCS,TEM1,TEM2,DM1)
CALL SIR(NSP,2*NSP,PAN,SUR,QDF1,QDF2,A-C,SR,SI,AMCC,AMCS,TEM1,TEM2,DM2)
FX=FX+.47579255841246392E-1*(APCC+AMCC)
FY=FY+.47579255841246392E-1*(APCS+AMCS)
FMEN=FMEN+.47579255841246392E-1*(DM1+DM2)
C=.37770220417750152E0*B
CALL SIR(NSP,2*NSP,PAN,SUR,QDF1,QDF2,A+C,SR,SI,APCC,APCS,TEM1,TEM2,DM1)
CALL SIR(NSP,2*NSP,PAN,SUR,QDF1,QDF2,A-C,SR,SI,AMCC,AMCS,TEM1,TEM2,DM2)
FX=FX+.62314485627766936E-1*(APCC+AMCC)
FY=FY+.62314485627766936E-1*(APCS+AMCS)
FMEN=FMEN+.62314485627766936E-1*(DM1+DM2)
C=.30893812220132197E0*B
CALL SIR(NSP,2*NSP,PAN,SUR,QDF1,QDF2,A+C,SR,SI,APCC,APCS,TEM1,TEM2,DM1)

```
CALL SIR(NSP,2*NSP,PAN,SUR,QDF1,QDF2,A-C,SR,SI,AMCC,AMCS,TEM1,TEM2,DM2)
FX=FX+.7479799440828837E-1*(APCC+AMCC)
FY=FY+.7479799440828837E-1*(APCS+AMCS)
FMEN=FMEN+.7479799440828837E-1*(DM1+DM2)
C=.22900838882861369E0*B
CALL SIR(NSP,2*NSP,PAN,SUR,QDF1,QDF2,A+C,SR,SI,APCC,APCS,TEM1,TEM2,DM1)
CALL SIR(NSP,2*NSP,PAN,SUR,QDF1,QDF2,A-C,SR,SI,AMCC,AMCS,TEM1,TEM2,DM2)
FX=FX+.8457825969750127E-1*(APCC+AMCC)
FY=FY+.8457825969750127E-1*(APCS+AMCS)
FMEN=FMEN+.8457825969750127E-1*(DM1+DM2)
C=.14080177538962946E0*B
CALL SIR(NSP,2*NSP,PAN,SUR,QDF1,QDF2,A+C,SR,SI,APCC,APCS,TEM1,TEM2,DM1)
CALL SIR(NSP,2*NSP,PAN,SUR,QDF1,QDF2,A-C,SR,SI,AMCC,AMCS,TEM1,TEM2,DM2)
FX=FX+.9130170752246179E-1*(APCC+AMCC)
FY=FY+.9130170752246179E-1*(APCS+AMCS)
FMEN=FMEN+.9130170752246179E-1*(DM1+DM2)
C=.47506254918818720E-1*B
CALL SIR(NSP,2*NSP,PAN,SUR,QDF1,QDF2,A+C,SR,SI,APCC,APCS,TEM1,TEM2,DM1)
CALL SIR(NSP,2*NSP,PAN,SUR,QDF1,QDF2,A-C,SR,SI,AMCC,AMCS,TEM1,TEM2,DM2)
FX=B*(FX+.9472530522753425E-1*(APCC+AMCC))
FY=B*(FY+.9472530522753425E-1*(APCS+AMCS))
FMEN=B*(FMEN+.9472530522753425E-1*(DM1+DM2))
SUMX=SUMX+FX
SUMY=SUMY+FY
SUMMEN=SUMMEN+FMEN
20 CONTINUE
C...TOTAL DRIFTING FORCE AND MOMENT
DRFX=DRFX+TEMP2*SUMX
DRFY=DRFY+TEMP2*SUMY
DRMZ=DRMZ+TEMP2*SUMMEN
RETURN
END
```

```
PROGRAM OUT72
DIMENSION PAN(36,3),UN(36,3),UNN(36,3),SUR(36),
1      DG11R(36,36),DG11I(36,36),DG12R(36,36),DG12I(36,36),
2      G11R(36,36),G11I(36,36),G12R(36,36),G12I(36,36),
3      PHI7R(36),PHI7I(36),PHI8R(36),PHI8I(36),QDF1(72),QDF2(72),
4      POT135(72,4),POT246(72,4),Q135(72,4),Q246(72,4),
5      AM(6,6),DEMP(6,6),RM(6,6),C(6,6),FOR(12),AMP(12)

COMMON /C2/ GRAV,DEN,FREQ,DEPTH,MNUM,ANU,HEAD
COMMON /C3/ VOL,XB,YB,ZB,AREA,PR2AMP,XG,YG,ZG
COMMON /SER/ UK(1000),GAMMA(1000),ALPHA
DATA NSP/42/
DATA GRAV,DEN/9.8,1000.0/
DATA XG,YG,ZG/0.0,0.0,10.62/
DATA RI44,RI55,RI66/33.04,32.09,32.92/
DATA DEPTH,HEAD/500.0,0.0/

C*****  

VOL=324000.0  

SLL=90.0  

AA1=DEN*VOL  

BB1=DEN*VOL*SQRT(GRAV/SLL)  

AA5=AA1*SLL*SLL  

BB5=BB1*SLL*SLL  

C*****  

CALL ASSIGN (2,'COM.DAT')
CALL ASSIGN (3,'PRNT2.DAT')

WRITE(3,*)'*****'  

WRITE(3,*)'RESULT OF 72 PANELS FOR RECTANGULAR BOX'  

WRITE(3,*)'*****'

DO 17 KI=1,6
READ (2)PAN,SUR,FOR,AMP,AM,DEMP,C,RM,
1      GRAV,DEN,FREQ,DEPTH,MNUM,ANU,HEAD,DRIPX,DRIFTY,DRMZ
C*****  

WRITE (3,*)'PERIOD = ',2.0*3.14159/FREQ
WRITE (3,*)'HEADING = ',HEAD*180./3.14159
WRITE (3,*)'A(11) = ',AM(1,1)/AA1,'A(33) = ',AM(3,3)/AA1
WRITE (3,*)'A(55) = ',AM(5,5)/AA5,'A(66) = ',AM(6,6)/AA5
WRITE (3,*)'B(11) = ',DEMP(1,1)/BB1,'B(33) = ',DEMP(3,3)/BB1
WRITE (3,*)'B(55) = ',DEMP(5,5)/BB5,'B(66) = ',DEMP(6,6)/BB5

PHASE=90.0-FTAN(AMP(1),AMP(7))
AMIG =SQRT(AMP(1)*AMP(1)+AMP(7)*AMP(7))
WRITE (3,*) 'SURGE MOTION = ',AMIG,' PHASE = ',PHASE

PHASE=90.0-FTAN(AMP(3),AMP(9))
AMIG =SQRT(AMP(3)*AMP(3)+AMP(9)*AMP(9))
WRITE (3,*) 'HEAVE MOTION = ',AMIG,' PHASE = ',PHASE

PHASE=90.0-FTAN(AMP(5),AMP(11))
AMIG =SQRT(AMP(5)*AMP(5)+AMP(11)*AMP(11))
```

- 119 -

```
      WRITE (3,*) 'PITCH MOTION =',AMIG*SLL,' PHASE =',PHASE  
      PHASE=90.0-FTAN(POR(1),POR(7))  
      AMIG =SQRT(POR(1)*POR(1)+POR(7)*POR(7))  
      WRITE (3,*) 'SURGE EX.FORCE =',AMIG/(GRAV*MA1/SLL),' PHASE =',PHASE  
  
      PHASE=90.0-FTAN(POR(3),POR(9))  
      AMIG =SQRT(POR(3)*POR(3)+POR(9)*POR(9))  
      WRITE (3,*) 'HEAVE EX.FORCE =',AMIG/(GRAV*MA1/SLL),' PHASE =',PHASE  
  
      PHASE=90.0-FTAN(POR(5),POR(11))  
      AMIG =SQRT(POR(5)*POR(5)+POR(11)*POR(11))  
      WRITE (3,*) 'PITCH EX.FORCE =',AMIG/(GRAV*MA1),' PHASE =',PHASE  
  
      WRITE (3,*) 'DRIFT FORCE(X) =', DRIFX/(DEN*GRAV*SLL)  
      WRITE (3,*) 'DRIFT FORCE(Y) =', DRIFY/(DEN*GRAV*SLL)  
      WRITE (3,*) 'DRIFT MOMENT(Z) =', DRMZ/(DEN*GRAV*SLL*SLL)  
      WRITE (3,*) '*****  
      WRITE (3,*) '
```

17 CONTINUE
STOP
END

FUNCTION FTAN(AR,AI)
C.....THIS FUNCTION COMPUTE THE ARGUMENT OF (AR,AI) IN THE RANGE
C.....FROM -90 DEG. TO +270 DEG.
D=ABS(AI/AR)
D=ATAN(D)/3.1416*180.0
IF(AI .GT. 0.0 .AND. AR .LT. 0.0) D=180.0-D
IF(AI .LT. 0.0 .AND. AR .GT. 0.0) D=-D
IF(AI .LT. 0.0 .AND. AR .LT. 0.0) D=+180.0+D
FTAN=D
RETURN
END

POR005.DAT : INPUT OF THE PROGRAM

1	45.	7.5	-10.	1.0	0.0	0.0	300.0
2	45.	7.5	-30.	1.0	0.0	0.0	300.0
3	45.	22.5	-10.	1.0	0.0	0.0	300.0
4	45.	22.5	-30.	1.0	0.0	0.0	300.0
5	45.	37.5	-10.	1.0	0.0	0.0	300.0
6	45.	37.5	-30.	1.0	0.0	0.0	300.0
7	37.5	45.	-10.	0.0	1.0	0.0	300.0
8	37.5	45.	-30.	0.0	1.0	0.0	300.0
9	22.5	45.	-10.	0.0	1.0	0.0	300.0
10	22.5	45.	-30.	0.0	1.0	0.0	300.0
11	7.5	45.	-10.	0.0	1.0	0.0	300.0
12	7.5	45.	-30.	0.0	1.0	0.0	300.0
13	37.5	33.75	-40.	0.0	0.0	-1.0	337.5
14	37.5	11.25	-40.	0.0	0.0	-1.0	337.5
15	22.5	33.75	-40.	0.0	0.0	-1.0	337.5
16	22.5	11.25	-40.	0.0	0.0	-1.0	337.5
17	7.5	33.75	-40.	0.0	0.0	-1.0	337.5
18	7.5	11.25	-40.	0.0	0.0	-1.0	337.5

PRNT2.DAT : OUTPUT OF THE PROGRAM

RESULT OF 72 PANELS FOR RECTANGULAR BOX

PERIOD = 9.999999

HEADING = 0.000000E+00

A(11) = 0.1779451 A(33) = 0.6936716

A(55) = 4.0283702E-02 A(66) = 5.7746455E-02

B(11) = 0.9037306 B(33) = 3.1050753E-02

B(55) = 1.8677386E-02 B(66) = 4.5083300E-03

SURGE MOTION = 0.2023692 PHASE = -46.46820

HEAVE MOTION = 2.6818879E-02 PHASE = -103.8198

PITCH MOTION = 0.2177859 PHASE = 135.5104

SURGE EX.FORCE = 0.9025733 PHASE = 106.8761

HEAVE EX.FORCE = 0.1043513 PHASE = 75.30950

PITCH EX.FORCE = 0.1205921 PHASE = -71.56024

DRIFT FORCE(X) = 0.4890130

DRIFT FORCE(Y) = -1.1289563E-08

DRIFT MOMENT(Z) = -7.5263756E-10

PERIOD = 12.000000

HEADING = 0.0000000E+00

A(11) = 0.4019165 A(33) = 0.6734779

A(55) = 4.5369517E-02 A(66) = 5.0772507E-02

B(11) = 0.9664637 B(33) = 7.7199653E-02

B(55) = 1.7726453E-02 B(66) = 2.3326605E-04

SURGE MOTION = 0.3462898 PHASE = -73.69241

HEAVE MOTION = 0.1399764 PHASE = -127.2732

PITCH MOTION = 0.3302048 PHASE = 106.0551

SURGE EX.FORCE = 1.331019 PHASE = 79.48020

HEAVE EX.FORCE = 0.2753643 PHASE = 49.15677

PITCH EX.FORCE = 0.1761464 PHASE = -100.9704

DRIFT FORCE(X) = 0.3758127

DRIFT FORCE(Y) = 1.0888847E-08

DRIFT MOMENT(Z) = 1.2098719E-10

PERIOD = 14.000000

HEADING = 0.0000000E+00

A(11) = 0.6638447 A(33) = 0.6657764

A(55) = 4.9814995E-02 A(66) = 4.8433807E-02

B(11) = 0.8056340 B(33) = 0.1296488

B(55) = 1.3000505E-02 B(66) = 1.7320217E-05

SURGE MOTION = 0.4901692 PHASE = -83.02115

HEAVE MOTION = 0.5476664 PHASE = -135.1987

PITCH MOTION = 0.4152229 PHASE = 96.09303

SURGE EX.FORCE = 1.616891 PHASE = 75.34177

HEAVE EX.FORCE = 0.4654126 PHASE = 32.82574

PITCH EX.FORCE = 0.2063015 PHASE = -104.9533

DRIFT FORCE(X) = 0.2471173
DRIFT FORCE(Y) = -1.1755061E-08
DRIFT MOMENT(Z) = 6.5305893E-11

PERIOD = 16.00000
HEADING = 0.0000000E+00
A(11) = 0.8342986 A(33) = 0.6773978
A(55) = 5.1916514E-02 A(66) = 4.7341917E-02
B(11) = 0.5253953 B(33) = 0.1700688
B(55) = 7.5277337E-03 B(66) = 1.7596584E-06
SURGE MOTION = 0.6040380 PHASE = -86.78464
HEAVE MOTION = 2.761543 PHASE = -98.99474
PITCH MOTION = 0.4516027 PHASE = 92.33227
SURGE EX. FORCE = 1.630511 PHASE = 78.55598
HEAVE EX. FORCE = 0.6577757 PHASE = 22.82619
PITCH EX. FORCE = 0.1988162 PHASE = -101.5796
DRIFT FORCE(X) = 0.6720425
DRIFT FORCE(Y) = -2.0671662E-08
DRIFT MOMENT(Z) = 9.0917031E-11

PERIOD = 18.00007
HEADING = 0.0000000E+00
A(11) = 0.8786014 A(33) = 0.7036057
A(55) = 5.1954225E-02 A(66) = 4.6719987E-02
B(11) = 0.2963249 B(33) = 0.1925385
B(55) = 3.8218205E-03 B(66) = 2.3890027E-07
SURGE MOTION = 0.6893444 PHASE = -88.44836
HEAVE MOTION = 2.098073 PHASE = -14.25278
PITCH MOTION = 0.4532574 PHASE = 90.88786
SURGE EX. FORCE = 1.476040 PHASE = 82.47288
HEAVE EX. FORCE = 0.8381730 PHASE = 16.39951
PITCH EX. FORCE = 0.1724154 PHASE = -97.58699
DRIFT FORCE(X) = 6.5767340E-02
DRIFT FORCE(Y) = -1.0753330E-09
DRIFT MOMENT(Z) = -2.7303377E-12

PERIOD = 20.00084
HEADING = 0.0000000E+00
A(11) = 0.8590820 A(33) = 0.7375016
A(55) = 5.1246542E-02 A(66) = 4.6323139E-02
B(11) = 0.1602608 B(33) = 0.1992931
B(55) = 1.8877644E-03 B(66) = 4.3368996E-08
SURGE MOTION = 0.7523804 PHASE = -89.22000
HEAVE MOTION = 1.426518 PHASE = -3.616913
PITCH MOTION = 0.4350950 PHASE = 90.33043
SURGE EX. FORCE = 1.278632 PHASE = 85.28959
HEAVE EX. FORCE = 1.000595 PHASE = 12.07687
PITCH EX. FORCE = 0.1438083 PHASE = -94.73732
DRIFT FORCE(X) = 6.5905107E-03
DRIFT FORCE(Y) = -4.4062243E-11
DRIFT MOMENT(Z) = 9.9446039E-14



